Bitumen properties and the shear resistance of asphalt mixtures

Towards a tool for bitumen selection

Jiqing Zhu
Abubeker Ahmed
Yared Dinegdae

vti

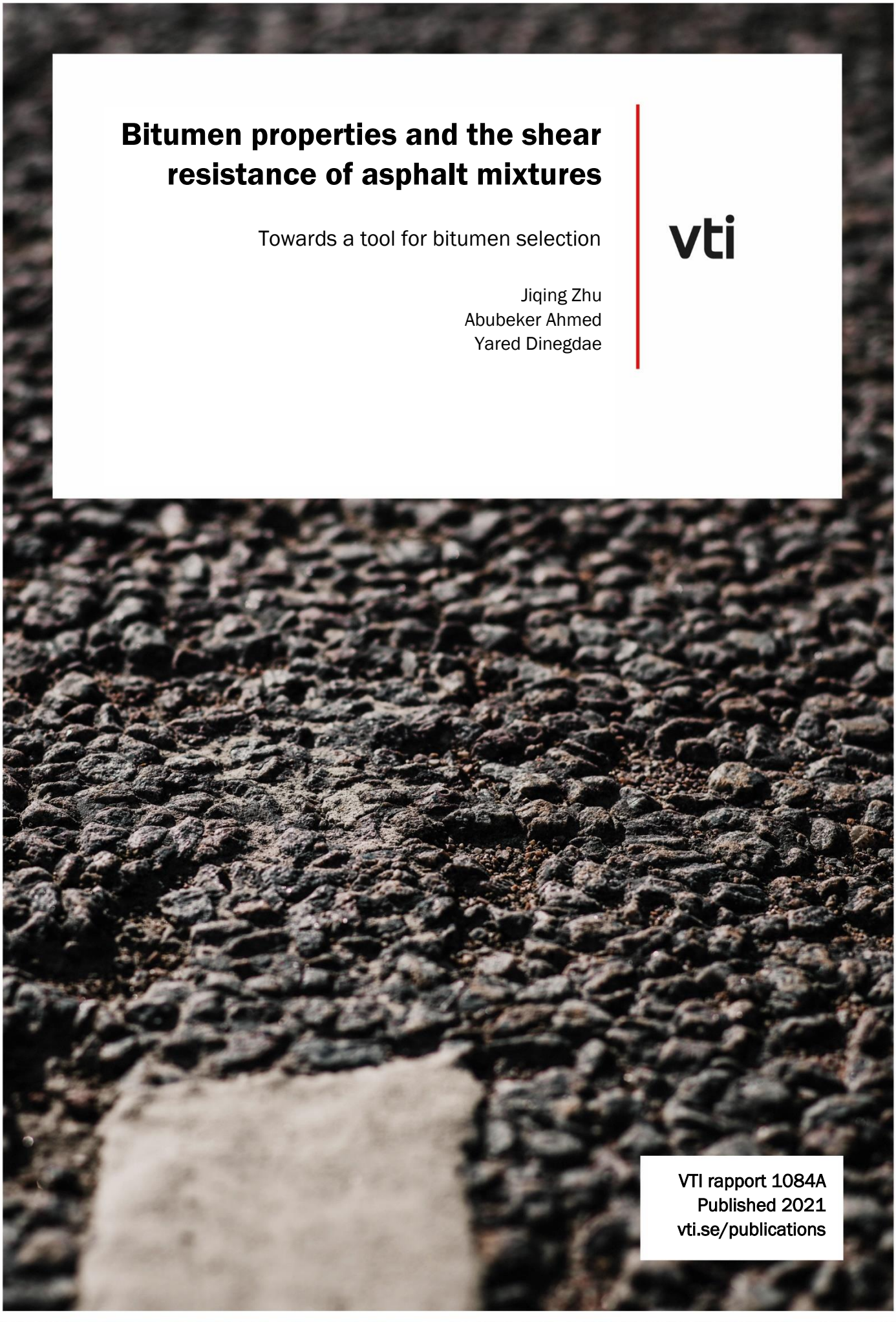

VTI rapport 1084A
Published 2021
vti.se/publications

Foto: Fotograf Satu AB, VTI

VTI rapport 1084A

Bitumen properties and the shear resistance of asphalt mixtures

Towards a tool for bitumen selection

Jiqing Zhu

Abubeker Ahmed

Yared Dinegdae

vti

Authors: Jiqing Zhu (VTI), Abubeker Ahmed (VTI), Yared Dinegdae (VTI)
Reg. No., VTI: 2018/0519-9.2
Publication No.: VTI rapport 1084A
Published by VTI, 2021

Publication Information – Publikationsuppgifter

Titel/ Title

Bitumenegenskaper och skjuvmotstånd hos asfaltbeläggningar. Framtagning av en urvalsmodell för bitumen./ Bitumen properties and the shear resistance of asphalt mixtures. Towards a tool for bitumen selection

Författare/Authors

Jiqing Zhu (VTI, https://orcid.org/0000-0003-1779-1710)

Abubeker Ahmed (VTI, https://orcid.org/0000-0002-6327-4709)

Yared Dinegdae (VTI, https://orcid.org/0000-0001-7174-7214)

Utgivare/Publisher

VTI, Statens väg- och transportforskningsinstitut/
Swedish National Road and Transport Research Institute (VTI)
www.vti.se/

Serie och nr/Publication No.

VTI rapport 1084A

Utgivningsår/ Published

2021

VTI:s diarienr/Reg. No., VTI

2018/0519-9.2

ISSN

0347–6030

Projektnamn/Project

BVFF Framtagning av urvalsmodell för bitumen kopplat till skjuvrelaterad nedbrytning./
BVFF Bitumen selection protocol to minimize shear-related distresses of asphalt pavement.

Uppdragsgivare/Commissioned by

Trafikverket/Swedish Transport Administration

Språk/Language

Engelska/english

Antal sidor inkl. bilagor/No. of pages incl. appendices

66

Kort sammanfattning

Skjuvmotståndet hos asfaltmassor är en viktig materialegenskap för att säkerställa god kvalitet på asfaltbeläggningar och minimera skjuvrelaterade skador såsom deformationer orsakade av tung trafik. För att få ett högt skjuvmotstånd är modeller viktiga verktyg för att välja lämpliga råmaterial för asfaltmassor, främst bitumen och ballast. Studien som presenteras i denna rapport fokuserar på val av bitumen för asfaltmassor.

Denna studie syftar till att förstå förhållandet mellan asfaltmassans skjuvegenskaper och bindemedlets egenskaper för att skapa en urvalsmodell. I rapporten redovisas en experimentell undersökning av hur de dynamiska skjuvegenskaperna hos asfaltmassor korrelerar med bitumenegenskaper. Bindemedelshaltens inverkan beaktas också i studien. Sex bituminösa bindemedel, varav två var polymermodifierade, användes för att tillverka asfaltmassor i laboratorium. Bindemedlen testades med olika provningsmetoder, medan deras asfaltmassor karaktäriserades av dynamisk skjuvprovning varefter korrelationen mellan resultaten analyserades. Resultaten indikerar att bindemedlens iso-modultemperaturer efter korttidsåldring har mycket stark korrelation med asfaltmassans viskositet vid maximal fasvinkel. Iso-modultemperaturer mättes med dynamisk skjuvreometer (DSR, dynamic shear rheometer) vid 10 rad/s. Sambandet gällde både omodifierade och polymermodifierade bitumen även om antalet testade modifierade bindemedel var lågt i studien.

Baserat på korrelationsanalysen kunde asfaltmassans viskositet vid maximal fasvinkel kopplas till bindemedelsparametrar genom regressionsanalys vid minimal tillåten bindemedelshalt. Detta möjliggjorde ett genomförbart tillvägagångssätt från utvärdering av bitumen till prognos av spårbildning i asfaltbeläggningar med PEDRO-modellen (PErmanent Deformation of asphalt concrete layer for ROads). Genom detta tillvägagångssätt kan en urvalsmodell för bitumen läggas fram, bestående av två länkade delar för utvärdering av bitumen samt prognos av spårbildning i asfaltbeläggningar. Blackdiagram föreslås som ett effektivt verktyg för linjär viskoelastisk utvärdering av bituminösa bindemedel, medan PEDRO-modellen kan användas för utvärdering av bindemedlets långsiktiga påverkan på asfaltbeläggningen med provningsresultat av bindemedlet.

Nyckelord

Asfaltmassa, bitumen, skjuvmotstånd, reologi, masterkurva

Abstract

The shear resistance of asphalt mixtures is a crucial material property to ensure the pavement quality and minimize shear-related distresses. For a high shear resistance, proper protocols to select suitable raw materials for asphalt mixtures, mainly bitumen and mineral aggregates, are of great importance. The study presented in this report focuses on the selection of bitumen for asphalt mixtures.

Towards a tool for bitumen selection, this study aims to understand the relationship between asphalt mixture shear properties and bitumen. The research objective is to identify the correlation between them. Following this direction, this report presents an experimental investigation on the dynamic shear properties of asphalt mixtures and their relationships with the bitumen properties. The influence of binder content is also considered. Six bituminous binders, two of which were polymer-modified, were used to prepare asphalt mixtures in laboratory. The binders were tested with various methods, while their asphalt mixtures were characterized by the dynamic shear test. With the test results, the correlation between them was analysed. It is indicated that the iso-modulus temperatures of bitumen after short-term ageing by dynamic shear rheometer testing at 10 rad/s have very strong correlations with the asphalt mixture viscosity at the maximum phase angle. This was valid for both the studied neat (unmodified) bitumen and polymer-modified bitumen (PMB), although the number of studied PMB samples was limited in this study.

Based on the correlation analysis, the asphalt mixture viscosity at the maximum phase angle could be linked to binder parameters by regression analysis at the minimum allowable binder content. This enabled a feasible approach from bitumen evaluation to the rutting performance prediction of asphalt pavements with the PEDRO (PErmanent Deformation of asphalt concrete layer for ROads) model. Through this approach, a bitumen selection tool could be put forward, consisting of two linked parts respectively for bitumen evaluation and performance prediction. The Black space diagram is proposed as an efficient tool for the linear viscoelastic evaluation of bituminous binders, while the PEDRO model can be employed for the evaluation of bitumen's long-term influence on pavement (rutting) performance with the binder testing results.

Keywords

Asphalt mixture, bitumen, shear resistance, rheology, master curve

Sammanfattning

Skjuvspänningen och skjuvtöjningen som framkallas av trafikbelastning spelar en avgörande roll för utvecklingen av flera typer av nedbrytningsmekanismer hos asfaltbeläggningar, såsom spår- och sprickbildning. Skjuvmotståndet hos asfaltmassor är således en viktig materialegenskap för att minimera skjuvrelaterade skador och säkerställa god kvalitet på asfaltbeläggningar. För att erhålla ett högt skjuvmotstånd är det viktigt med adekvata metoder för att välja lämpliga råmaterial för asfaltmassor, främst bitumen och ballast. Studien som presenteras i denna rapport fokuserar på val av bitumen för asfaltmassor.

Denna studie syftar till att förstå förhållandet mellan asfaltmassans skjuvegenskaper och bindemedlets egenskaper för att skapa en urvalsmodell för bitumen. Syftet är att identifiera korrelationen mellan dem. I rapporten redovisas en experimentell undersökning av hur de dynamiska skjuvegenskaperna hos asfaltmassor korrelerar med bitumenegenskaper. Bindemedelshaltens inverkan beaktas också i studien. Sex bituminösa bindemedel användes för att tillverka asfaltmassor i laboratorium, inklusive fyra varianter av omodifierade bitumen och två varianter av polymermodifierade bitumen (PMB). Bindemedlen testades med olika provningsmetoder, medan deras motsvarande asfaltmassor karaktäriserades av dynamisk skjuvprovning.

I denna rapport demonstreras att Blackdiagram (Black space diagram) är ett effektivt verktyg för linjär viskoelastisk utvärdering av bituminösa bindemedel. Det kombinerar bitumenets modul och fasvinkel i samma domän och kan därmed integrera olika linjära viskoelastiska parametrar i ett enda diagram. Detta möjliggör enkla utvärderingar av bitumen, särskilt tillsammans med den vanliga provnings-metoden för temperatursvep med dynamisk skjuvreometer (DSR, dynamic shear rheometer) vid 10 rad/s. Användningen av Blackdiagram är inte bara kompatibel med de nuvarande tekniska specifikationerna för utvärdering av bitumen vid höga temperaturer, den har också stor potential att täcka ett bredare temperaturområde samt även inkludera nya linjära parametrar.

Med de experimentella resultaten analyserades korrelationen mellan dynamiska skjuvegenskaper hos asfaltmassor och bitumenegenskaper. Resultaten indikerar att asfaltmassans skjuvmodul vid maximal fasvinkel ligger i ett relativt smalt område och varierar inte särskilt mycket. Därmed är asfaltmassans viskositet vid maximal fasvinkel i hög grad beroende av frekvensen för maximal fasvinkel. Dessutom har bindemedlens iso-modultemperaturer efter korttidsåldring mätt med DSR vid 10 rad/s en mycket stark korrelation med asfaltmassans viskositet vid maximal fasvinkel. Sambandet gällde både omodifierade och polymermodifierade bitumen även om antalet testade modifierade bindemedel var lågt i studien.

Endast för omodifierade bitumen har mjukpunkten efter korttidsåldring en mycket stark korrelation med asfaltmassans viskositet vid maximal fasvinkel. När både omodifierade bitumen och PMB ingår i analysen är korrelationen dock inte längre stark. Bindemedlets viskositet vid låg skjuvning (LSV) vid 0,001 Hz och 10 °C efter korttidsåldring har en mycket stark korrelation med asfaltmassans viskositet vid maximal fasvinkel. Däremot är korrelationen av LSV vid 60 °C efter korttidsåldring inte lika stark som vid 10 °C. Trots korrelationerna kan den stora mätosäkerheten för LSV från både modellanpassning och val av målfrekvens begränsa dess användning i praktiken för utvärdering av bitumen samt relaterade prognoser av bindemedlets långsiktiga påverkan på asfaltbeläggningen.

Baserat på korrelationsanalysen kunde asfaltmassans viskositet vid maximal fasvinkel kopplas till valda bindemedelsparametrar genom regressionsanalys vid minimal tillåten bindemedelshalt. Detta möjliggjorde ett genomförbart tillvägagångssätt att prognostisera spårbildning i asfaltbeläggningar med PEDRO-modellen (PErmanent Deformation of asphalt concrete layer for ROads) och analysresultat av bitumen. Genom detta tillvägagångssätt kan en urvalsmodell för bitumen läggas fram, bestående av två länkade delar för utvärdering av bitumen samt prognos av spårbildning i asfaltbeläggningar. Blackdiagram föreslås som ett effektivt verktyg för linjär viskoelastisk utvärdering

av bituminösa bindemedel, medan PEDRO-modellen kan användas för utvärdering av bindemedlets långsiktiga påverkan på asfaltbeläggningen med provningsresultat av bindemedlet.

Summary

The shear stress and strain induced by traffic loading play a critical role in the development of major distresses in asphalt pavements, such as rutting and top-down cracking. The shear resistance of asphalt mixtures is thus a crucial material property to minimize shear-related distresses and ensure the pavement quality. For a high shear resistance, proper protocols to select suitable raw materials for asphalt mixtures, mainly bitumen and mineral aggregates, are of great importance. The study presented in this report focuses on the selection of bitumen for asphalt mixtures.

Towards a tool for bitumen selection, this study aims to understand the relationship between asphalt mixture shear properties and bitumen. The research objective is to identify the correlation between them. Following this direction, this report presents an experimental investigation on the dynamic shear properties of asphalt mixtures and their relationships with the bitumen properties. The influence of binder content is also considered. Six bituminous binders were used to prepare asphalt mixtures in laboratory, including four variants of neat (unmodified) bitumen and two variants of polymer-modified bitumen (PMB). The binders were tested with various methods, while their asphalt mixtures were characterized by the dynamic shear test.

In this report, it is demonstrated that the Black space diagram is an efficient tool for the linear viscoelastic evaluation of bituminous binders. It combines the modulus and phase angle of bitumen in the same space and can thus integrate various linear viscoelastic parameters into one single diagram. This enables straightforward evaluations of bitumen, especially together with the common test method of temperature sweep by dynamic shear rheometer (DSR) at 10 rad/s. The adoption of the Black space diagram is not only compatible with the current technical specifications regarding high-temperature evaluation, but it also holds great potential to cover a wider service temperature range and even to include new linear parameters based on the up-to-date research.

With the experimental results, the correlation between dynamic shear properties of asphalt mixtures and bitumen properties was analysed. It is indicated that the shear modulus of asphalt mixtures at the maximum phase angle is in a relatively narrow range and does not vary very much. The asphalt mixture viscosity at the maximum phase angle is thus largely dependent on the frequency of the maximum phase angle. Furthermore, the iso-modulus temperatures of bitumen after short-term ageing by DSR testing at 10 rad/s have very strong correlations with the asphalt mixture viscosity at the maximum phase angle. This was valid for both the studied unmodified bitumen and PMB, although the number of studied PMB samples was limited in this study.

For unmodified bitumen only, the softening point of bitumen after short-term ageing has a very strong correlation with the asphalt mixture viscosity at the maximum phase angle. When both unmodified bitumen and PMBs are included in the analysis, however, the correlation is not strong anymore. The low shear viscosity (LSV) at 0.001 Hz and 10 °C after short-term ageing has a very strong correlation with the asphalt mixture viscosity at the maximum phase angle. In contrast, the correlation of the LSV at 60 °C after short-term ageing is not as strong as at 10 °C. Despite the correlations, the great determination uncertainty of LSV from both the model fitting and the selection of target frequency can limit its practical use for bitumen evaluation and the related pavement performance prediction.

Based on the correlation analysis, the asphalt mixture viscosity at the maximum phase angle could be linked to the selected binder parameters by regression analysis at the minimum allowable binder content. This enabled a feasible approach to the rutting performance prediction of asphalt pavements with the PEDRO (PErmanent Deformation of asphalt concrete layer for ROads) model and analysis results of bitumen. Through this approach, a bitumen selection tool could be put forward, consisting of two linked parts respectively for bitumen evaluation and performance prediction. The Black space diagram is proposed as an efficient tool for the linear viscoelastic evaluation of bituminous binders, while the PEDRO model can be employed for the evaluation of bitumen's long-term influence on pavement (rutting) performance with the binder testing results.

Foreword

This report presents an experimental study as a part of the research project “Bitumen selection protocol to minimize shear-related distresses of asphalt pavement”. The project is financed by the BVFF (Bana väg för framtiden) programme with funding from the Swedish Transport Administration (Trafikverket) and co-funding from Nynas AB, Peab Asfalt AB and VTI. All support is gratefully acknowledged.

The bituminous binders analysed in this report were provided by Nynas AB. I would like to express my thanks to Xiaohu Lu and Bengt Sandman, both from Nynas AB, for their help with the materials. The preparation of asphalt mixtures and most of the reported tests were conducted at the Road Material Laboratory of VTI. Andreas Waldemarson and Terence (Terry) McGarvey, both my colleagues at VTI, are acknowledged for their hard work in the laboratory. In addition, the microscopic investigation of polymer-modified bitumen was done by Peab Asfalt AB. Many thanks to Michael Langfjell, from Peab Asfalt AB, for his assistance with the analysis. Last but not least, my appreciation goes to my co-authors and also colleagues at VTI, Abubeker Ahmed and Yared Dinegdae, for their valuable contributions to this report.

An external expert group was formed for steering the project, consisting of the following members:

- Henrik Arnerdal, Trafikverket
- Xiaohu Lu, Nynas AB
- Anders Gudmarsson, Peab Asfalt AB
- Michael Langfjell, Peab Asfalt AB

The experts gave me constructive advice and suggestions during the whole period of this study, from the experimental plan to result analysis. Their input is gratefully appreciated.

Linköping, December 2020

Jiqing Zhu
Project leader

Granskare/Examiner

Safwat Said.

Table of contents

1. Introduction

1.1. Background

In order to ensure good pavement conditions of the road network, it is important to select and use materials of proper quality in the pavement structures, namely the materials quality assurance. Improper quality grades of road materials may cause early pavement distresses that usually cost extra expenses to repair. Different forms and mechanisms of pavement distresses often lead to quality requirements on different material properties. For major distresses in asphalt pavements, such as rutting and top-down cracking, the shear resistance of asphalt mixtures is a crucial material property to ensure the pavement quality and minimize the related distresses.

Asphalt mixtures are composed of the bitumen (as binder), mineral aggregates, filler, and air voids. The shear resistance of asphalt mixtures depends on the specific composition and internal structure of the mixture as well as properties of the raw materials. As a binder-bound material, however, asphalt mixture has a very different shear behaviour from unbound materials. The viscoelastic nature of bitumen endows the asphalt mixture with unique rheological properties and viscoelasticity. The content and properties of bitumen in an asphalt mixture significantly affects its resistance to shear loadings, especially to dynamic shear loadings.

For ensuring a high shear resistance of asphalt mixtures, it is thus of great importance to understand its relationship with the bitumen (content and properties) and find the correlation between them. This may assist in the asphalt mixture design and bitumen selection processes to minimize the potential of shear-related distresses in asphalt pavements. Following a previous literature study (Zhu *et al.*, 2020), this report presents an experimental investigation on shear resistance of asphalt mixtures and the bitumen properties and analyses the correlation between them. The influence of binder content is also considered in this laboratory study.

Based on the correlation analysis, this report seeks a feasible approach from bitumen evaluation to rutting performance prediction of asphalt pavements with the PEDRO (PErmanent Deformation of asphalt concrete layer for ROads) model (Said *et al.*, 2020). Through such an approach, a bitumen selection tool can be put forward, consisting of two linked parts respectively for bitumen evaluation and performance prediction. This tool is expected to enable not only the control of bitumen parameters but also the evaluation of bitumen's long-term influence on pavement (rutting) performance with the binder testing results.

1.2. Objectives and scope

Towards a tool for bitumen selection, the laboratory study presented in this report aims to identify the effects of bitumen on shear properties of asphalt mixtures and to understand the binder-mixture correlation. With the improved understanding as a basis, this study seeks solutions for better control of bitumen parameters and explores a feasible approach from bitumen evaluation to rutting performance prediction of asphalt pavements with the PEDRO model.

In this report, the shear properties of asphalt mixtures are limited to the dynamic shear properties within the linear viscoelastic range. The bitumen properties, however, are not limited. Common binder performance indicators, either within or out of the linear viscoelastic range, are investigated and analysed. The rutting performance prediction in this report is based on the PEDRO model, which uses linear viscoelastic properties of asphalt mixtures at the maximum phase angle for the input material parameters. Thus, the correlation analysis in this report focuses on the bitumen's correlation with asphalt mixture properties at the maximum phase angle. This helps to identify the link between binder performance indicators and PEDRO model parameters.

1.3. Report organization

This report consists of seven chapters. After this introduction chapter, Chapter 2 describes the experimental plan with an asphalt mixture testing part and a bitumen testing part. Chapter 3 analyses the test results of asphalt mixtures and demonstrates the ordinary steps of rutting performance prediction with the PEDRO model. Chapter 4 discusses the bitumen testing results and lists the potential performance indicators. Chapter 5 presents the correlation analysis between bitumen properties and the shear resistance of asphalt mixtures. Chapter 6 puts forward the two linked parts of a possible bitumen selection tool and demonstrates its feasibility. At the end, Chapter 7 summarises the main findings of this study and gives recommendations based on the research outcomes.

2. Experimental plan

2.1. Materials

In this study, six bituminous binders of different types were used to prepare asphalt mixture samples in laboratory. Four of them were unmodified binders (paving grade bitumen according to EN 12591): one of penetration grade 50/70, one of penetration grade 70/100, and two of penetration grade 160/220. The other two of the studied binders were modified binders with a linear-type styrene-butadiene-styrene (SBS) copolymer. The polymer-modified bitumen (PMB) was prepared in laboratory by mixing the SBS modifier with a base bitumen of penetration grade 100/150. The polymer contents of the two PMBs were respectively 3% and 5% by weight of the blends. The studied binders are denoted in this report as follow:

- Pen. 50/70
- Pen. 70/100
- Pen. 160/220 #1
- Pen. 160/220 #2
- PMB 1 (Pen. 100/150+3% SBS)
- PMB 2 (Pen. 100/150+5% SBS)

It should be noted that the Pen. 160/220 #1 and Pen. 160/220 #2 are two different binder variants of the same penetration grade.

Dense-graded asphalt mixtures of ABT16 type were designed and prepared according to the specification of the Swedish Transport Administration (Trafikverket, 2020). The six bituminous binders resulted in six different asphalt mixtures, all of ABT16 type with identical mineral aggregates (granite), filler, and gradation. The used aggregates were from the Skärlunda quarry in Sweden, while the gradation curve is shown in Figure 1. Asphalt mixture samples were made in laboratory with a gyratory compactor. The target air void content was 3.0% for all asphalt mixtures. So, the difference among the asphalt mixtures were only in the binder.

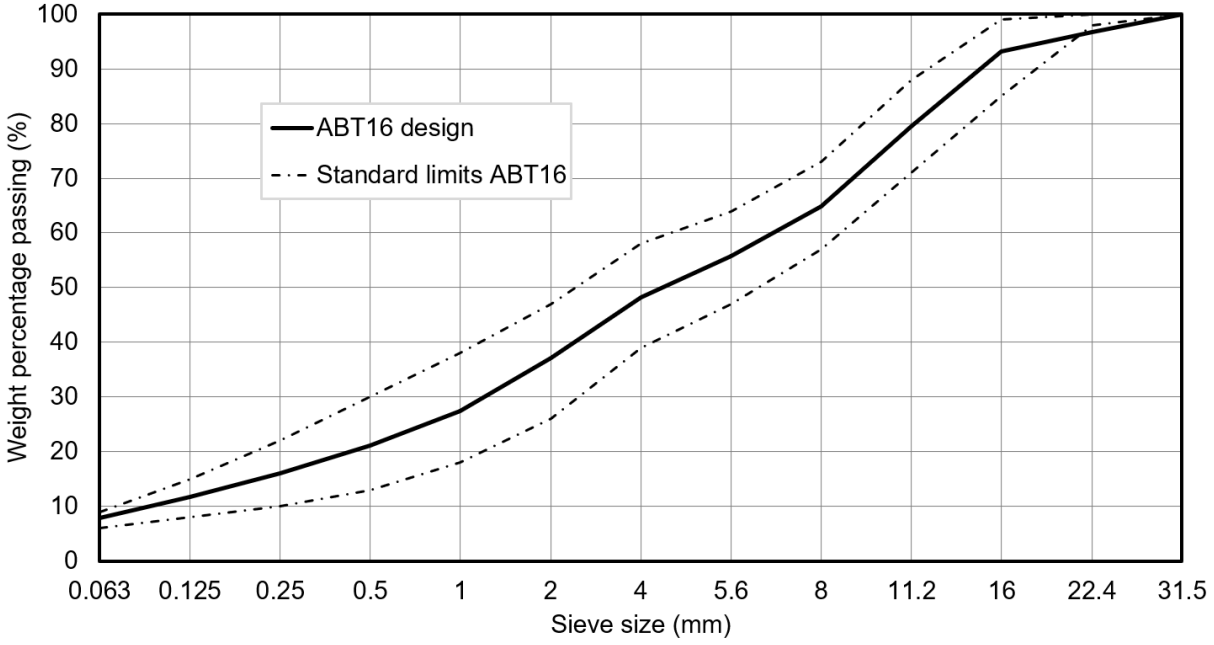

Figure 1. Gradation curve of the ABT16 asphalt mixtures.

In practice, the binder content of asphalt mixtures usually varies when binders of different grades/types are used in the mixtures. The specification of the Swedish Transport Administration (Trafikverket, 2020) requires different values as the minimum allowable binder content for different binders, which is an empirical adjustment based on the experience of practice. This study considers these varying minimum allowable values as the benchmark of the analysis. So, the expected outcomes from the analysis would include and reflect the effects of this empirical adjustment, and thus enable practical implementations.

It should be noted that, in the Swedish specification, the minimum allowable binder content for PMBs in ABT16 asphalt mixtures is not specified according to the PMB type and grade. This study considers the same value for PMB 1 (3% SBS) as for the Pen. 70/100 paving grade bitumen, while an empirically increased value (0.2% higher) for PMB 2 with 5% SBS modifier. In addition, to consider the influence of binder content change, the asphalt mixture using Pen. 160/220 #1 bitumen was prepared with an increased binder content, i.e. 0.4% higher than the minimum allowable. This also enables the comparison among three of the ABT16 asphalt mixtures at exactly the same binder content (6.0%). All binder content values for preparing the ABT16 asphalt mixtures are listed in Table 1.

Table 1. Binder content values for preparing the ABT16 asphalt mixtures.

Binder type	Pen. 50/70	Pen. 70/100	Pen. 160/220 #1	Pen. 160/220 #2	PMB 1 (3% SBS)	PMB 2 (5% SBS)
Binder content	6.2%	6.0%	6.0%	5.6%	6.0%	6.2%

2.2. Methodology and methods

2.2.1. Methodology

The laboratory study presented in this report aims to link the bitumen and asphalt mixture properties and seeks a feasible approach from bitumen evaluation to rutting performance prediction of asphalt pavements with the PEDRO model. To analyse the binder-mixture correlation, the potentially related bitumen and asphalt mixture properties must be firstly identified. As the PEDRO model uses linear shear properties of asphalt mixtures for the input material parameters, the linear viscoelastic properties in shear are of the interest of this study from the asphalt mixture perspective. It is thus necessary to construct and analyse the master curves of shear modulus and phase angle of the asphalt mixtures. The reference temperature (T_{ref}) for constructing master curves was chosen at 10 °C. The focus of analysis was placed on parameters at the maximum phase angle of the asphalt mixture, where material parameters are calculated for inputting to the PEDRO model.

As for the related bitumen properties and performance indicators, previous studies (Christensen *et al.*, 2003; Bari and Witczak, 2006) have suggested the significant role of linear viscoelastic properties of bitumen in determining the asphalt mixture properties. Thus, the comparison of master curves between asphalt mixture and bitumen, as shown in Figure 2, may help to identify the potentially related linear viscoelastic parameters of bitumen. This needs the construction of bitumen master curves to be at the same reference temperature (10 °C) as that of the asphalt mixtures. Based on the time-temperature superposition principle, however, the bitumen parameters from master curves at a reference temperature can be equivalently converted to temperature sweep parameters at a reference frequency (e.g. the commonly used 10 rad/s). These temperature sweep parameters are probably more practical and easier for the implementation. Furthermore, as some popular linear parameters of bitumen combine both the modulus and phase angle such as the American performance grading parameters and Glover-Rowe parameter (Glover *et al.*, 2005; Rowe, 2014), the plot of linear viscoelastic parameters of bitumen in the Black space, i.e. the modulus-phase angle space, may integrate various linear parameters into one single diagram as shown in Figure 3. It enables straightforward and efficient

evaluations of bitumen with the temperature sweep testing. This report demonstrates its usefulness in terms of bitumen evaluation and explores the possibility of combining it with the PEDRO model for a bitumen selection tool.

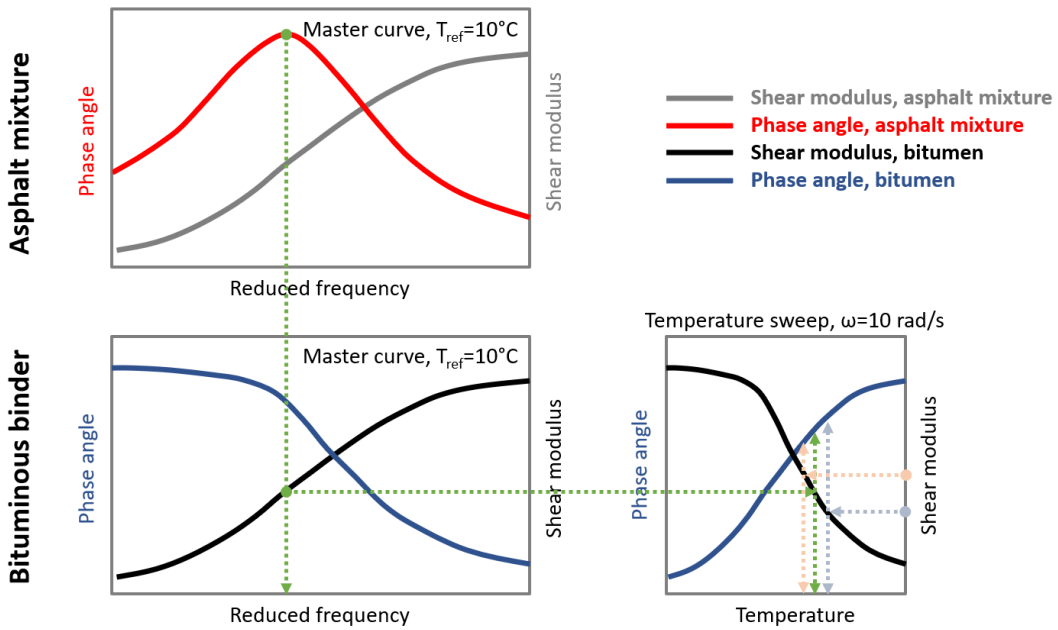

Figure 2. Comparison of master curves between asphalt mixture and bitumen to identify potentially related linear viscoelastic parameters of bitumen.

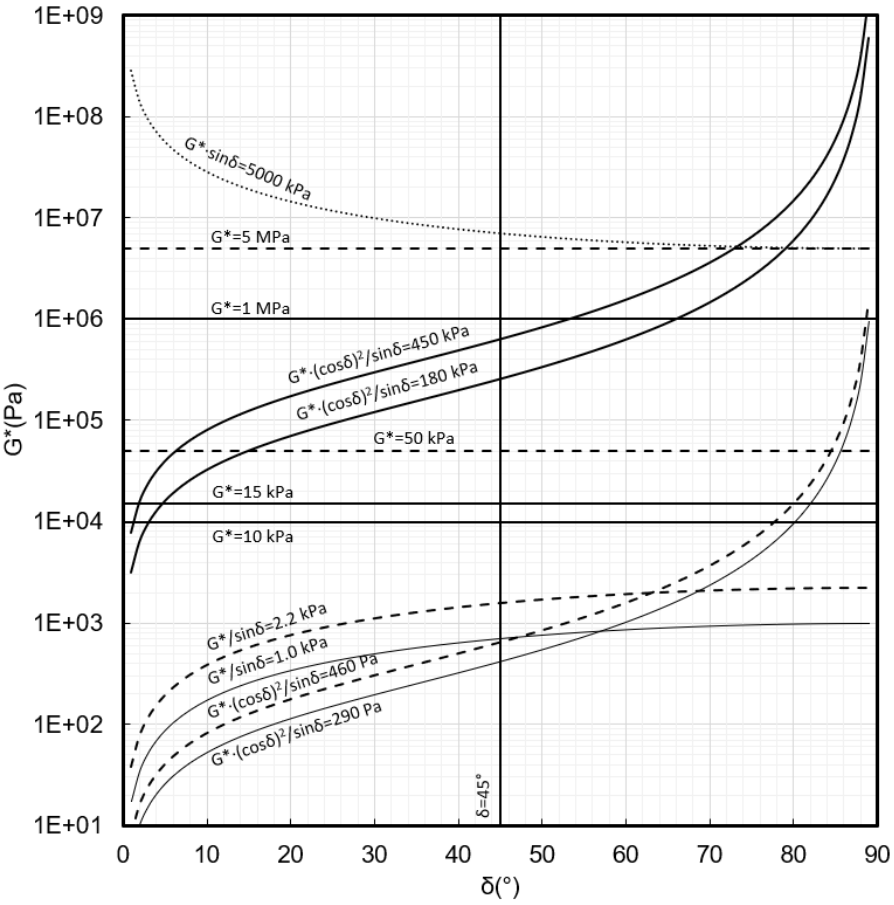

Figure 3. The Black space diagram of bitumen.

Besides the bitumen master curves and temperature sweep parameters, the low shear viscosity (LSV) of bitumen was also investigated as a potential performance indicator in this study. This is a response to the viscosity concept that the PEDRO model uses for asphalt mixtures (Oscarsson, 2011; Said *et al.*, 2013). Furthermore, the popular multiple stress creep and recovery (MSCR) test was also employed to analyse the binders. Although both the original and short-term aged binders were investigated in this study, it is the bitumen properties after the short-term ageing that were analysed for the possible correlation with the shear resistance of asphalt mixtures. Based on the correlation analysis, a feasible approach was investigated from bitumen evaluation to rutting performance prediction of asphalt pavements with the PEDRO model.

2.2.2. Methods

To characterize the linear viscoelastic properties in shear, the prepared ABT16 asphalt mixtures were analysed by dynamic shear test (frequency sweep at various temperatures) with the VTI shear box (Said *et al.*, 2013), as shown in Figure 4. The asphalt mixture samples were in the disc shape of 150 mm in diameter and about 38 mm in thickness. Two duplicates were done for each of the asphalt mixtures. With the test results, the PEDRO model (web version at https://pedro.vti.se/) was used to demonstrate the ordinary steps of rutting performance prediction.

The bitumen testing was done with the European standard methods, including the needle penetration according to EN 1426, ring and ball softening point according to EN 1427, temperature sweep and frequency sweep with dynamic shear rheometer (DSR) according to EN 14770, and the MSCR test according to EN 16659. The short-term ageing of bitumen was conducted in laboratory with the rolling thin film oven test (RTFOT) method according to EN 12607-1. The morphology of PMB samples was investigated with a fluorescence microscope. Regarding the correlation between bitumen and asphalt mixture properties, the Pearson product-moment correlation coefficient was employed for the analysis.

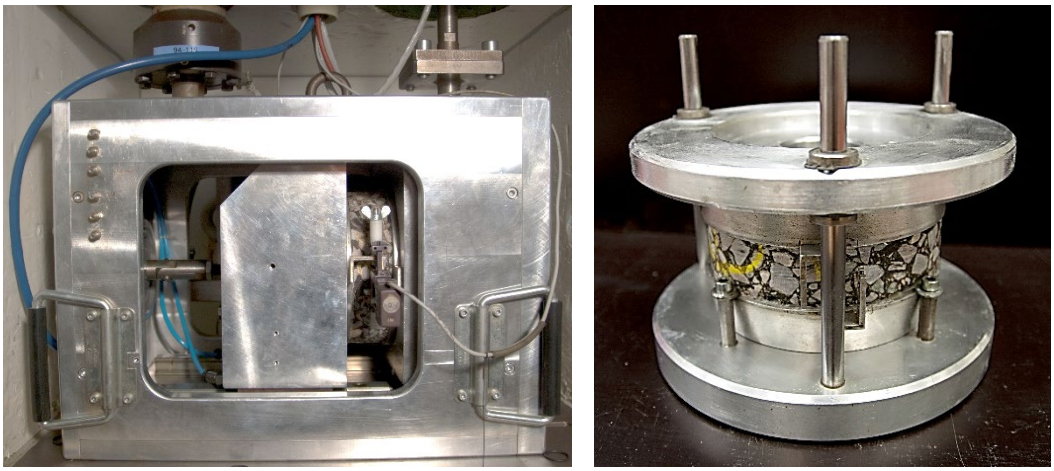

Figure 4. Dynamic shear test of asphalt mixtures: The left image shows the VTI shear box setup. The right image shows a sample with platens attached. Photo: VTI.

3. Dynamic shear characterization of asphalt mixtures and rutting performance prediction

This chapter analyses the results of asphalt mixtures by the dynamic shear test and demonstrates the ordinary steps of rutting performance prediction with the PEDRO model. The basic characteristics of the prepared asphalt mixture samples are presented firstly. The construction and analyses of master curves are then described, with a focus on the asphalt mixture properties at the maximum phase angle. At the end, the use of the PEDRO model is demonstrated.

3.1. Basic characteristics of the prepared asphalt mixture samples

After the preparation processes, the asphalt mixture samples were measured for their dimension and volumetric properties. The measured dimension data of samples were used to calculate the shear modulus and phase angle, while the results of volumetric properties are listed in Table 2. As mentioned previously, the target air void content was 3.0% for all asphalt mixtures. Not unexpectedly, the prepared asphalt mixture samples ended up with certain variations in the air void content. These variations, as well as the respective binder content values, will be put into the correlation analysis later and be investigated for their influences on the asphalt mixture properties of interest. It should be noted that the air void content was measured on the cut "test-ready" samples of the needed size, not the uncut samples of a bigger size. This helps to limit possible errors from the sample preparation.

Furthermore, the volumetric parameters VMA (Voids in the Mineral Aggregate) and VFA (Voids Filled with Asphalt, with the term "asphalt" actually meaning the binder) were calculated as well. This is because there were previous studies suggesting their significant roles in determining the asphalt mixture properties (Christensen *et al.*, 2003; Christensen and Bonaquist, 2015). All these volumetric parameters will be included and investigated in the planned correlation analysis.

Table 2. Volumetric properties of the prepared asphalt mixture samples of ABT16 type.

Binder type in the asphalt mixture (binder content)	**Pen. 50/70 (6.2%)**	**Pen. 70/100 (6.0%)**	**Pen. 160/220 #1 (6.0%)**	**Pen. 160/220 #2 (5.6%)**	**PMB 1 (6.0%)**	**PMB 2 (6.2%)**
Air voids	2.8%	3.3%	3.0%	3.1%	2.6%	2.8%
VMA	17.0%	17.1%	16.8%	16.0%	16.4%	17.0%
VFA*	83.4%	80.8%	82.2%	80.5%	84.3%	83.5%

3.2. Master curves of shear modulus and phase angle

To construct master curves for the asphalt mixtures, the first step was to shift the dynamic shear test results according to the time-temperature superposition principle. And then, the following step was to fit the shifted data with certain fitting model that can, to a great extent, represent the measurement results. In this study, the Arrhenius equation was used for shifting the test data, as Equation 1.

$$\log(a_T) = K_a \left(\frac{1}{T + 273} - \frac{1}{T_{ref} + 273} \right)$$

Equation 1. Calculation of the shift factor with the Arrhenius equation.

* The term VFA is according to the American terminology. By the European standard EN 12697-8, however, the same concept as VFA is named as VFB, namely voids filled with binder.

In Equation 1, a_T is the shift factor; K_a is the activation energy constant in K (usually around 10000 K); T is the test temperature in °C; and T_{ref} is the reference temperature (chosen at 10 °C in this study). The same equation will be used for shifting the bitumen test data as well.

As for the curve fitting, there are different fitting models that can be used, e.g., the Havriliak-Negami model of empirical expression (Havriliak and Negami, 1966), 2S2P1D model of rheological elements (Olard and Di Benedetto, 2003), and sigmoidal/compound unimodal-sigmoidal model of mathematical fitting (Pellinen *et al.*, 2004; Said *et al.*, 2013). The fitting model needed in this study is a model that can fit the measurement data very well. The good fitting of phase angle data is particularly important for the asphalt mixtures in this study. This is because the model-fitted master curves of asphalt mixtures will lead to the material parameter values input to the PEDRO model, while the PEDRO model uses the maximum phase angle as the determination basis. So, the fitting model should be able to represent the measured phase angle data to a great precision, in addition to the usually high precision for the shear modulus. Furthermore, the same type of model is also expected to be applicable to bituminous binders.

A comparison of different fitting models was done by fitting the same measurement data of an asphalt mixture with several available models. Based on the comparison, as presented in the Appendix 1 of this report, the sigmoidal model (Equation 2) was selected to fit the shear modulus data in this study, and the compound unimodal-sigmoidal model (Said *et al.*, 2013), as Equation 3, was selected for the phase angle of asphalt mixtures. They gave the best fitting, especially for the phase angle data.

$$G = \upsilon + \frac{\alpha}{1 + e^{\beta - \gamma \log(f_r)}}$$

Equation 2. Fitting equation of the sigmoidal model for shear modulus master curve of asphalt mixture.

$$\phi = \frac{c}{1 + \left(\frac{\log(f_r) - a}{b}\right)^2} + \frac{d}{1 + e^{\left(\frac{\log(f_r) - a}{g}\right)}}$$

Equation 3. Fitting equation of the compound unimodal-sigmoidal model for phase angle master curve of asphalt mixture.

In Equations 2 and 3, f_r is the reduced frequency in Hz, G is the shear modulus of asphalt mixtures (in MPa in this study), ϕ is the phase angle of asphalt mixtures in degree (°), and the fitting parameters include υ, α, β, γ, a, b, c, d, and g. This is a slightly higher number of parameters than other available models, which results in a higher degree of freedom for the model. Especially, the two separate terms of Equation 3 make a great flexibility for better fitting of the phase angle data.

For each asphalt mixture, a one-step optimisation was done to obtain the values of all fitting parameters as well as the constant K_a for determining the shift factor. This is believed to have the same effect as the optimisation of complex shear modulus as a complex number by other models (e.g. the Havriliak-Negami model and 2S2P1D model), because the shear modulus G and phase angle ϕ are basically interconvertible with the elastic (storage) modulus and viscous (loss) modulus.

The obtained values of the constant K_a are listed in Table 3, while the values of other parameters for fitting master curves of asphalt mixtures are presented in the Appendix 2 of this report. In Table 3, it can be seen that the K_a values slightly vary from one asphalt mixture to another, with the mean value around 10000 K. This fact, that the K_a values do not greatly vary, makes it reasonable to assume constant shift factors for estimating asphalt mixture parameters for predictions later in this study.

Table 3. Constant values for determining shift factors of asphalt mixture master curves.

Binder type in the asphalt mixture (binder content)	**Pen. 50/70 (6.2%)**	**Pen. 70/100 (6.0%)**	**Pen. 160/220 #1 (6.0%)**	**Pen. 160/220 #2 (5.6%)**	**PMB 1 (6.0%)**	**PMB 2 (6.2%)**
K_a (K)	10742	10320	9543	11207	9997	10420

One example of the master curve fitting is presented in Figure 5, for the ABT16 asphalt mixture with PMB 1 (binder content 6.0%). It indicates a good fitting for both the shear modulus G and phase angle ϕ. The other asphalt mixtures had similar good fitting as well. All the model-fitted master curves of all asphalt mixtures are shown in Figure 6. The results suggest that the asphalt mixture with Pen. 50/70 bitumen (6.2%) has the highest shear modulus, and its maximum phase angle appears at the lowest frequency. The asphalt mixture Pen. 160/220 #1 (6.0%) has the lowest shear modulus, and its maximum phase angle appears at the highest frequency. If changing the binder to a harder bitumen, i.e. from Pen. 160/220 #1 to Pen. 70/100 with the same binder content (6.0%), the shear modulus of asphalt mixture would increase, and the maximum phase angle would move to a lower frequency. Decreasing the binder content while maintaining the bitumen grade, namely from Pen. 160/220 #1 (6.0%) to Pen. 160/220 #2 (5.6%), would have similar effects. The asphalt mixtures with PMBs reach lower values for the maximum phase angle, comparing with those with unmodified bitumen. Between the two asphalt mixtures with PMBs, there is only a very limited difference in the shear modulus. However, the maximum phase angle of asphalt mixture PMB 2 (6.2%) appears at a lower frequency than PMB 1 (6.0%), despite a higher binder content. This is probably due to the higher polymer content in PMB2 than PMB1.

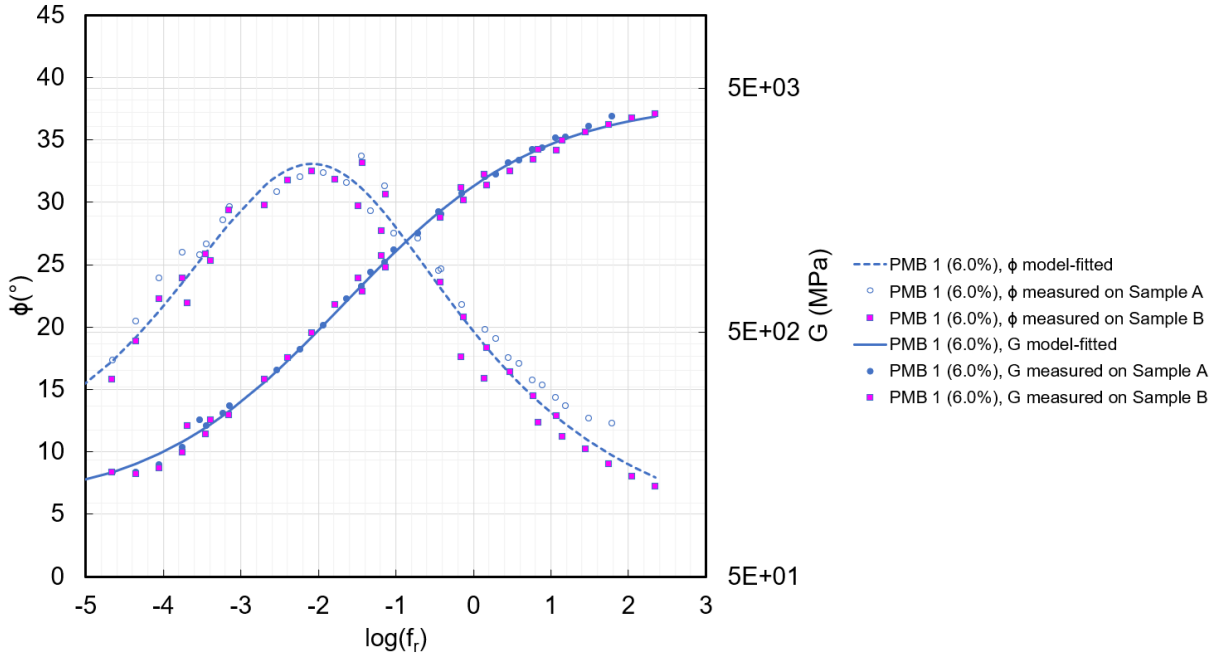

Figure 5. Master curve fitting of the ABT16 asphalt mixture PMB 1 (6.0%), T_{ref}=10 °C.

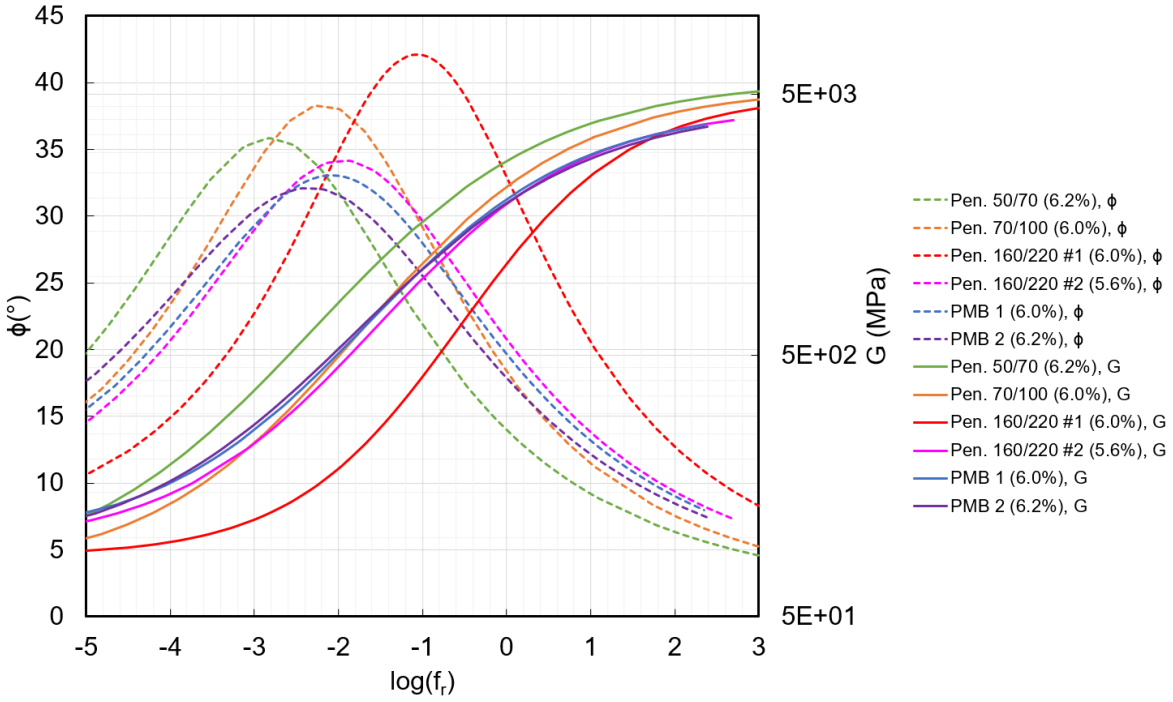

Figure 6. Model-fitted master curves of the ABT16 asphalt mixtures, T_{ref}=10 °C.

3.3. Asphalt mixture properties at the maximum phase angle

As the PEDRO model considers the maximum phase angle of asphalt mixtures as the basis for determining input material parameters, the asphalt mixture properties at the maximum phase angle are of great interest in this study. These properties are to be investigated for their potential correlations with the bitumen, which will eventually help to identify the link between binder performance indicators and PEDRO model parameters.

For this, the model-fitted master curves shown in Figure 6 were analysed to locate the maximum phase angle and the corresponding shear modulus of asphalt mixtures. Furthermore, since the PEDRO model employs the concept of viscosity for asphalt mixtures and uses it for determining the input material parameters, the asphalt mixture viscosity η was also calculated at the maximum phase angle according to Equation 4.

$$\eta = \frac{G}{\omega_r}$$

Equation 4. Definition of the asphalt mixture viscosity.

In Equation 4, ω_r is the reduced angular frequency in rad/s. The determined values of all these parameters are listed in Table 4 for all types of asphalt mixtures. It is observed that the shear modulus G of asphalt mixtures at the maximum phase angle does not vary very much (all around 400-500 MPa). The asphalt mixture viscosity η at the maximum phase angle is thus largely dependent on the frequency of the maximum phase angle. In Table 4 are basically the asphalt mixture properties of interest to be correlated with the bitumen later in this study, while they are also the properties to be put into the PEDRO model for predicting the rutting development.

Table 4. Asphalt mixture properties at the maximum phase angle, T_{ref}=10 °C.

Binder type in the asphalt mixture (binder content)	Pen. 50/70 (6.2%)	Pen. 70/100 (6.0%)	Pen. 160/220 #1 (6.0%)	Pen. 160/220 #2 (5.6%)	PMB 1 (6.0%)	PMB 2 (6.2%)
Maximum phase angle (°)	35.8	38.3	42.1	34.1	33.1	32.1
log(f_r) of the maximum phase angle	-2.81	-2.19	-1.07	-1.95	-2.08	-2.35
G (MPa) at the maximum phase angle	423	425	390	470	479	414
log(η) at the maximum phase angle (η in MPa·s)	4.64	4.02	2.86	3.82	3.96	4.17

3.4. Prediction of rutting development with the PEDRO model

This section demonstrates the steps of rutting prediction with the PEDRO model. The PEDRO model has been implemented for several roads in Sweden by now (Said *et al.*, 2020). While further work of model calibration and validation is going on, this study seeks an alternative approach from bitumen evaluation to rutting performance prediction of asphalt pavements with the PEDRO model. It is expected that this alternative approach would ease the future implementation of the PEDRO model by enabling options bypassing certain potential restrictions such as the equipment accessibility, etc.

Furthermore, for the purpose of bitumen selection, it is often comparative analyses that are conducted to rank the candidate binders. For comparative analyses, the precise calibration and extensive validation of the model are not of the same importance as for other applications. As follow, a comparative analysis of the studied binders with the PEDRO model is presented with a fixed structure and fixed traffic and climate conditions. This analysis is based on the testing results of asphalt mixtures described previously in this chapter. The outcomes of this analysis will be considered as the reference for evaluating the prediction results based on binder testing later in this report.

The input material parameters into the PEDRO model are values of the constants a_1, a_2 and a_3 according to Equation 5.

$$\log(\eta) = a_1 T^2 + a_2 T + a_3$$

Equation 5. Fitting equation used by the PEDRO model for material constants.

In Equation 5, T is the temperature in °C. To determine these material parameters, the asphalt mixture viscosity η was calculated at the maximum phase angle at different reference temperatures, i.e. 0 °C, 10 °C, 20 °C, 30 °C, 40 °C, and 50 °C. The $\log(\eta)$-T plot, as shown in Figure 7, led to the determined values of PEDRO input parameters listed in Table 5. These values were put into the PEDRO model (web version at https://pedro.vti.se/) for the prediction of rutting development in a pre-defined structure of asphalt mixture under pre-defined traffic and climate conditions.

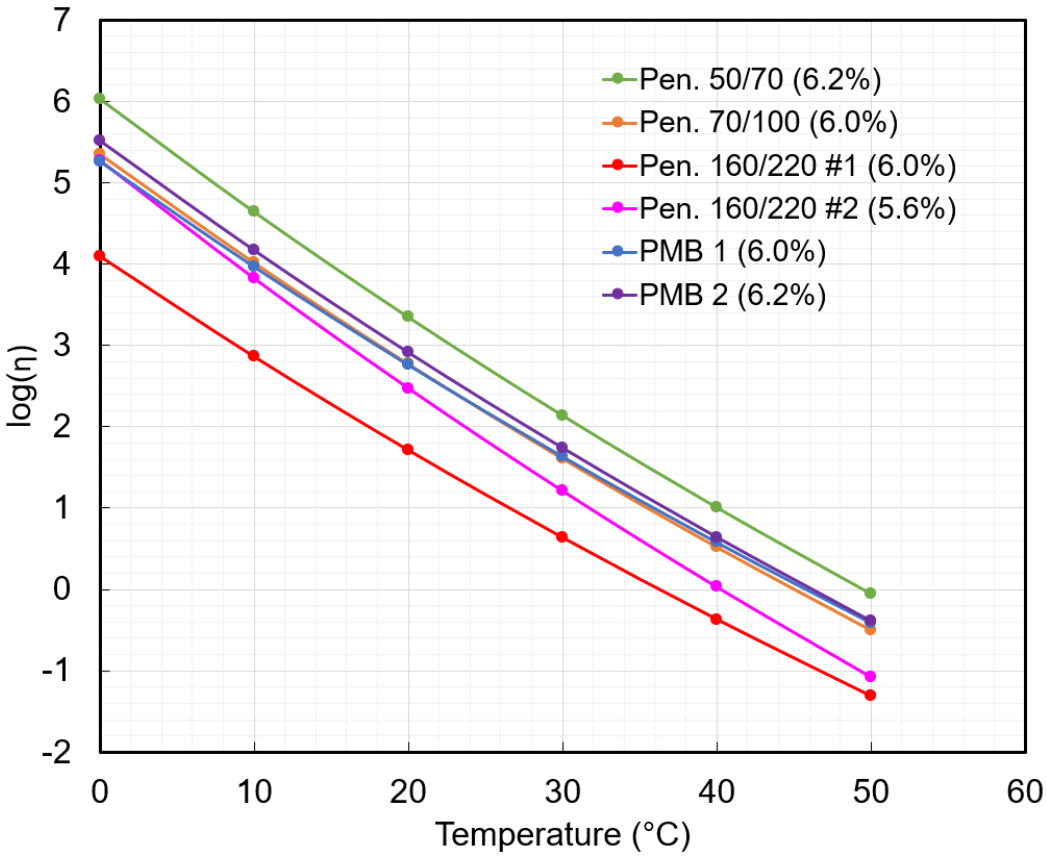

Figure 7. Asphalt mixture viscosity at the maximum phase angle at different reference temperatures.

Table 5. Determined PEDRO material parameters with asphalt mixture testing.

Binder type in the asphalt mixture (binder content)	**Pen. 50/70 (6.2%)**	**Pen. 70/100 (6.0%)**	**Pen. 160/220 #1 (6.0%)**	**Pen. 160/220 #2 (5.6%)**	**PMB 1 (6.0%)**	**PMB 2 (6.2%)**
a_1	4.09×10^{-4}	3.93×10^{-4}	3.63×10^{-4}	4.27×10^{-4}	3.81×10^{-4}	3.97×10^{-4}
a_2	-0.142	-0.137	-0.126	-0.148	-0.132	-0.138
a_3	6.027	5.348	4.093	5.270	5.254	5.513

A one-layer structure of asphalt mixture with a thickness of 50 mm was considered for the comparative analysis. The six asphalt mixtures were compared by respectively putting their material parameters, as listed in Table 5, into the PEDRO model for predicting their rutting performance. Except the material parameters, the other input parameters were the same for all asphalt mixtures. Namely, the standard (default) parameter values were used. The input parameters for the comparative analysis are summarised and listed as follow:

- General
  - Layers: 1 layer, 50 mm thickness, ABT16 asphalt mixture
  - Calibration factor: 0.02
- Material constants
  - Viscosity: a_1, a_2, a_3 values from Table 5 (each asphalt mixture), n=0 (ignoring ageing)
  - Poisson's ratio: y_{span}=0.35, y_{min}=0.16, lamda=0.08, x_{shift}=15.18

- Traffic
    - Traffic data: by ESALs, standard axle load 100 kN, load equivalency factor 1.3
    - Vehicle configuration: 1 axle with tyre pressure of 0.8 MPa
    - Axle configuration: calculated from contact pressure (0.8 MPa), 50% dual wheels of 0.3 m centre to centre spacing
    - Daily traffic distribution: d_1=0.61, d_2=13.54, d_3=0.04, d_4=0.02
- Climate
    - By monthly average temperature as below
        - January -2 °C
        - February -1 °C
        - March 3 °C
        - April 10 °C
        - May 15 °C
        - June 20 °C
        - July 25 °C
        - August 20 °C
        - September 15 °C
        - October 10 °C
        - November 5 °C
        - December 0 °C

The prediction results by the PEDRO model are presented in Figures 8 and 9. Figure 8 shows the predicted rut profiles at the end of a period of 20 years. It is indicated that the ABT16 asphalt mixture with Pen. 160/220 #1 (binder content 6.0%) would deform dramatically if it lasts for the whole period of 20 years. In reality, however, such a structure would probably fail very early without reaching the 20th year. If decreasing the binder content while maintaining the bitumen grade, namely from Pen. 160/220 #1 (6.0%) to Pen. 160/220 #2 (5.6%), the rutting resistance of the structure would be improved. Using harder binder would have the same effect. The predicted rut profile of the asphalt mixture with PMB 1 (6.0%) is almost identical to that of the one with Pen. 70/100 (6.0%). The increased SBS polymer content in PMB 2 makes the asphalt mixture more resistant to rutting. Figure 9 presents the development of predicted rut depth (downward deformation plus upheaval at the profile centre distance=0 m) during the whole period of 20 years.

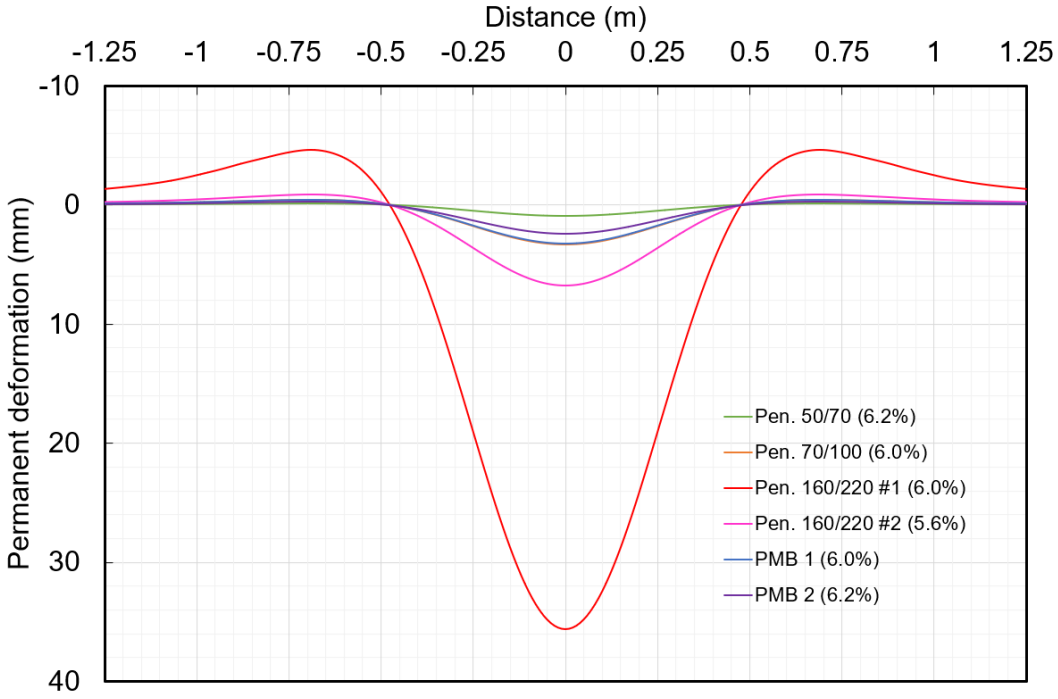

Figure 8. Predicted rut profiles in 20 years by the PEDRO model based on asphalt mixture testing.

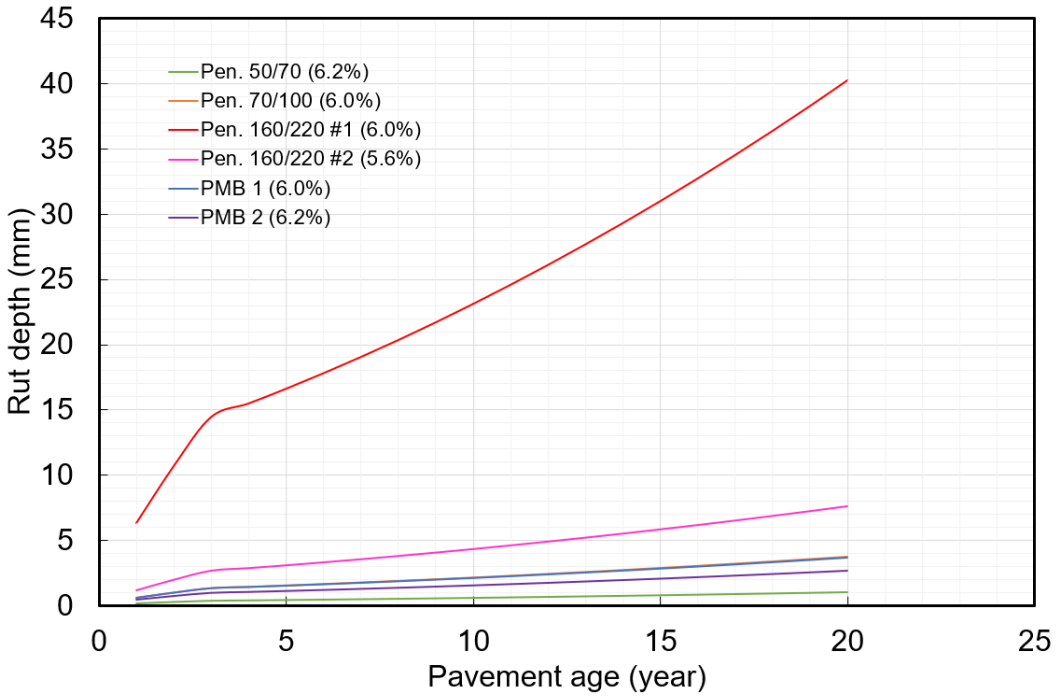

Figure 9. Predicted rut development (profile centre) during 20 years by the PEDRO model based on asphalt mixture testing.

4. Bitumen properties and performance indicators

This chapter analyses the results of bitumen testing. The basic properties of bitumen are presented firstly. Linear viscoelastic properties and related performance indicators by DSR measurements are then discussed. At last, the MSCR parameters are analysed. Both the original and RTFOT-aged binders are investigated in this chapter. It should be noted, however, that only the properties of RTFOT-aged bitumen will be analysed for possible correlations with the shear resistance of asphalt mixtures later in this report.

4.1. Basic properties

The studied binders were tested for the needle penetration at 25 °C (original binder only) and softening point (before and after RTFOT ageing). The test results are listed in Table 6. It is suggested that the softening point of unmodified binders all increased by about 5 °C after the RTFOT ageing. Comparing with the base bitumen (penetration grade 100/150), the modification with SBS copolymer decreased the needle penetration and increased the softening point. The PMBs showed lower softening point increase after the RTFOT ageing, i.e. by about 1 °C. Based on the test results listed in Table 6, PMB 1 could be classified as 65/105-50 and PMB 2 as 40/100-75 according to the framework specification EN 14023, although other additional tests were not conducted to confirm the classes. Furthermore, the PMB morphology was investigated with a fluorescence microscope. Figure 10 shows that both PMBs have very fine microstructures without significant phase separation.

Table 6. Basic properties of the studied binders.

Parameters	Pen. 50/70	Pen. 70/100	Pen. 160/220 #1	Pen. 160/220 #2	PMB 1 (3% SBS)	PMB 2 (5% SBS)
Needle penetration @25 °C (0.1 mm)	49	80	182	192	93	71
Softening point, original (°C)	50.8	46.6	38.0	40.0	51.2	75.4
Softening point, after RTFOT (°C)	56.0	51.6	43.2	44.6	52.4	76.4
Softening point change (°C)	5.2	5.0	5.2	4.6	1.2	1.0

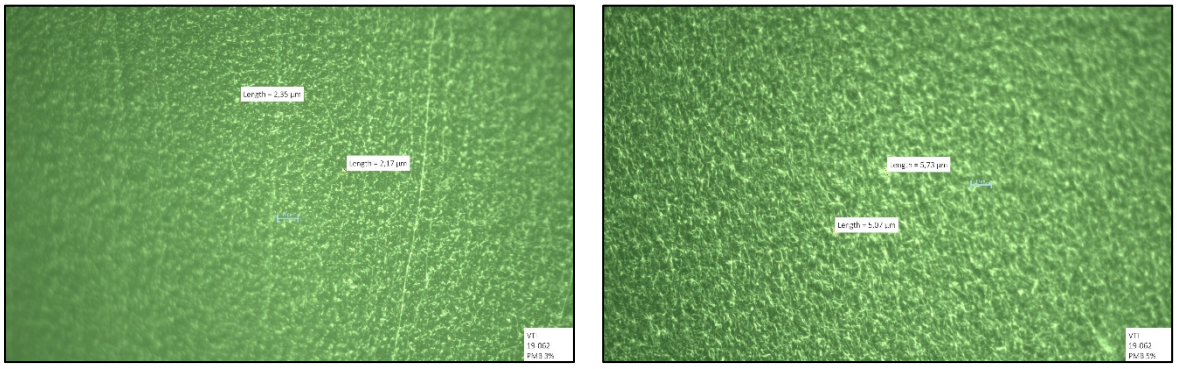

Figure 10. Morphology of the studied PMBs: The left image shows PMB 1 with 3% SBS. The right image shows PMB 2 with 5% SBS. Photo: Michael Langfjell.

4.2. Linear viscoelastic parameters by DSR

This section discusses the linear viscoelastic parameters of bitumen by DSR measurements. Both temperature sweep and frequency sweep were employed to test the studied binders. The temperature

sweep was done at 10 rad/s, while the frequency sweep was done at various temperatures to construct master curves for the binders. Both the original and RTFOT-aged binders were investigated.

4.2.1. Temperature sweep at 10 rad/s

The temperature sweep at 10 rad/s is one of the most common methods for testing bitumen with DSR in practice. It leads to the calculation of various linear viscoelastic parameters. Examples include the iso-modulus parameters (complex shear modulus G*=5 MPa, 1 MPa, 50 kPa, 15 kPa and 10 kPa), crossover temperature (phase angle δ=45°), and other derivative parameters combining G* and δ such as the performance grading (PG) parameters G*/sinδ, G*·sinδ and the Glover-Rowe parameter $G^*\cdot(\cos\delta)^2/\sin\delta$. To integrate all these linear parameters into one single diagram, this study uses the Black space diagram for evaluating binders.

4.2.1.1. Original binders

Figures 11-14 present the temperature sweep results of the original binders in the Black space. Each data point was labelled with its test temperature. With the help of criterion lines, the binders could be quickly evaluated by various parameters in a single diagram. For example, in Figure 11, the Pen. 50/70 original binder reaches the G*=15 kPa criterion line at a temperature lower than but almost 52 °C. Previous studies (Schrader and Wistuba, 2019; Alisov *et al.*, 2020) suggested that this criterion corresponds to the softening point of unmodified bitumen, which is confirmed by the test result listed in Table 6. Furthermore, it is also indicated in Figure 11 that the Pen. 50/70 original binder passes the G*/sinδ=1.0 kPa criterion of PG grading at 70 °C. Similar evaluations by some other criteria can be done as well.

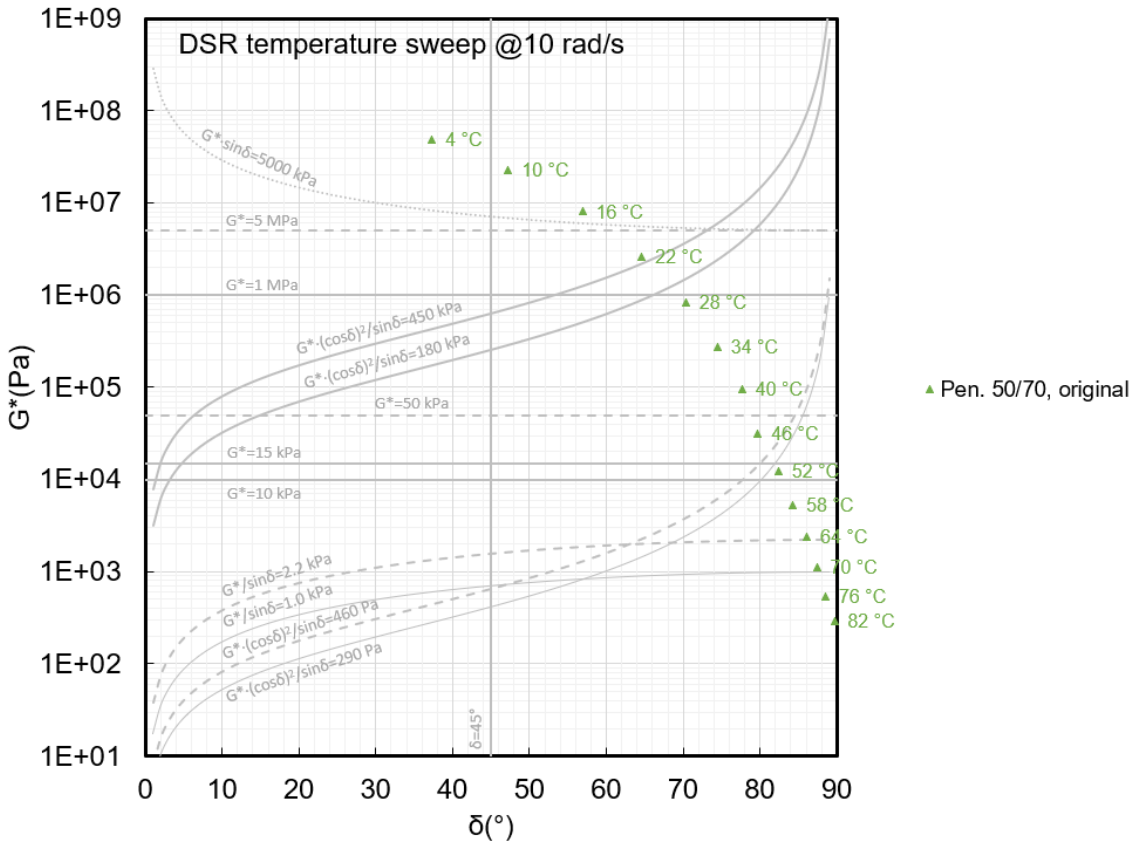

Figure 11. Temperature sweep results of Pen. 50/70 original binder in Black space.

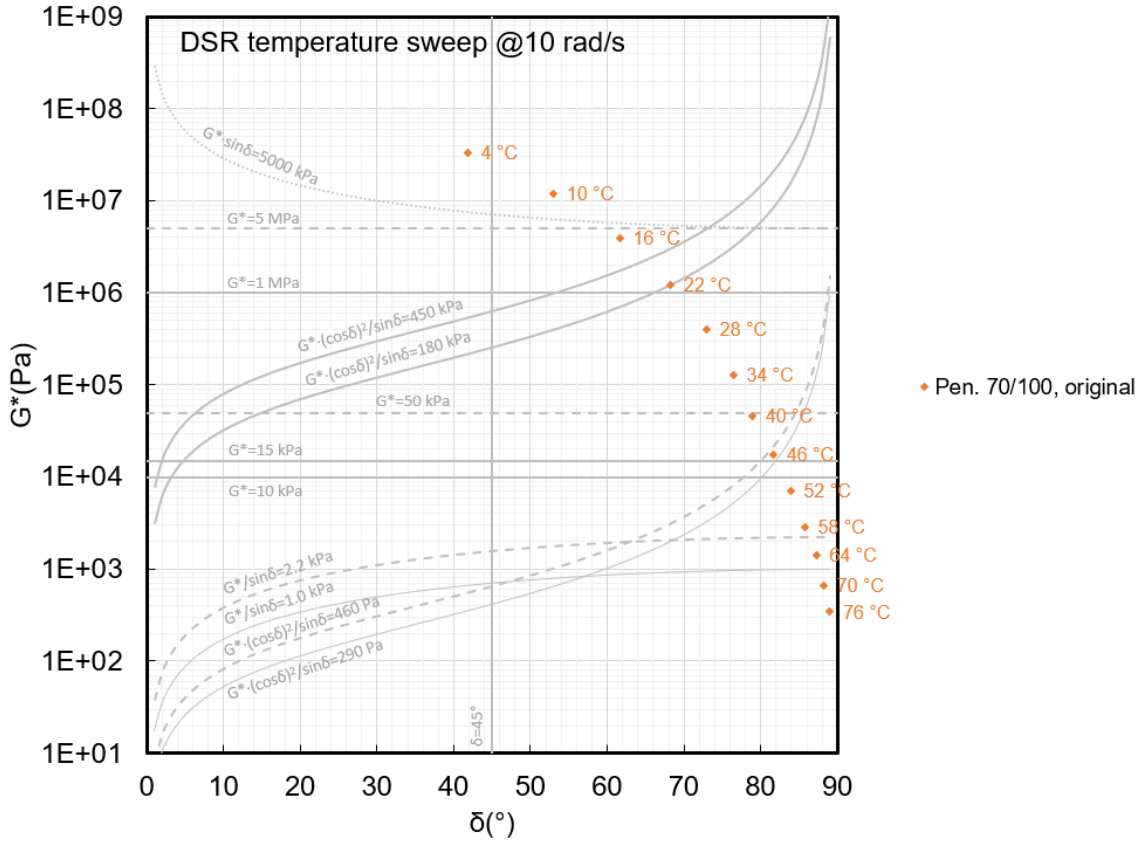

Figure 12. Temperature sweep results of Pen. 70/100 original binder in Black space.

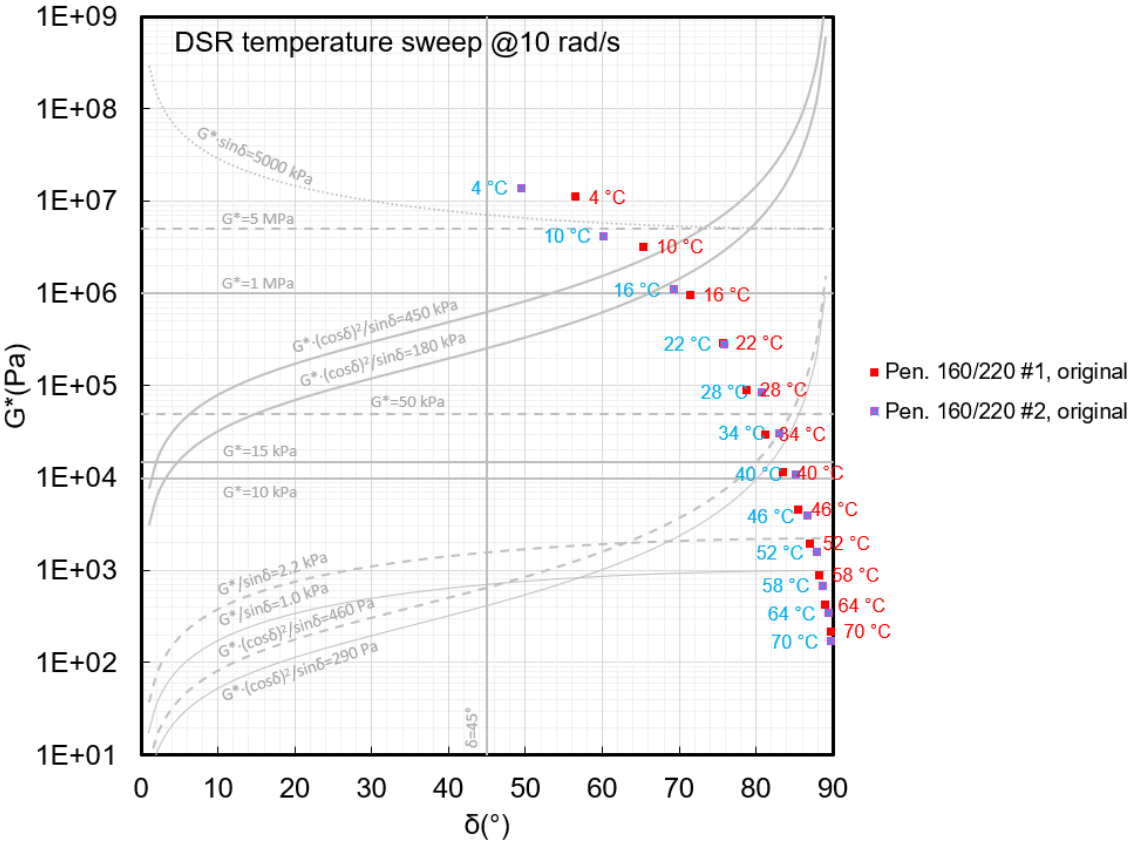

Figure 13. Temperature sweep results of Pen. 160/220 (#1 and #2) original binders in Black space.

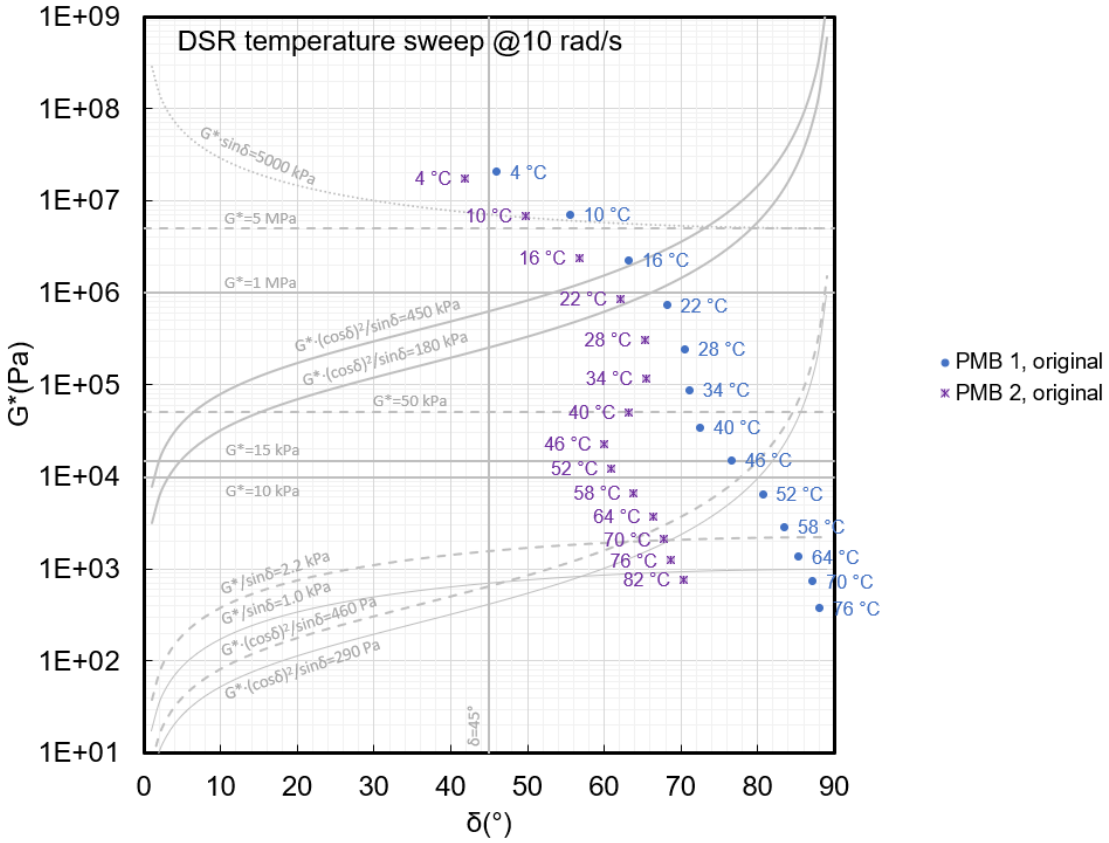

Figure 14. Temperature sweep results of PMB 1 and PMB 2 original binders in Black space.

Figure 13 indicates the difference between binders Pen. 160/220 #1 and Pen. 160/220 #2. At lower temperatures, especially 4 °C, Pen. 160/220 #2 shows slightly higher G* but much lower δ than Pen. 160/220 #1. Figure 14 suggests the influence of polymer content in PMBs. Comparing with PMB 1, the increased polymer content in PMB 2 led to increased G* and decreased δ, especially at higher temperatures. PMB 1 passes the G*/sinδ=1.0 kPa criterion of PG grading at 64 °C, while PMB 2 passes the same criterion at 76 °C.

For precise quantitative evaluations, Equation 6 was used to determine the iso-modulus temperatures of the studied binders by interpolation.

$$T_{G*=Y} = \frac{T_1 - T_2}{log\ (G_1^*) - log\ (G_2^*)}[log(Y) - log(G_2^*)] + T_2$$

Equation 6. Equation for determining the iso-modulus temperatures by interpolation.

In Equation 6, $T_{G*=Y}$ is the iso-modulus temperature with Y being the modulus level of interest. The levels of 5 MPa, 1 MPa, 50 kPa, 15 kPa and 10 kPa were investigated in this study. The subscript 1 represents a level higher than Y, while subscript 2 represents a level lower than Y. Equation 7 was used to determine the phase angle at the iso-modulus temperature.

$$\delta\ @T_{G*=Y} = \frac{\delta_{T1} - \delta_{T2}}{T_1 - T_2}[T_{G*=Y} - T_1] + \delta_{T1}$$

Equation 7. Equation for determining the phase angle at the iso-modulus temperature.

The calculation results of original binders are listed in Tables 7 and 8. It is indicated, in general, that stiffer binders have higher iso-modulus temperatures. PMBs have lower phase angle than unmodified bitumen at the iso-modulus temperatures. In addition to these iso-modulus parameters, two derivative parameters combining G* and δ were investigated in this study as well, i.e. the temperatures at which the PG grading parameter G*/sinδ and the Glover-Rowe parameter G*·(cosδ)²/sinδ reach certain

levels. For original binders, the G*/sinδ level of interest was 1.0 kPa according to the American PG grading specification, while the $G^*\cdot(\cos\delta)^2/\sin\delta$ level was selected at 290 Pa on the basis of a previous study (Zhu *et al.*, 2021). This level of $G^*\cdot(\cos\delta)^2/\sin\delta$ corresponds to the softening point of both unmodified bitumen and PMB. The same interpolation as Equation 6 (but replacing G* with the derivative parameters) was done to determine the additional parameters for all studied binders. The calculation results are listed in Table 9. The values based on G*/sinδ indicate the expected PG high-temperature grades of the binders, while those based on $G^*\cdot(\cos\delta)^2/\sin\delta$ suggest the estimated softening point.

Table 7. Iso-modulus temperatures of original binders.

Parameters	Pen. 50/70, original	Pen. 70/100, original	Pen. 160/220 #1, original	Pen. 160/220 #2, original	PMB 1, original	PMB 2, original
$T_{G^*=5\ MPa}$ (°C)	18.6	14.7	7.9	9.1	11.8	11.8
$T_{G^*=1\ MPa}$ (°C)	27.0	23.1	15.8	16.4	20.3	21.1
$T_{G^*=50\ kPa}$ (°C)	43.5	39.5	31.2	31.1	37.6	40.1
$T_{G^*=15\ kPa}$ (°C)	50.8	47.1	38.3	38.2	46.0	50.0
$T_{G^*=10\ kPa}$ (°C)	53.5	49.8	40.9	40.6	48.9	54.1

Table 8. Phase angle at the iso-modulus temperature of original binders.

Parameters	Pen. 50/70, original	Pen. 70/100, original	Pen. 160/220 #1, original	Pen. 160/220 #2, original	PMB 1, original	PMB 2, original
$\delta\ @T_{G^*=5\ MPa}$ (°)	60.2	59.8	62.1	58.5	57.9	51.8
$\delta\ @T_{G^*=1\ MPa}$ (°)	69.5	69.1	71.2	69.7	66.8	61.3
$\delta\ @T_{G^*=50\ kPa}$ (°)	78.9	78.7	80.1	81.9	71.9	63.1
$\delta\ @T_{G^*=15\ kPa}$ (°)	81.9	82.1	82.9	84.5	76.6	60.6
$\delta\ @T_{G^*=10\ kPa}$ (°)	82.9	83.1	83.8	85.3	78.6	61.9

Table 9. Additional derivative parameters combining G and δ of original binders.*

Parameters	Pen. 50/70, original	Pen. 70/100, original	Pen. 160/220 #1, original	Pen. 160/220 #2, original	PMB 1, original	PMB 2, original
T @G*/sinδ=1.0 kPa (°C)	70.9	66.7	57.1	55.2	67.1	79.5
T @$G^*\cdot(\cos\delta)^2/\sin\delta$ =290 Pa (°C)	50.9	47.0	37.4	35.6	50.0	71.1

4.2.1.2. RTFOT-aged binders

The same analyses as described in the last section were done for the RTFOT-aged binders. Figures 15-18 present the temperature sweep results of the RTFOT-aged binders in the Black space. If comparing these results with those of the original binders (Figures 11-14), a stiffening effect can be observed due to the short-term ageing, i.e., increased G* after RTFOT. This led to increased iso-modulus temperatures at all the investigated G* levels.

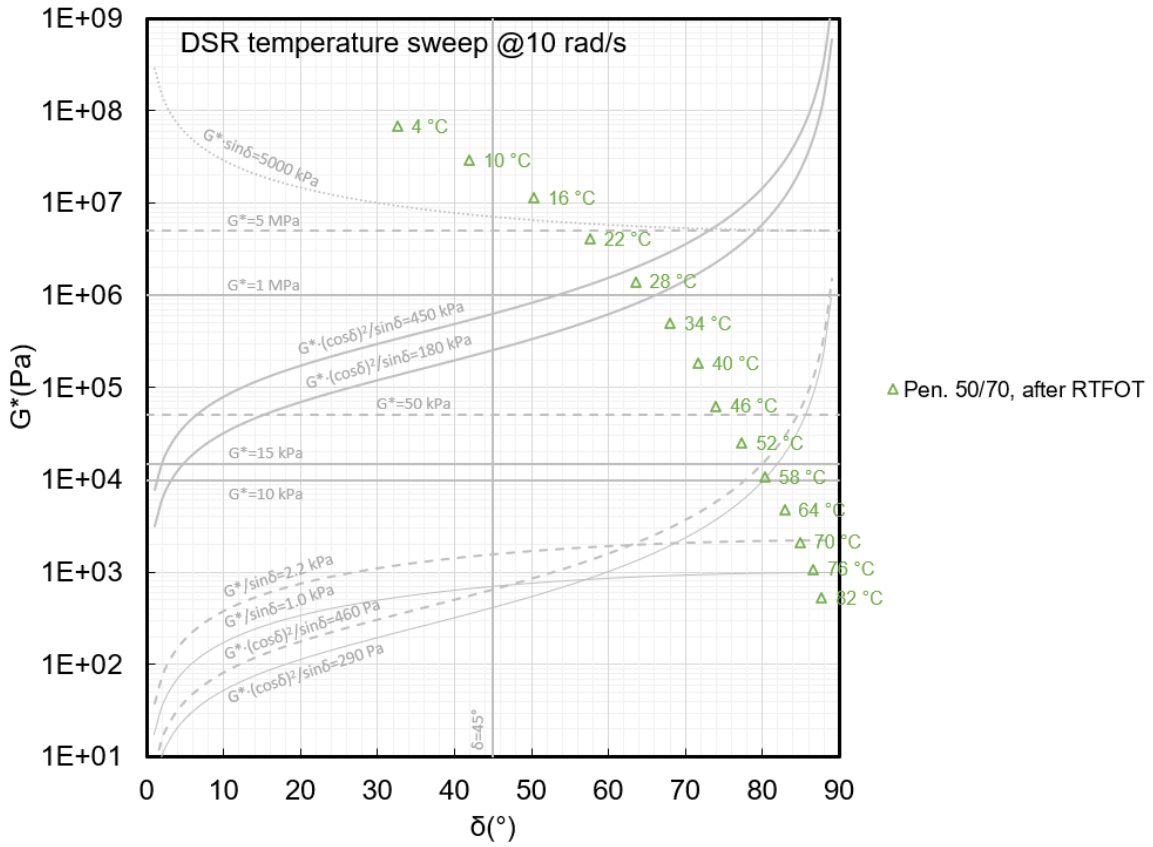

Figure 15. Temperature sweep results of Pen. 50/70 RTFOT-aged binder in Black space.

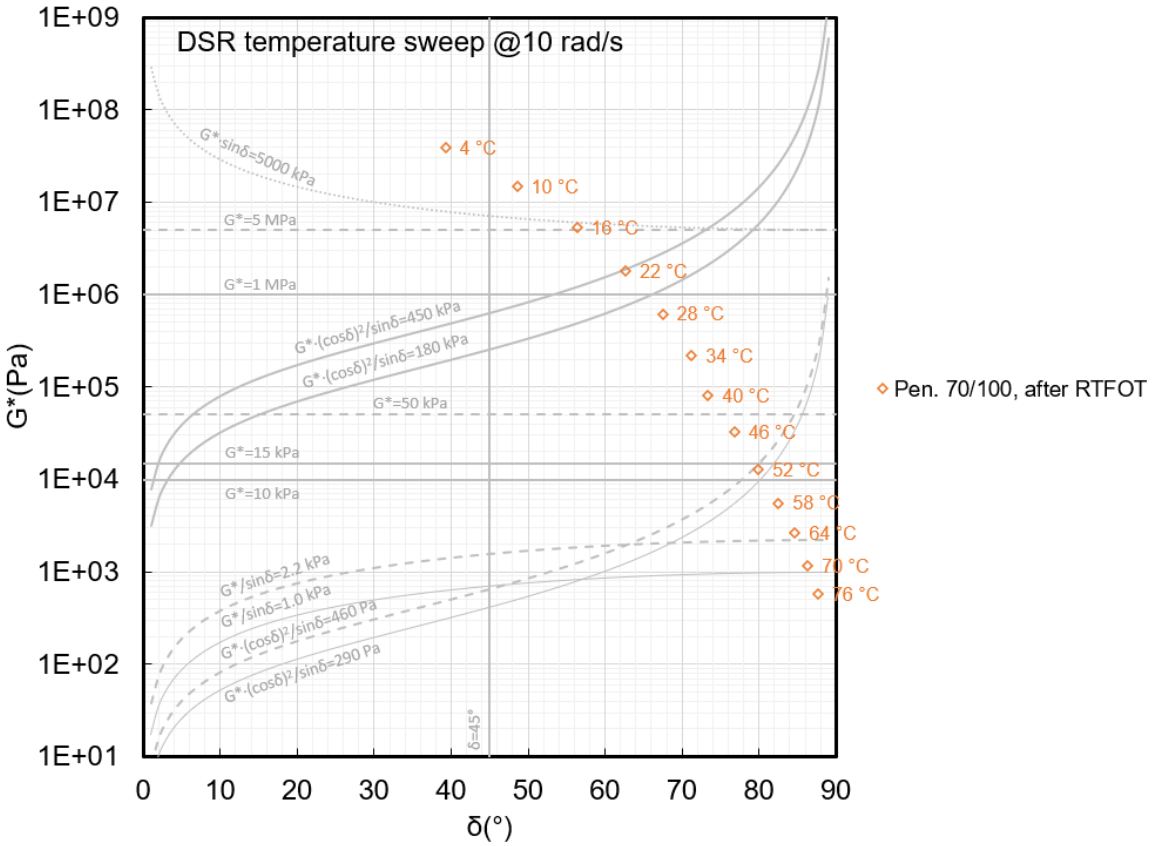

Figure 16. Temperature sweep results of Pen. 70/100 RTFOT-aged binder in Black space.

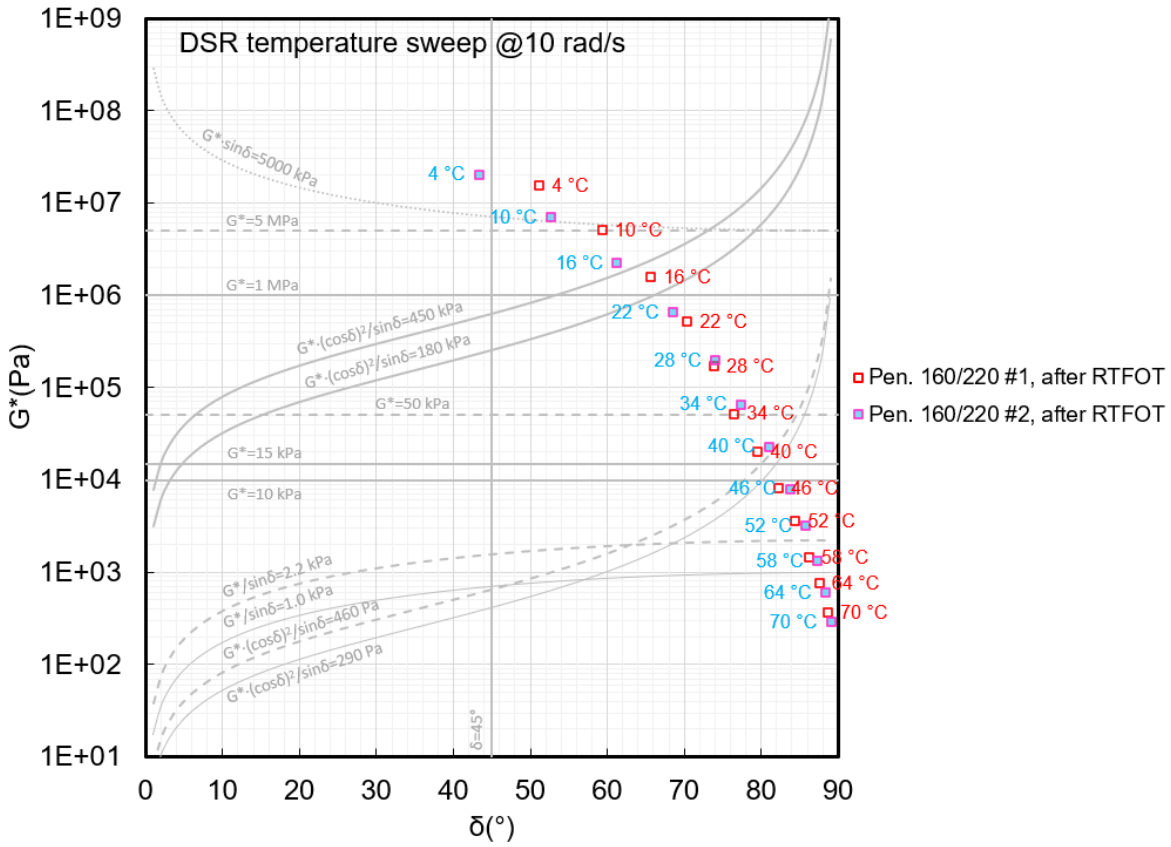

Figure 17. Temperature sweep results of Pen. 160/220 (#1 and #2) RTFOT-aged binders in Black space.

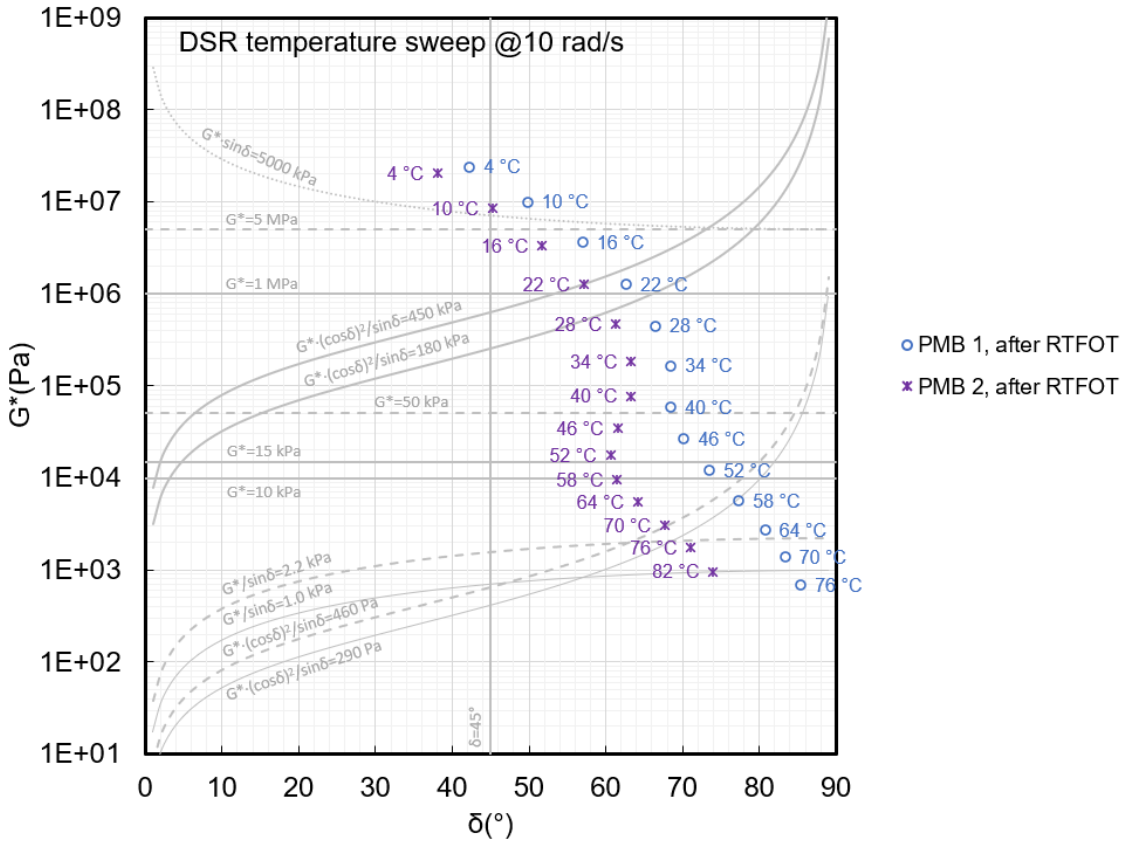

Figure 18. Temperature sweep results of PMB 1 and PMB 2 RTFOT-aged binders in Black space.

The quantitative analyses by Equation 6 confirmed the increase of iso-modulus temperatures after RTFOT, as results show in Table 10. Meanwhile, the calculation by Equation 7 (results listed in Table 11) suggested a decrease of phase angle at the iso-modulus temperature after RTFOT. Furthermore, the investigation of the two additional derivative parameters, namely $G^*/\sin\delta$ and $G^*\cdot(\cos\delta)^2/\sin\delta$, was done for RTFOT-aged binders at different levels from those for original binders. For RTFOT-aged binders, the $G^*/\sin\delta$ level of interest was 2.2 kPa regarding the PG system, while the previous study (Zhu *et al.*, 2021) proposed the $G^*\cdot(\cos\delta)^2/\sin\delta$ level of 460 Pa for corresponding to the softening point after RTFOT. The calculation results are listed in Table 12. All these binder parameters after RTFOT will be included and investigated in the planned correlation analysis later in this report.

Table 10. Iso-modulus temperatures of RTFOT-aged binders.

Parameters	Pen. 50/70, after RTFOT	Pen. 70/100, after RTFOT	Pen. 160/220 #1, after RTFOT	Pen. 160/220 #2, after RTFOT	PMB 1, after RTFOT	PMB 2, after RTFOT
$T_{G^*=5\ MPa}$ (°C)	20.8	16.3	10.2	11.9	14.1	13.4
$T_{G^*=1\ MPa}$ (°C)	29.9	25.3	18.6	20.0	23.3	23.4
$T_{G^*=50\ kPa}$ (°C)	47.5	43.2	34.4	35.7	41.2	43.3
$T_{G^*=15\ kPa}$ (°C)	55.6	51.0	42.0	42.5	50.3	53.6
$T_{G^*=10\ kPa}$ (°C)	58.5	53.8	44.7	44.8	53.4	57.6

Table 11. Phase angle at the iso-modulus temperature of RTFOT-aged binders.

Parameters	Pen. 50/70, after RTFOT	Pen. 70/100, after RTFOT	Pen. 160/220 #1, after RTFOT	Pen. 160/220 #2, after RTFOT	PMB 1, after RTFOT	PMB 2, after RTFOT
$\delta\ @T_{G^*=5\ MPa}$ (°)	56.1	56.7	59.4	55.2	54.7	48.9
$\delta\ @T_{G^*=1\ MPa}$ (°)	65.0	65.3	67.6	66.0	63.5	58.1
$\delta\ @T_{G^*=50\ kPa}$ (°)	74.8	75.2	76.6	78.3	68.8	62.3
$\delta\ @T_{G^*=15\ kPa}$ (°)	79.2	79.4	80.3	82.0	72.6	60.9
$\delta\ @T_{G^*=10\ kPa}$ (°)	80.5	80.7	81.6	83.1	74.4	61.4

Table 12. Additional derivative parameters combining G and δ of RTFOT-aged binders.*

Parameters	Pen. 50/70, after RTFOT	Pen. 70/100, after RTFOT	Pen. 160/220 #1, after RTFOT	Pen. 160/220 #2, after RTFOT	PMB 1, after RTFOT	PMB 2, after RTFOT
T @G*/sinδ=2.2 kPa (°C)	69.8	65.3	55.4	54.6	66.0	74.2
T @G*·(cosδ)²/sinδ =460 Pa (°C)	56.2	51.4	41.6	40.9	55.7	70.2

4.2.2. Frequency sweep

The frequency sweep at various temperatures enables the construction of master curves for binders. When master curves of asphalt mixtures and their binders are constructed at the same reference temperature, it is possible to compare them in pairs of asphalt mixture and binder. This may help to identify the potentially related linear viscoelastic parameters of bitumen to asphalt mixture properties. In addition, the frequency sweep results at an individual temperature allow the analysis of zero/low

shear viscosity, which is particularly relevant for this study regarding the bitumen's correlation with the asphalt mixture viscosity used by the PEDRO model.

4.2.2.1. Master curves of bituminous binders

Similar as the master curves of asphalt mixtures, the binder master curves were also constructed by two steps: shifting the frequency sweep results first, and then fitting the shifted data with certain model. The Arrhenius equation (Equation 1) was used for shifting the binder data. The same reference temperature was chosen for the binders as for asphalt mixtures, i.e., 10 °C.

As for the fitting model, the intention was to use the same type of model for the binders as for asphalt mixtures. Equation 8 was thus derived from Equation 2 for fitting the binder G* data.

$$G^* = \frac{\alpha}{1 + e^{\beta - \gamma \log(f_r)}}$$

Equation 8. Fitting equation of the sigmoidal model for G master curve of binder.*

In Equation 8, α, β and γ are the fitting parameters. To fit the phase angle δ of unmodified binders, Equation 9 could be derived from Equation 3.

$$\delta = \frac{90}{1 + e^{\left(\frac{\log(f_r) - a}{g}\right)}}$$

Equation 9. Fitting equation of the compound unimodal-sigmoidal model for phase angle master curve of unmodified binder.

In Equation 9, a and g are the fitting parameters. This equation, however, is not able to fit the phase angle δ of PMBs, due to the limitation of its mathematical form. None of other simple models is actually able to fit the δ data of both unmodified bitumen and PMB (Asgharzadeh et al., 2015). Thus, this study employs different models for fitting the δ data of unmodified binders and PMBs. For PMBs, the double-logistic model (Asgharzadeh *et al.*, 2013) was used, as Equation 10.

$$\delta = \delta_P - \delta_P \cdot H(f_r - f_P) \cdot \left\{1 - e^{-\left[S_R \cdot \log\left(\frac{f_r}{f_P}\right)\right]^2}\right\} + \delta_L \cdot H(f_P - f_r) \cdot \left\{1 - e^{-\left[S_L \cdot \log\left(\frac{f_P}{f_r}\right)\right]^2}\right\}$$

Equation 10. Fitting equation of the double-logistic model for phase angle master curve of PMB.

In Equation 10, δ_P, f_P, S_R, δ_L and S_L are the fitting parameters; and H is the Heaviside step function. For each binder, both the original and after RTFOT, a one-step optimisation was done to obtain the values of all fitting parameters as well as the activation energy constant K_a for determining the shift factor. The obtained K_a values are listed in Table 13, while the values of other parameters for fitting bitumen master curves are presented in the Appendix 3 of this report. One example of the bitumen master curve fitting is presented in Figure 19, for the PMB 1 original binder. It indicates a good fitting for both the G* and phase angle δ. The other binders had similar good fitting as well.

Table 13. Constant values for determining shift factors of bitumen master curves.

Binder type	**Pen. 50/70**	**Pen. 70/100**	**Pen. 160/220 #1**	**Pen. 160/220 #2**	**PMB 1**	**PMB 2**
K_a, original binder (K)	8751	8591	7983	8585	8404	8700
K_a, after RTFOT (K)	8836	8873	8253	8974	8663	8624

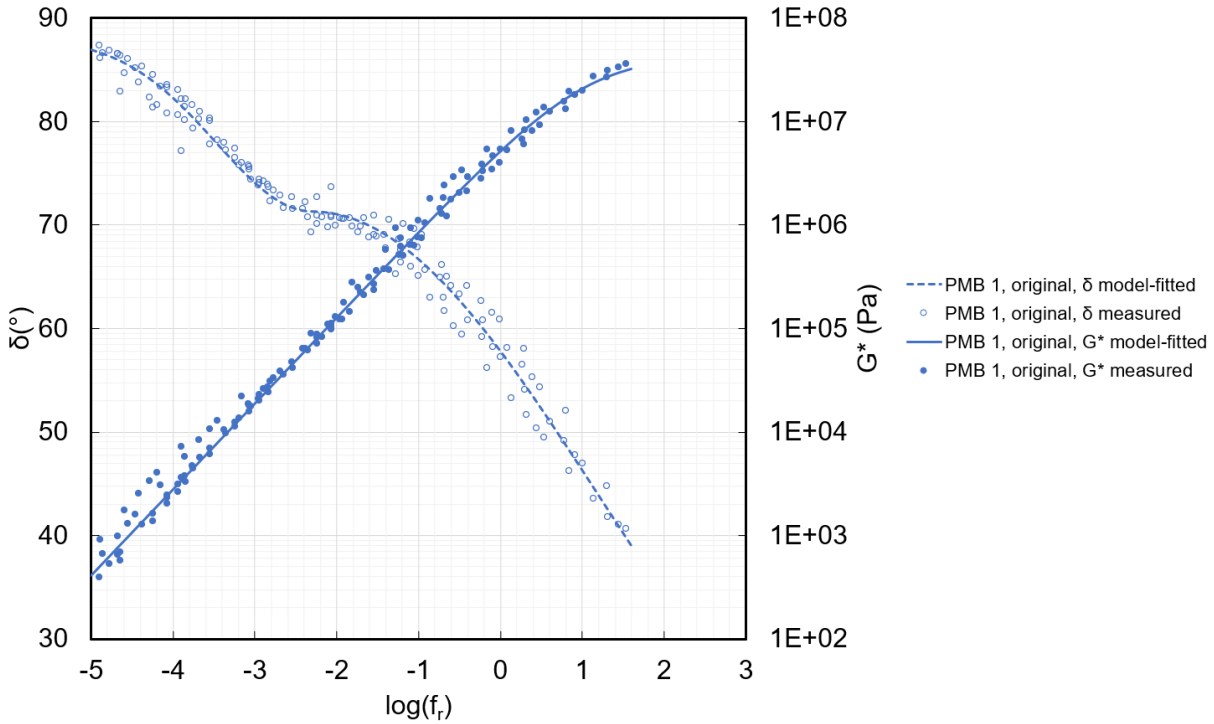

Figure 19. Master curve fitting of the PMB 1 original binder, T_{ref}=10 °C.

All the model-fitted master curves of original binders are shown in Figure 20. The results suggest that the master curves of unmodified binders are firmly in the order of their penetration grades. The bitumen Pen. 160/220 #2 shows slightly higher G* than Pen. 160/220 #1. At higher frequencies, Pen. 160/220 #2 shows lower δ than Pen. 160/220 #1. The modification with SBS copolymer significantly increases the G* (reaching harder grades despite the 100/150 base bitumen) at lower frequencies while decreases the δ. At higher frequencies, the base bitumen has more influence on the master curves of PMBs.

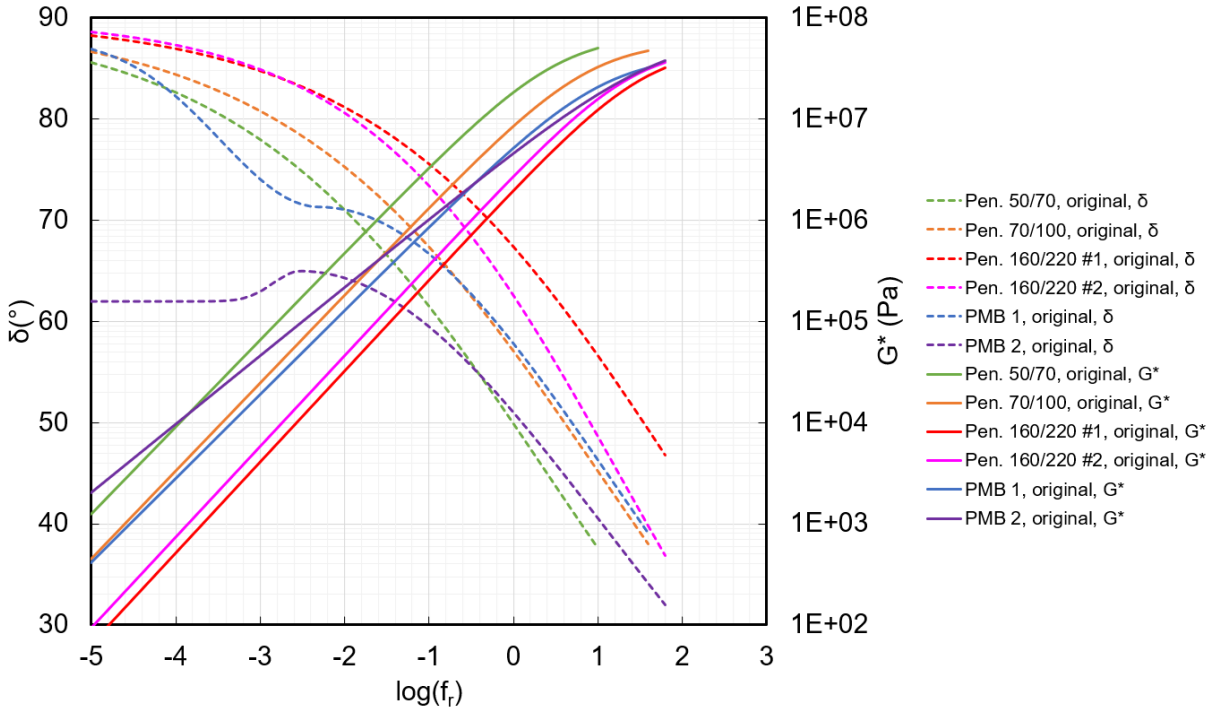

Figure 20. Model-fitted master curves of the original binders, T_{ref}=10 °C.

Figure 21 shows the model-fitted master curves of the RTFOT-aged binders. If comparing between binders in Figure 21, similar conclusions can be drawn as the comparison between original binders (Figure 20). If comparing the results before and after RTFOT, however, a stiffening effect can be observed due to the short-term ageing, namely increased G* and decreased δ after RTFOT. Furthermore, it is worth noting here that these binder master curves after RTFOT will be compared with the master curves of asphalt mixtures later in this report.

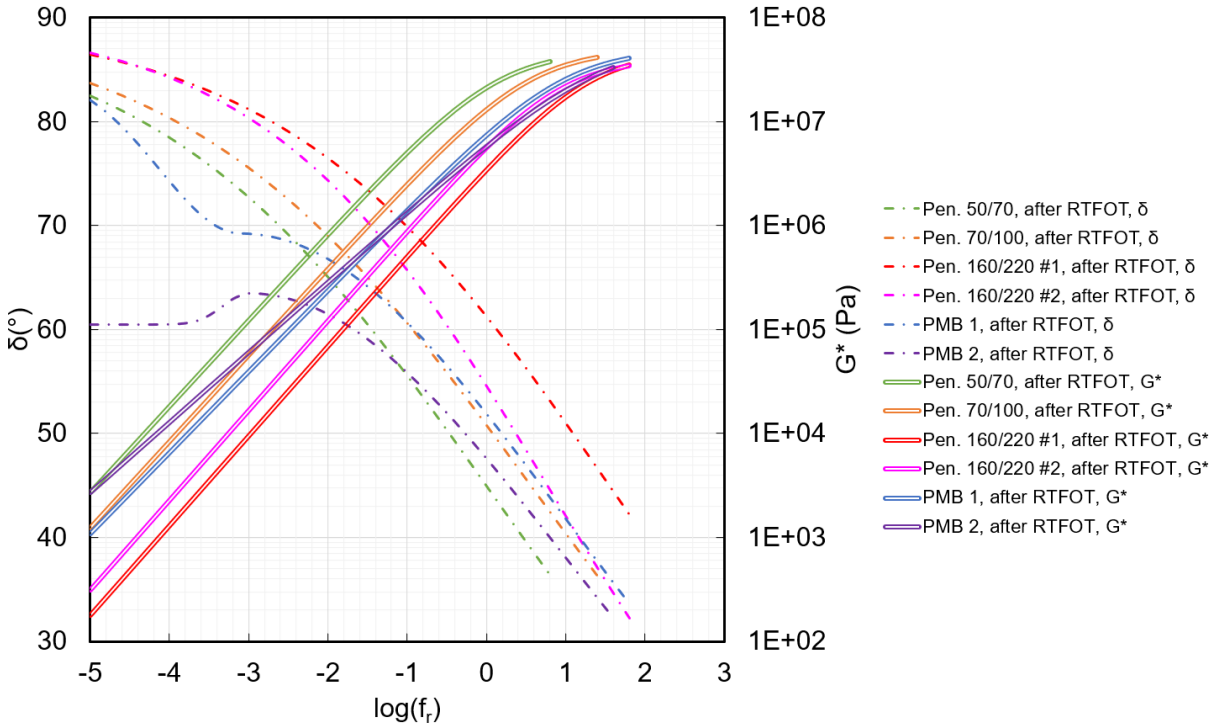

Figure 21. Model-fitted master curves of the RTFOT-aged binders, T_{ref}=10 °C.

4.2.2.2. Low shear viscosity

As the PEDRO model employs the concept of viscosity for asphalt mixtures, it is particularly relevant for this study to investigate the similar concept of viscosity for binders and see if there is a correlation existing between them. For this, the first idea was to analyse the zero-shear viscosity (ZSV) of binders. This is because the ZSV has been studied as a potential performance indicator of bitumen for permanent deformation (Sybilski, 1994, 1996, 1997), while the PEDRO model uses the asphalt mixture viscosity for predicting the permanent deformation in asphalt pavements. They target on the same type of pavement performance.

However, the practical measurement method of ZSV works mostly for unmodified binders only. For certain PMB (and some unmodified bitumen at lower temperatures), the measurement by extrapolation can lead to unreliable ZSV results. This is because the extrapolated curve may not present a plateau (namely not reaching the steady state) at very low frequencies but can be curvilinear in many cases. Thus, a common practice for analysing PMB is to determine the LSV (low shear viscosity) at a relatively low frequency instead, e.g., at 0.001 Hz (approximately 0.006 rad/s) in some previous studies (De Visscher and Vanelstraete, 2004; Morea *et al.*, 2010, 2011).

This study analyses both unmodified bitumen and PMB, so the LSV at 0.001 Hz was selected as the parameter for evaluating all the binders within the same framework and also for the further correlation analysis with asphalt mixture properties. The LSV values of all binders, both before and after RTFOT, were determined at two temperatures: (1) 60 °C, which is a common temperature for the evaluation of high-temperature properties; and (2) 10 °C, which is the reference temperature chosen for the construction of master curves of both asphalt mixtures and binders in this study.

The simplified Cross model (Sybilski, 1996; Zhang et al., 2018), as Equation 11, was used to fit the frequency sweep results and extrapolate the data to 0.001 Hz.

$$\eta^* = \frac{\eta_0^*}{1 + (K\omega)^m}$$

Equation 11. The simplified Cross model for fitting the frequency sweep results.

In Equation 11, η^* is the complex viscosity; η_0^* is the extrapolated ZSV; ω is the angular frequency in rad/s; K and m are model constants. Figures 22 and 23 respectively show the data fitting of original binders and RTFOT-aged binders, both at 60 °C. It is indicated that, at 60 °C and 0.001 Hz, all the unmodified binders and even PMB1 reach or get very close to the steady state, but not PMB2. It is still so after RTFOT. The determined LSV values at 60 °C are listed in Table 14. The results suggest that the LSV values of unmodified binders are basically in the order of their penetration grades. The bitumen Pen. 160/220 #2 shows slightly lower LSV than Pen. 160/220 #1 at 60 °C, possibly due to the different crude oil sources and production processes. Despite the base bitumen of penetration grade 100/150, the modification with SBS copolymer significantly increases the LSV at 60 °C and 0.001 Hz, especially for PMB 2 that shows the highest LSV value.

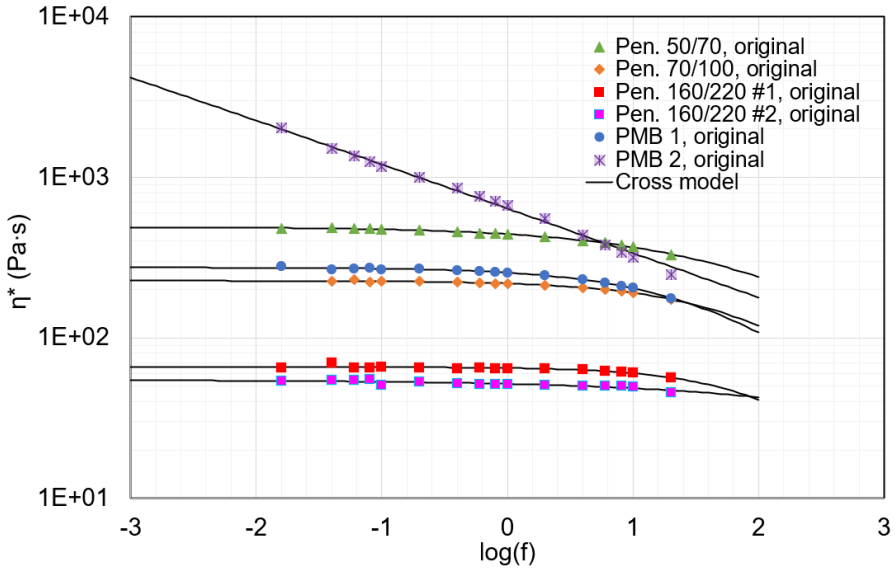

Figure 22. LSV determination of original binders at 60 °C.

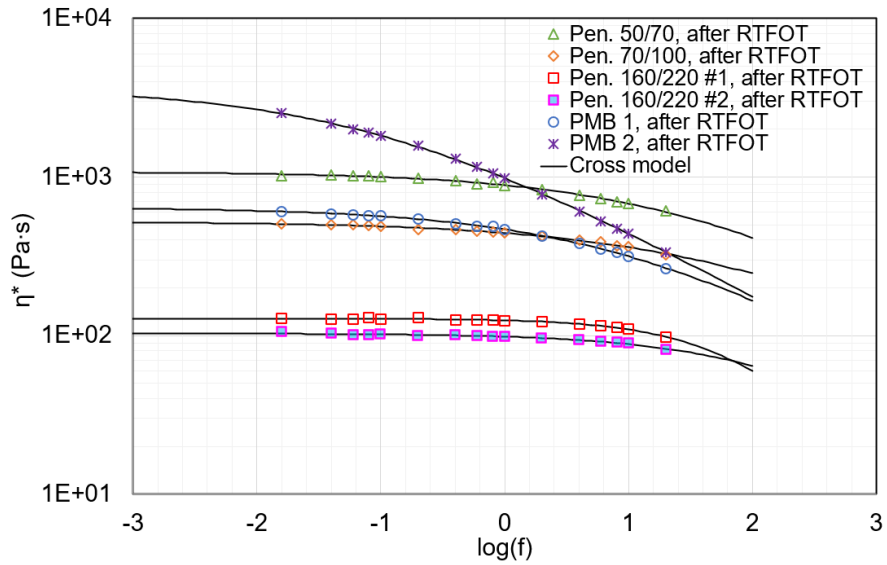

Figure 23. LSV determination of RTFOT-aged binders at 60 °C.

Table 14. Determined LSV values at 60 °C and 0.001 Hz.

Low shear viscosity (LSV) at 60 °C and 0.001 Hz	Pen. 50/70	Pen. 70/100	Pen. 160/220 #1	Pen. 160/220 #2	PMB 1	PMB 2
LSV, original binder (Pa·s)	488.7	226.8	65.8	54.3	274.2	4180.3†
LSV, after RTFOT (Pa·s)	1068.0	517.0	127.9	103.1	630.9	3218.9

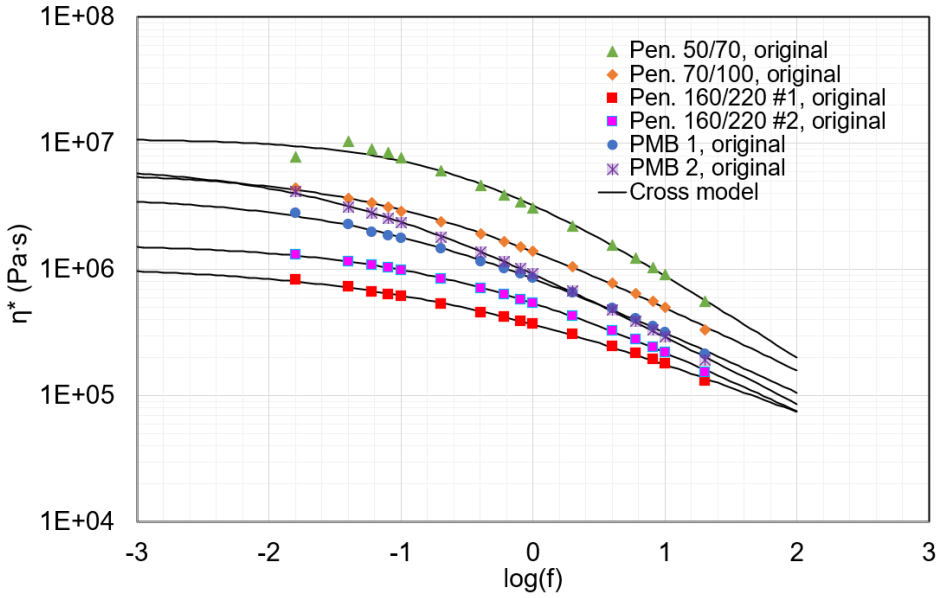

Figure 24. LSV determination of original binders at 10 °C.

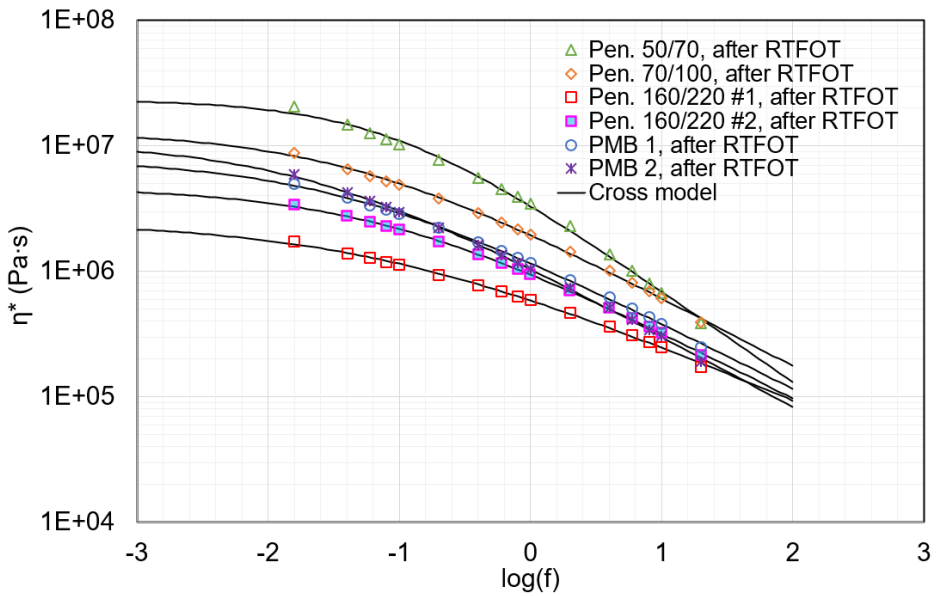

Figure 25. LSV determination of RTFOT-aged binders at 10 °C.

Figures 24 and 25 present the data fitting of original and RTFOT-aged binders at 10 °C. The results show that no binder reaches the typical steady state at 10 °C and 0.001 Hz. The determined LSV values at 10 °C are listed in Table 15. It is indicated again that the LSV values of unmodified binders

† Far from the steady state.

are in the order of their penetration grades. But the bitumen Pen. 160/220 #2 shows higher LSV than Pen. 160/220 #1 at 10 °C. Comparing with the results of PMBs at 60 °C, the results in Table 15 suggest that the base bitumen of PMB has more influence on the LSV at 10 °C. This led to a limited increase of LSV at 10 °C after the modification with SBS copolymer, while the Pen. 50/70 bitumen showing the highest LSV value among all the studied binders.

Table 15. Determined LSV values at 10 °C and 0.001 Hz.

Low shear viscosity (LSV) at 10 °C and 0.001 Hz	Pen. 50/70	Pen. 70/100	Pen. 160/220 #1	Pen. 160/220 #2	PMB 1	PMB 2
LSV, original binder (kPa·s)	10654.6	5415.4	966.6	1506.7	3454.7	5787.9
LSV, after RTFOT (kPa·s)	22534.4	11674.6	2161.0	4265.1	6923.8	9009.9

If comparing the LSV results between the two temperatures, a significant difference can be observed between the behaviour of PMB and unmodified bitumen in terms of temperature sensitivity. At higher temperatures, PMBs tend to show preferable properties. At lower temperatures, however, the superiority of PMBs tends to be smaller, while the base bitumen of PMB tends to have more influence on the properties. This agrees with the master curve analysis in the previous section, which suggested a difference in the binder behaviour between the high-frequency (equivalently low-temperature) and low-frequency (equivalently high-temperature) ranges. The LSV results at both temperatures will be included and investigated in the planned correlation analysis later in this report.

4.3. Multiple stress creep and recovery

This section analyses the MSCR test results of bitumen. The MSCR test is a relatively new but increasingly popular method for evaluating the high-temperature properties of bituminous binders. The tests were conducted with two stress levels (100 Pa and then immediately 3200 Pa) according to the standard EN 16659. The test temperature was chosen at 60 °C for all binders in this study. Both the original and RTFOT-aged binders were tested.

4.3.1. Original binders

The MSCR results of original binders are presented in Figure 26. The related parameters were calculated from these results according to the standard EN 16659, including the average values of the total strain at the end of the creep period $\varepsilon_1 100$ and $\varepsilon_1 3200$ (100 and 3200 representing the stress levels, the same below), percent recovery %R100 and %R3200, percent difference in recovery between stress levels R_{diff}, non-recoverable creep compliance $J_{nr}100$ and $J_{nr}3200$, and the percent difference in non-recoverable creep compliance between stress levels $J_{nr\text{-}diff}$. The calculation results were listed in Table 16.

The results indicate that, at 60 °C, the total strain ($\varepsilon_1 100$ and $\varepsilon_1 3200$) and non-recoverable creep compliance ($J_{nr}100$ and $J_{nr}3200$) values of unmodified binders are basically in the order of their penetration grades. The bitumen Pen. 160/220 #2 shows higher total strain and non-recoverable creep compliance values than Pen. 160/220 #1 at 60 °C. Despite the base bitumen of penetration grade 100/150, the modification with SBS copolymer significantly decreases the total strain and non-recoverable creep compliance values at 60 °C, especially for PMB 2 that shows the lowest values among all binders. These conclusions are in very good agreement with those from the LSV analysis at 60 °C.

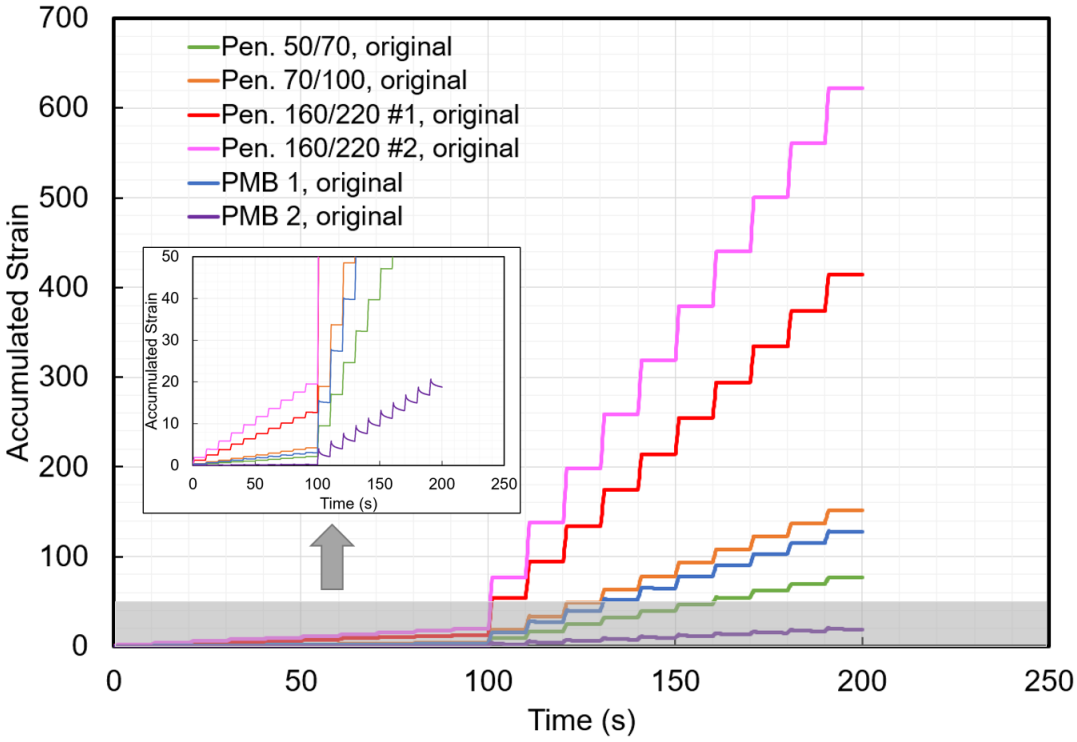

Figure 26. MSCR test results of original binders at 60 °C.

Table 16. Calculated MSCR parameters of original binders at 60 °C.

MSCR parameters	Pen. 50/70, original	Pen. 70/100, original	Pen. 160/220 #1, original	Pen. 160/220 #2, original	PMB 1, original	PMB 2, original
$\varepsilon_1$100	0.221	0.431	1.28	1.96	0.360	0.105
$\varepsilon_1$3200	7.54	14.8	39.9	59.6	12.9	3.78
%R100	3.6%	1.5%	0.3%	0.1%	14.8%	78.6%
%R3200	1.2%	0.4%	-0.6%	-1.0%	2.8%	50.9%
R_{diff}	66.3%	72.4%	314.5%	939.2%	80.8%	35.2%
J_{nr}100 (kPa^{-1})	2.13	4.25	12.7	19.5	3.07	0.226
J_{nr}3200 (kPa^{-1})	2.33	4.60	12.5	18.8	3.91	0.580
$J_{nr\text{-}diff}$	9.0%	8.2%	-1.4%	-3.7%	27.4%	157.2%

It was noted, in the MSCR results at 60 °C, that the original binders of penetration grade 160/220 (both #1 and #2) showed negative values for the percent recovery at 3200 Pa (%R3200). A probe into the MSCR test result, as Figure 27 probing for Pen. 160/220 #1, revealed that the shear strain did not stop increasing immediately after the creep stress was uploaded. This is a phenomenon observed by other researchers as well (Hagner, 2018; Soenen, 2018; Liu *et al.*, 2020). Although there is still a discussion on the possible reasons for this, it is likely that the inertial effect continued driving these soft binders (low viscosity at such a high temperature) a bit forward even without the applied stress. Thus, the negative recovery values of soft binders at high temperatures basically mean zero recovery.

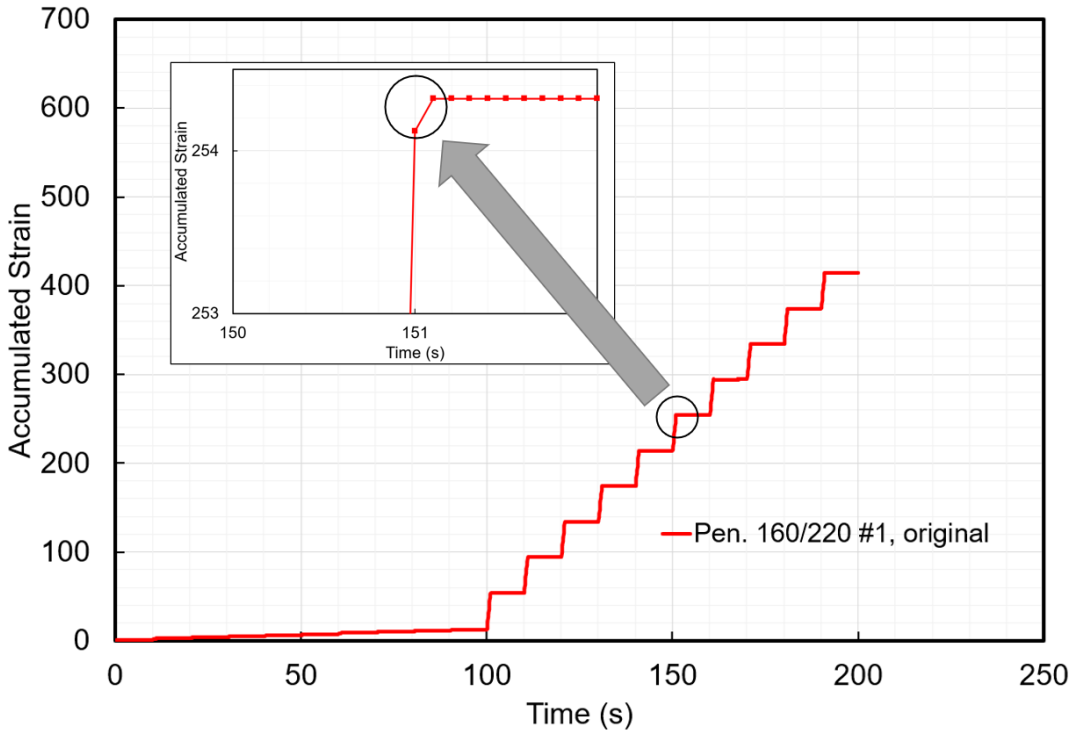

Figure 27. A probe into the MSCR test result of Pen. 160/220 #1 original binder.

4.3.2. RTFOT-aged binders

The same MSCR tests and analyses were done for the RTFOT-aged binders. Figure 28 presents the test results of RTFOT-aged binders at 60 °C, while Table 17 lists the calculated MSCR parameters. If comparing between RTFOT-binders, similar conclusions can be drawn as the comparison between original binders (the previous section). If comparing the results before and after RTFOT, however, a stiffening effect can be observed due to the short-term ageing, namely decreased total strain ($\varepsilon_1$100 and $\varepsilon_1$3200) and non-recoverable creep compliance (J_{nr}100 and J_{nr}3200) values after RTFOT. Additionally, for all the unmodified binders and even PMB1, the percent recovery values (%R100 and %R3200) increased after RTFOT. This resulted in a non-negative %R3200 value (actually 0.0%) for the Pen. 160/220 #1 RTFOT-aged binder, but still a negative %R3200 for Pen. 160/220 #2. Furthermore, it was noted that the %R100 and %R3200 values of PMB2 decreased after RTFOT. This is most probably due to the damage of the polymer network in PMB2 during the short-term ageing.

The MSCR test leads to the calculation of several parameters as the result. Among them, the percent recovery (%R100 and %R3200) and non-recoverable creep compliance (J_{nr}100 and J_{nr}3200) are the most common ones used for binder evaluation. In the American specification AASHTO M 332, J_{nr}3200 after RTFOT has been employed as the basis for PG grading of binders. Thus, the J_{nr}3200 value after RTFOT is selected as a single result of the MSCR test in this study and will be investigated in the planned correlation analysis later in this report.

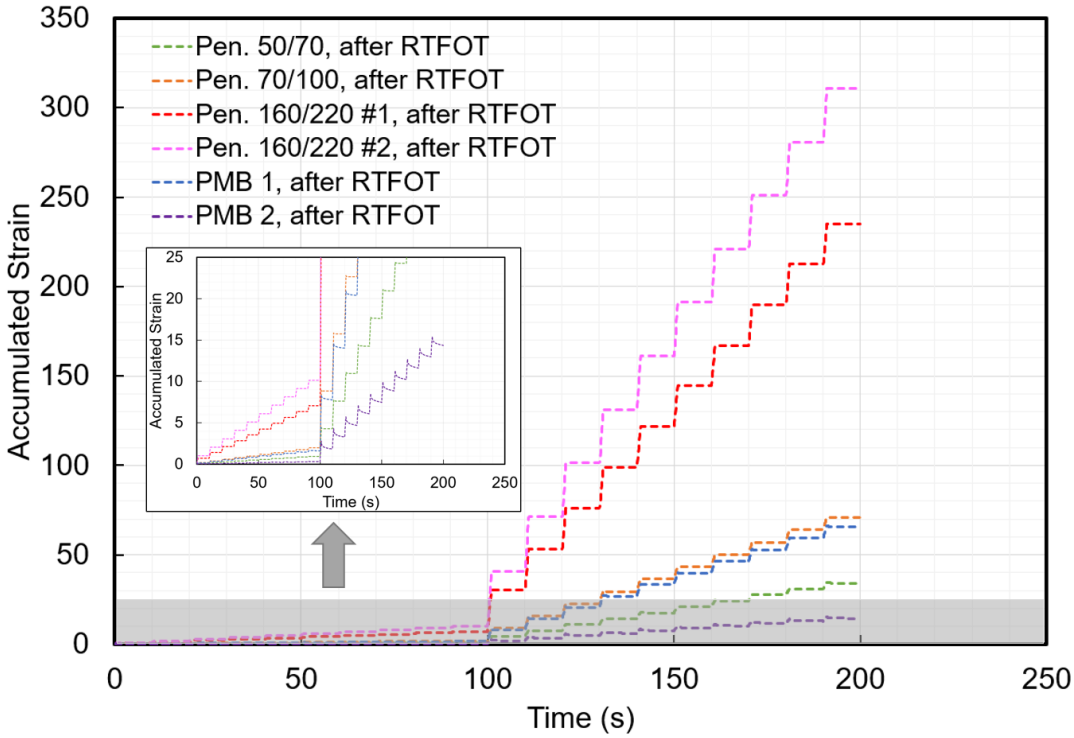

Figure 28. MSCR test results of RTFOT-aged binders at 60 °C.

Table 17. Calculated MSCR parameters of RTFOT-aged binders at 60 °C.

MSCR parameters	Pen. 50/70, after RTFOT	Pen. 70/100, after RTFOT	Pen. 160/220 #1, after RTFOT	Pen. 160/220 #2, after RTFOT	PMB 1, after RTFOT	PMB 2, after RTFOT
$\varepsilon_1$100	0.105	0.208	0.720	1.02	0.197	0.0717
$\varepsilon_1$3200	3.50	7.02	22.8	29.9	6.90	2.48
%R100	9.5%	5.1%	1.7%	0.6%	17.7%	59.1%
%R3200	4.9%	1.8%	0.0%	-0.4%	7.0%	43.3%
R_{diff}	48.2%	64.6%	100.0%	163.8%	60.6%	26.7%
J_{nr}100 (kPa^{-1})	0.950	1.97	7.08	10.2	1.62	0.294
J_{nr}3200 (kPa^{-1})	1.04	2.15	7.13	9.39	2.01	0.439
$J_{nr\text{-}diff}$	9.5%	9.1%	0.7%	-7.5%	23.5%	49.7%

5. Correlation analysis between bitumen properties and asphalt mixture performance

Based on the test results presented in the previous chapters, this chapter analyses the correlation between bitumen properties and the shear resistance of asphalt mixtures. The master curves of asphalt mixtures and binders are firstly compared to get an indication of the potential correlations.

5.1. Master curve comparison between asphalt mixtures and binders

The master curves of asphalt mixtures and binders were constructed at the same reference temperature (10 °C) in this study. It is thus possible to directly compare them to get an indication of the potential correlations, i.e., what are the G* and δ levels of binder (after RTFOT) at the maximum phase angle of the asphalt mixture. One example of the comparison is presented in Figure 29, for the asphalt mixture Pen. 70/100 (6.0%) and its binder after RTFOT.

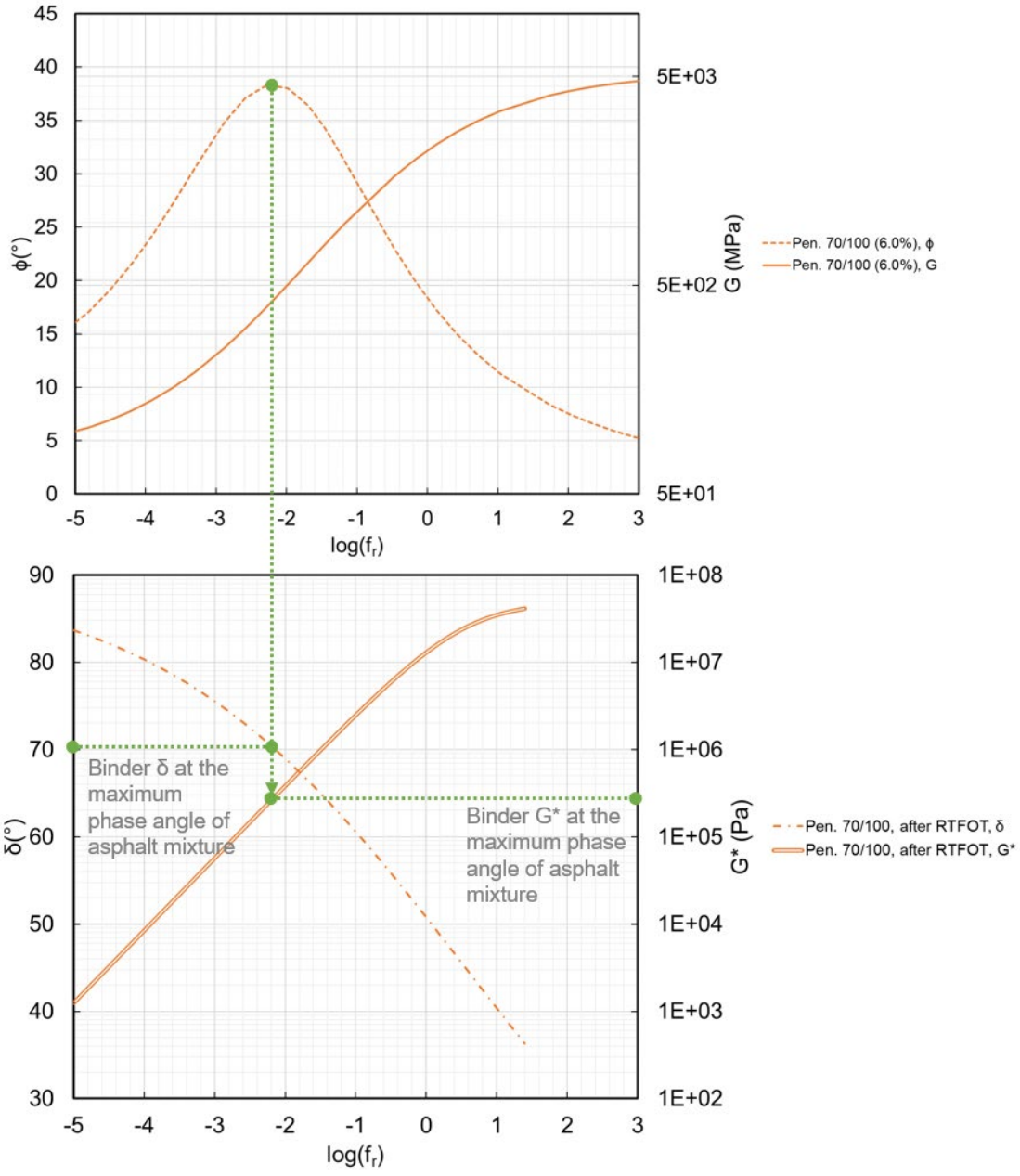

Figure 29. Master curve comparison between the asphalt mixture Pen. 70/100 (6.0%) and its binder after RTFOT, T_{ref}=10 °C.

The comparisons between other asphalt mixtures and their binders were done in the same way. These comparisons led to the determined G* and δ values of binders (after RTFOT) at the maximum phase angle of asphalt mixtures, as listed in Table 18. It is indicated that all the binder G* values at the maximum phase angle of asphalt mixtures were in the range of about 100-500 kPa, which is relatively narrow in the whole G* range (1 kPa to 10 MPa) that a bituminous binder can normally reach in the asphalt pavement. For asphalt mixtures with unmodified binders, the binder δ values at the maximum phase angle of asphalt mixtures were in the range of about 70-75°. For asphalt mixtures with PMBs, however, the binder δ values were lower. These determined values of binder G* and δ will be included as a part of the asphalt mixture parameters (because they are more associated with the asphalt mixture properties) in the correlation analysis and will be investigated to figure out if their levels are related to the properties of the used binders.

Table 18. Determined binder (after RTFOT) G and δ at the maximum phase angle of asphalt mixture.*

Binder type in the asphalt mixture (binder content)	Pen. 50/70 (6.2%)	Pen. 70/100 (6.0%)	Pen. 160/220 #1 (6.0%)	Pen. 160/220 #2 (5.6%)	PMB 1 (6.0%)	PMB 2 (6.2%)
Binder G* (kPa) at the maximum phase angle of asphalt mixture	175	268	437	134	204	166
Binder δ (°) at the maximum phase angle of asphalt mixture	71.5	70.3	70.4	74.0	64.7	56.8

5.2. Correlation to asphalt mixture properties at the maximum phase angle

This section analyses the correlation between bitumen properties and the shear resistance of asphalt mixtures. From the perspective of asphalt mixtures, the focus of analysis was placed on parameters at the maximum phase angle, including the results listed in Tables 4 and 18. These parameters allow a direct coupling with the PEDRO model. As for binders, their properties after RTFOT discussed in Chapter 4 were the main focus. In addition, the volumetric parameters listed in Table 2 were also included in the correlation analysis, because they play significant roles in determining the asphalt mixture properties as well. The analysis was conducted firstly for unmodified bitumen only, and then again for all binders including the unmodified bitumen and PMBs. This helps to figure out if different correlations exist depending on the binder type, because it is known that unmodified bitumen and PMB may behave very differently in asphalt mixtures.

The Pearson product-moment correlation coefficient, as defined by Equation 12, was employed to analyse the binder-mixture correlation.

$$r_{xy} = \frac{\sum_{i=1}^{n}(x_i - \bar{x})(y_i - \bar{y})}{\sqrt{\sum_{i=1}^{n}(x_i - \bar{x})^2 \sum_{i=1}^{n}(y_i - \bar{y})^2}}$$

Equation 12. Calculation of the Pearson product-moment correlation coefficient.

In Equation 12, r_{xy} is the Pearson product-moment correlation coefficient; x and y are the variables to be analysed for their correlation; and $\bar{x}$ and $\bar{y}$ are the mean values of the variables. This equation produces a correlation coefficient, ranging between +1 and -1, as the measure of the linear correlation between the two variables. A r_{xy} value of +1 represents a total positive linear correlation; 0 represents no linear correlation at all; and -1 represents a total negative linear correlation.

Each pair of the binder and asphalt mixture parameters were analysed for their correlation by Equation 12. However, it should be noted that this correlation coefficient measures only the linear correlation between two individual parameters. This is to say that, if an asphalt mixture parameter depends on multiple binder and/or volumetric parameters (which is probable for most asphalt mixture parameters)

and no parameter dominates the correlation, a moderate correlation coefficient around +0.5 or -0.5 can be obtained. Such a correlation coefficient does not lead to a simple quantitative relationship between the binder and mixture. Rather, the multi-factor modelling is needed to quantify the relationship. Thus, the analysis in this study focuses only on the very strong correlations (r_{xy} value greater than +0.85 or less than -0.85) and very weak correlations (r_{xy} value between +0.15 and -0.15). The boundaries were arbitrarily chosen, but their levels of significance will be evaluated with respect to the sample size.

Furthermore, the Pearson product-moment correlation coefficient measures only the linear correlation. Therefore, the analysis in this study considers the logarithm to the base 10 of the frequency- and viscosity-related variables, including the reduced frequency f_r, asphalt mixture viscosity η, and binder LSV. It is also usual to consider the logarithm of modulus for linear relationships. But the modulus variables (G for asphalt mixtures and G* for binders) in this study are both in relatively narrow ranges and do not vary very much. Thus, they were not considered in logarithm in this analysis.

5.2.1. Correlation analysis for unmodified bitumen only

The correlation analysis was conducted firstly for unmodified bitumen only, with four samples. The calculated values of the Pearson product-moment correlation coefficient are listed in Table 19, where the green colour represents very strong correlations, and the red colour represents very weak correlations. However, it should be noted that not all these highlighted correlations have a solid physical basis to support that such correlations really exist. Some of them can be biased results due to the limited number of samples in this study. Thus, this report discusses only those very strong and very weak correlations with a solid physical basis, while ignoring the others for time being. The very strong correlations reveal potential parameters for the bitumen selection.

Among the analysed asphalt mixture parameters, the viscosity η is the one that represents the shear resistance of asphalt mixtures in the PEDRO model. The results in Table 19 suggest that the softening point of unmodified bitumen, iso-modulus temperatures by DSR, and even LSV at 10 °C after RTFOT have the strongest correlations with η at the maximum phase angle. This is basically due to the very strong correlations of these parameters with the reduced frequency f_r of the maximum phase angle, but very weak correlations with the shear modulus G of asphalt mixtures at the maximum phase angle.

From the binder parameters of the strongest correlations with η at the maximum phase angle, several were selected for further analysis of quantitative relationship, including the iso-modulus temperatures by DSR $T_{G^*=5\ MPa}$ (correlation coefficient over 0.9), $T_{G^*=15\ kPa}$, softening point $T_{R\&B}$ (both great popularity), and the LSV at 10 °C (correlation coefficient over 0.9). They can be the parameters for the selection of unmodified bitumen. Quantitative regression analyses were done between these selected parameters and the asphalt mixture viscosity η at the maximum phase angle. In this way, the binder parameters could be linked to the asphalt property and thus further coupled with the PEDRO model.

Figure 30 presents the regression analysis between $T_{G^*=5\ MPa}$ of unmodified bitumen after RTFOT and the asphalt mixture viscosity η at the maximum phase angle. There are two alternative ways to analyse the quantitative relationship: (1) based on all the data points, which mixes up the effects of binder properties and binder content; and (2) based on the minimum allowable binder content, which separately considers the effects of binder properties and binder content. The latter was selected for this study because this approach emphasises binder properties (rather than confusing with the mixture design) and is thus more applicable for the purpose of bitumen selection. Additionally, the approach based on the minimum allowable binder content allows the future complement with a study separately considering the effect of binder content. So, a comprehensive and clear understanding is achievable.

Table 19. Correlation analysis with the Pearson product-moment correlation coefficient for unmodified bitumen only. The green colour represents very strong correlations, and the red colour represents very weak correlations.

Correlation coefficient (unmodified bitumen only) between	Maximum phase angle of asphalt mixture	log(f_r) of the maximum phase angle	G (MPa) at the maximum phase angle	log(η) at the maximum phase angle	Binder G* at the maximum phase angle of asphalt mixture	Binder δ at the maximum phase angle of asphalt mixture
Binder content	0.390	-0.336	-0.725	0.298	0.316	-0.762
Air voids	0.111	0.249	0.212	-0.234	0.096	-0.112
VMA	0.506	-0.240	-0.730	0.204	0.418	-0.910
VFA	0.190	-0.278	-0.564	0.247	0.164	-0.358
Softening point, after RTFOT	-0.346	-0.905	-0.014	0.887	-0.432	-0.248
$T_{G^*=5\ MPa}$, after RTFOT	-0.413	-0.930	0.039	0.915	-0.493	-0.162
$T_{G^*=1\ MPa}$, after RTFOT	-0.375	-0.916	0.003	0.899	-0.458	-0.206
$T_{G^*=50\ kPa}$, after RTFOT	-0.333	-0.899	-0.024	0.881	-0.420	-0.264
$T_{G^*=15\ kPa}$, after RTFOT	-0.282	-0.874	-0.079	0.854	-0.371	-0.312
$T_{G^*=10\ kPa}$, after RTFOT	-0.259	-0.862	-0.103	0.841	-0.348	-0.334
δ @$T_{G^*=5\ MPa}$, after RTFOT	0.980	0.748	-0.909	-0.774	0.989	-0.723
δ @$T_{G^*=1\ MPa}$, after RTFOT	0.703	0.967	-0.468	-0.970	0.772	-0.153
δ @$T_{G^*=50\ kPa}$, after RTFOT	-0.223	0.525	0.534	-0.492	-0.128	0.734
δ @$T_{G^*=15\ kPa}$, after RTFOT	-0.343	0.414	0.632	-0.378	-0.252	0.811
δ @$T_{G^*=10\ kPa}$, after RTFOT	-0.314	0.442	0.608	-0.407	-0.222	0.794
T @G*/sinδ=2.2 kPa, after RTFOT	-0.203	-0.832	-0.153	0.809	-0.295	-0.390
T @G*·(cosδ)^2/sinδ =460 Pa, after RTFOT	-0.212	-0.837	-0.147	0.815	-0.304	-0.379
log(LSV) at 60 °C, after RTFOT	-0,175	-0,815	-0,187	0,792	-0.266	-0,411
log(LSV) at 10 °C, after RTFOT	-0,491	-0,959	0,160	0,948	-0.573	-0,104
J_{nr}3200 by MSCR at 60°C, after RTFOT	-0.013	0.690	0.337	-0.662	0.084	0.587

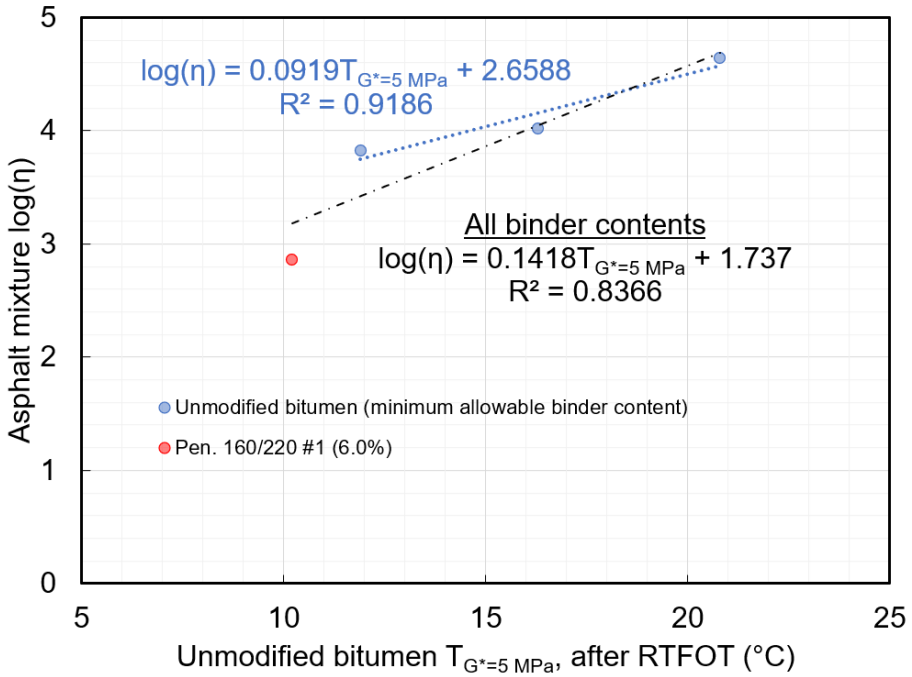

Figure 30. Regression analysis between $T_{G^*=5\ MPa}$ of unmodified bitumen after RTFOT and the asphalt mixture viscosity η at the maximum phase angle.

The regression analyses between the other selected binder parameters and the asphalt mixture viscosity η at the maximum phase angle were also done with the minimum allowable binder content as the benchmark. The results are shown in Figures 31-33. The obtained regression relationships link the binder parameters to the asphalt mixture property. This enables not only the evaluation of binder's influence on the asphalt mixture property for the purpose of bitumen selection but also the estimation of input material parameters into the PEDRO model from binder data for pavement performance prediction.

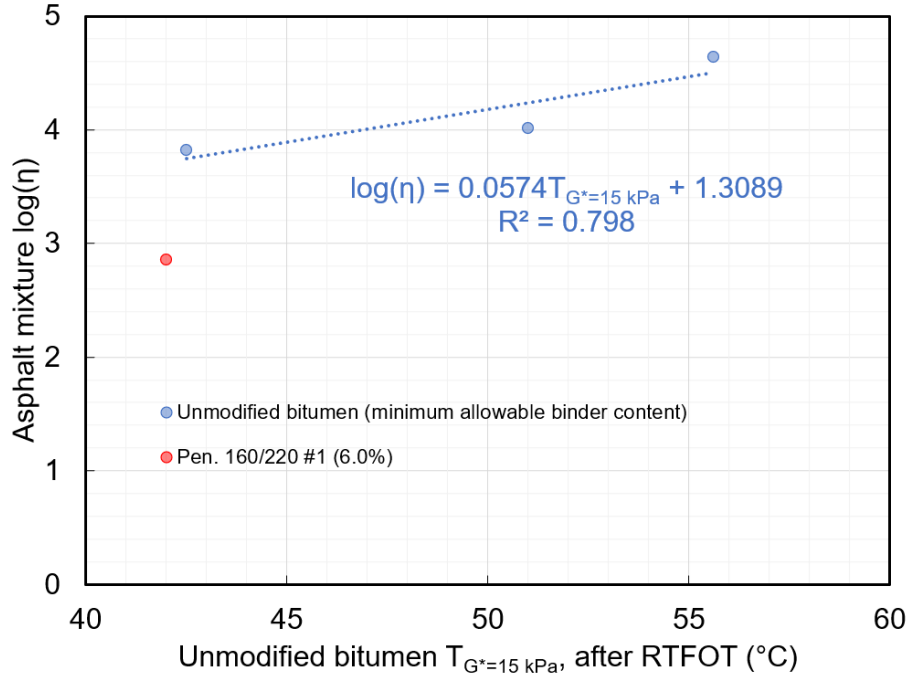

Figure 31. Regression analysis between $T_{G^*=15\ kPa}$ of unmodified bitumen after RTFOT and the asphalt mixture viscosity η at the maximum phase angle.

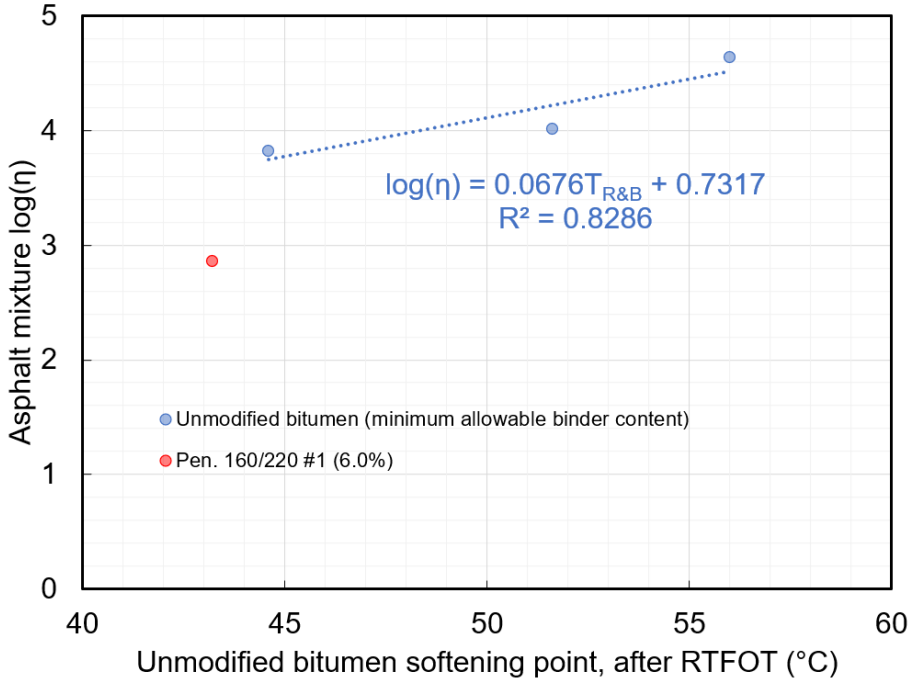

Figure 32. Regression analysis between softening point $T_{R\&B}$ of unmodified bitumen after RTFOT and the asphalt mixture viscosity η at the maximum phase angle.

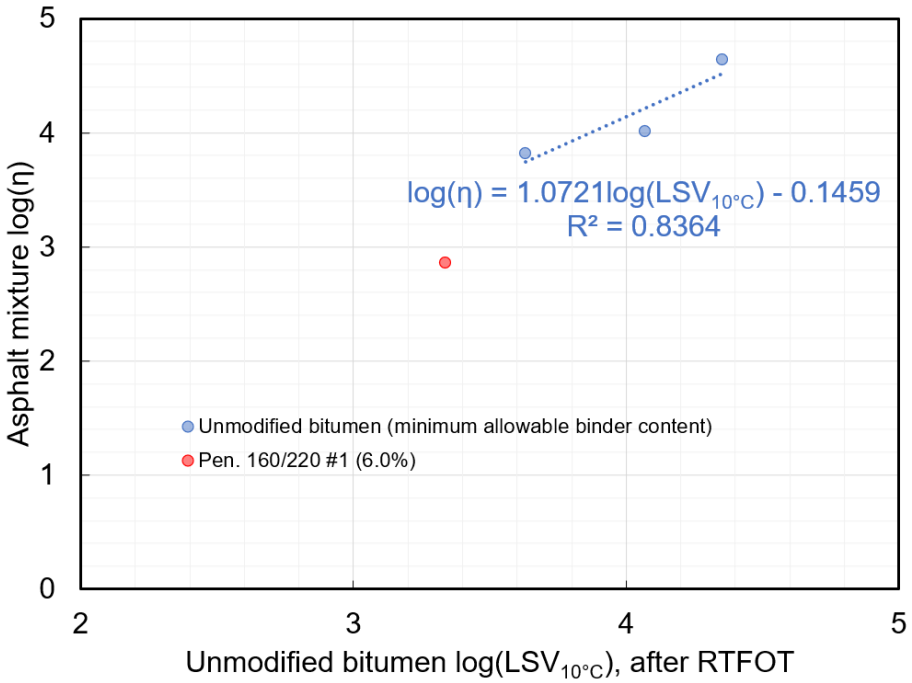

Figure 33. Regression analysis between LSV of unmodified bitumen at 10 °C after RTFOT and the asphalt mixture viscosity η at the maximum phase angle.

According to the regression analyses, the $T_{G^*=5\ MPa}$ after RTFOT showed the highest R^2 value and possibly would lead to the most reliable evaluation of unmodified bitumen and estimation of PEDRO material parameters among the discussed binder parameters. Considering the uncertainty of the regression analysis as well as the great popularity of $T_{G^*=15\ kPa}$ and softening point, however, it can be also practical to select unmodified bitumen and estimate PEDRO material parameters with $T_{G^*=15\ kPa}$ and softening point. As for the LSV at 10 °C, although a regression relationship was obtained, the great determination uncertainty from both the model fitting and the selection of target frequency might limit its practical use for bitumen evaluation and estimation of PEDRO material parameters.

5.2.2. Correlation analysis for all binders

After the analysis for unmodified bitumen only, the same correlation analysis was conducted again for all binders including the unmodified bitumen and PMBs, with six samples.

Table 20. Correlation analysis with the Pearson product-moment correlation coefficient for all binders including the unmodified bitumen and PMBs. The green colour represents very strong correlations, and the red colour represents very weak correlations.

Correlation coefficient (unmodified bitumen and PMB) between	Maximum phase angle of asphalt mixture	log(f_r) of the maximum phase angle	G (MPa) at the maximum phase angle	log(η) at the maximum phase angle	Binder G* at the maximum phase angle of asphalt mixture	Binder δ at the maximum phase angle of asphalt mixture
Binder content	-0.019	-0.400	-0.548	0.361	0.120	-0.575
Air voids	0.530	0.255	-0.264	-0.266	0.262	0.528
VMA	0.310	-0.268	-0.760	0.220	0.315	-0.323
VFA	-0.396	-0.294	0.032	0.290	-0.110	-0.632
Softening point, after RTFOT	-0.611	-0.561	-0.189	0.541	-0.441	-0.870
$T_{G^*=5\ MPa}$, after RTFOT	-0.187	-0.856	0.022	0.843	-0.406	0.119
$T_{G^*=1\ MPa}$, after RTFOT	-0.261	-0.888	-0.006	0.873	-0.428	-0.036
$T_{G^*=50\ kPa}$, after RTFOT	-0.389	-0.904	-0.035	0.887	-0.465	-0.297
$T_{G^*=15\ kPa}$, after RTFOT	-0.461	-0.868	-0.052	0.851	-0.458	-0.472
$T_{G^*=10\ kPa}$, after RTFOT	-0.478	-0.847	-0.073	0.828	-0.448	-0.533
δ @$T_{G^*=5\ MPa}$, after RTFOT	0.844	0.511	-0.173	-0.513	0.671	0.816
δ @$T_{G^*=1\ MPa}$, after RTFOT	0.741	0.486	-0.020	-0.479	0.514	0.921
δ @$T_{G^*=50\ kPa}$, after RTFOT	0.630	0.328	0.017	-0.321	0.305	0.986
δ @$T_{G^*=15\ kPa}$, after RTFOT	0.613	0.285	0.082	-0.275	0.301	0.989
δ @$T_{G^*=10\ kPa}$, after RTFOT	0.609	0.284	0.102	-0.274	0.305	0.984
T @G*/sinδ=2.2 kPa, after RTFOT	-0.539	-0.758	-0.113	0.739	-0.428	-0.714
T @G*·(cosδ)^2/sinδ =460 Pa, after RTFOT	-0.623	-0.635	-0.097	0.619	-0.432	-0.864
log(LSV) at 60 °C, after RTFOT	-0.552	-0.706	-0.147	0.686	-0.412	-0.778
log(LSV) at 10 °C, after RTFOT	-0.410	-0.953	0.077	0.942	-0.570	-0.130
J_{nr}3200 by MSCR at 60°C, after RTFOT	0.364	0.683	0.138	-0.663	0.248	0.625

The calculated values of the Pearson product-moment correlation coefficient are listed in Table 20, where the green colour represents very strong correlations, and the red colour represents very weak correlations. With a sample size of six, all the green-coloured correlations in Table 20 are statistically significant at a level lower than 0.05 (Siegle, 2015), namely at a confidence level higher than 95%.

The results in Table 20 suggest that, disregarding the binder type, some of the iso-modulus temperatures by DSR and the LSV at 10 °C after RTFOT still have the strongest correlations with the asphalt mixture viscosity η at the maximum phase angle. This is also due to the very strong correlations of these parameters with the reduced frequency f_r of the maximum phase angle, but very

weak correlations with the shear modulus G of asphalt mixtures at the maximum phase angle. It is noted that, when both unmodified bitumen and PMBs are included in the analysis, the softening point of bitumen does not have a strong correlation anymore with the η at the maximum phase angle.

In addition, when both unmodified bitumen and PMBs are included in the analysis, most binder parameters have very weak correlations with the shear modulus G of asphalt mixtures at the maximum phase angle. This basically means that whatever binder is used in the asphalt mixture, the shear modulus G of asphalt mixture at the maximum phase angle is not affected. It statistically confirms the previous observation that the shear modulus G of asphalt mixtures at the maximum phase angle is in a relatively narrow range and does not vary very much. The asphalt mixture viscosity η at the maximum phase angle is thus largely dependent on the frequency of the maximum phase angle. Furthermore, it is noted in Table 20 that the binder phase angle δ at the maximum phase angle of asphalt mixture is highly related to the binder phase angle δ at the iso-modulus temperatures and the softening point.

Similar as the analysis in the previous section, several binder parameters were also selected from those of the strongest correlations with η at the maximum phase angle in Table 20, for further analysis of quantitative relationship. When both unmodified bitumen and PMBs are included in the analysis, the selected parameters include the iso-modulus temperatures by DSR $T_{G^*=50\ kPa}$ (high correlation coefficient), $T_{G^*=15\ kPa}$ (great popularity), and the LSV at 10 °C (correlation coefficient over 0.9). Quantitative regression analyses were also done between these selected parameters and the asphalt mixture viscosity η at the maximum phase angle.

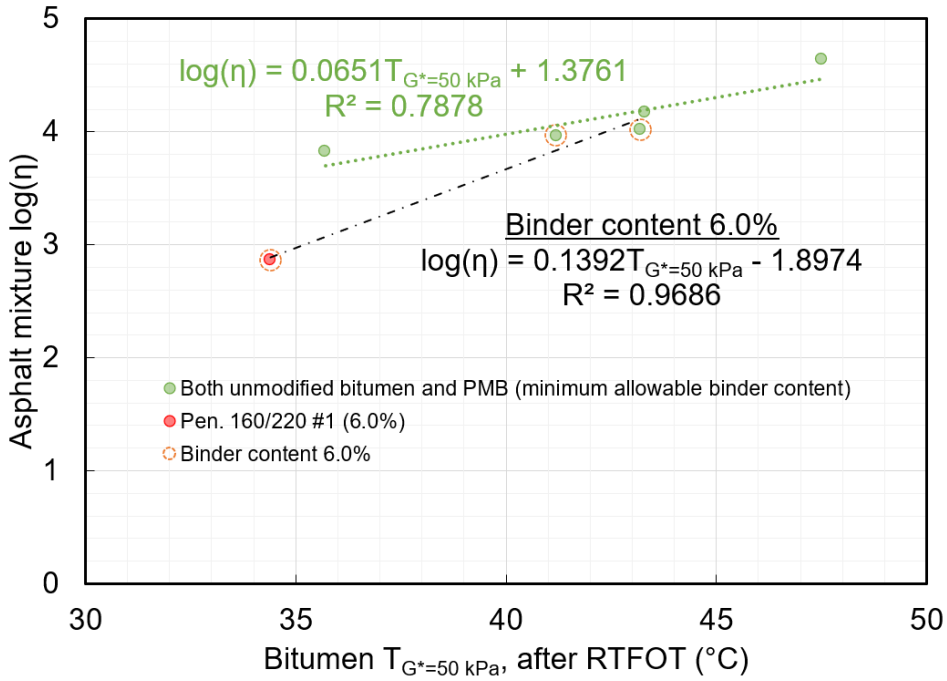

Figure 34. Regression analysis between $T_{G^*=50\ kPa}$ of bitumen after RTFOT and the asphalt mixture viscosity η at the maximum phase angle.

Figure 34 presents the regression analysis between $T_{G^*=50\ kPa}$ of bitumen after RTFOT and the asphalt mixture viscosity η at the maximum phase angle. There is a further alternative way to analyse the quantitative relationship in Figure 34, namely based on the exact same binder content (6.0%). This approach may make some sense for purely understanding the role of binders in asphalt mixtures, but it does not consider and reflect the empirical adjustment of binder content based on the binder type and grade in practice. Thus, it was not adopted in this study. The regression analyses between the selected binder parameters and η at the maximum phase angle were still done with the minimum allowable binder content as the benchmark. More results are shown in Figures 35 and 36.

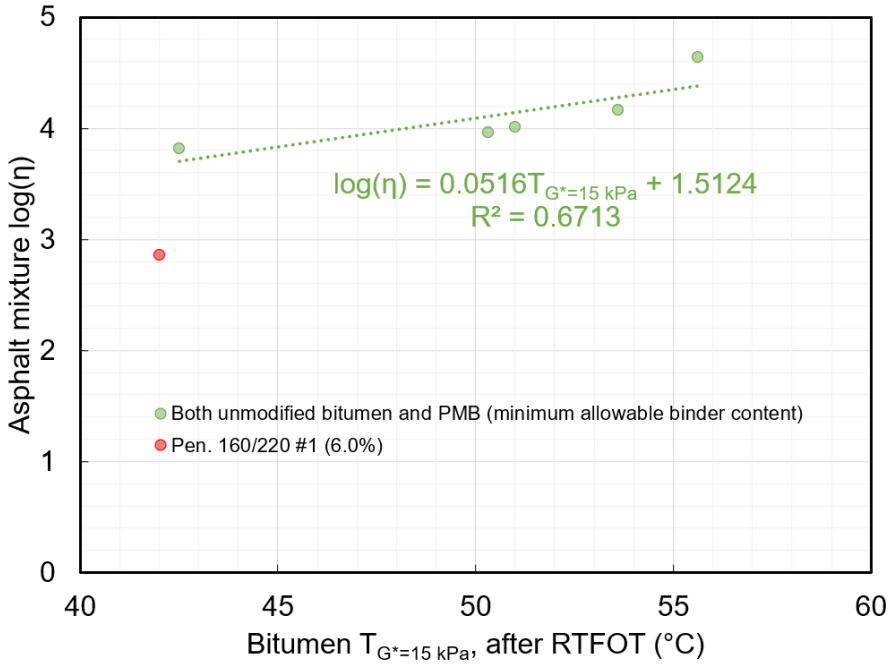

Figure 35. Regression analysis between $T_{G*=15\ kPa}$ of bitumen after RTFOT and the asphalt mixture viscosity η at the maximum phase angle.

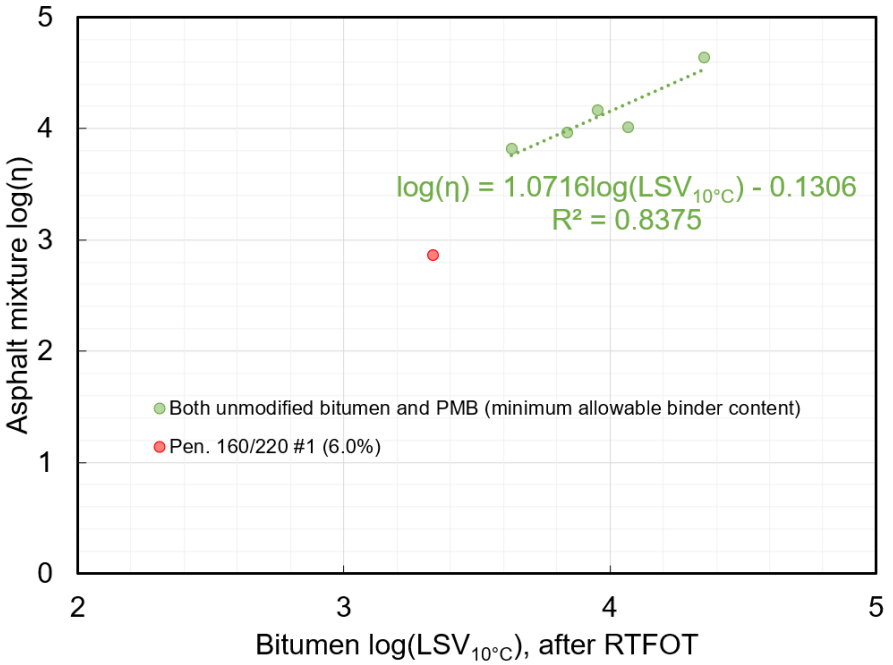

Figure 36. Regression analysis between LSV of bitumen at 10 °C after RTFOT and the asphalt mixture viscosity η at the maximum phase angle.

Also similar as the discussion in the previous section, the $T_{G*=50\ kPa}$ after RTFOT showed higher R^2 value than $T_{G*=15\ kPa}$. When the binder type is disregarded, it is possible that $T_{G*=50\ kPa}$ after RTFOT would lead to more reliable evaluation of bitumen and estimation of PEDRO material parameters than $T_{G*=15\ kPa}$. Considering the uncertainty of the regression analysis as well as the great popularity of $T_{G*=15\ kPa}$, however, it can be more practical to select bitumen and estimate PEDRO material parameters with $T_{G*=15\ kPa}$. Both parameters will be further investigated and evaluated in next chapter of this report in terms of their potential use in bitumen selection and pavement performance prediction. Yet, the use of LSV at 10 °C is probably limited due to the great determination uncertainty of LSV from both the model fitting and selection of target frequency. It will not be discussed in next chapter.

6. Black space diagram and PEDRO model for bitumen selection

This chapter puts forward the two linked parts of a possible bitumen selection tool: (1) the Black space diagram for bitumen evaluation, and (2) the PEDRO model for performance prediction based on the binder data. Such a tool not only allows the evaluation of bitumen itself in a more efficient way but also provides the possibility to predict the rutting performance of the bitumen in asphalt pavements based on binder testing. Its feasibility is discussed and demonstrated.

6.1. Black space diagram for bitumen evaluation

The Black space diagram of bitumen combines the modulus and phase angle in the same space and can thus integrate various linear viscoelastic parameters into one single diagram (Figure 3). It is compatible with both the American performance grading system and the iso-modulus approach at the angular frequency of 10 rad/s. By empirical determination and verification, the softening point of bitumen can be integrated into the Black space diagram as well. Therefore, it can be easily adopted based on the current specifications.

Furthermore, the Black space diagram of bitumen can go beyond the high-temperature evaluation. It is also possible to include criteria of fatigue performance at intermediate temperatures and even cracking resistance at low temperatures. New linear parameters based on the up-to-date research can be integrated into the Black space diagram as well, such as the crossover temperature and Glover-Rowe parameter. This diagram holds great potential in terms of linear viscoelastic evaluation of bitumen.

In a Black space diagram, the temperature and/or frequency information is not presented on an axis. Avoiding using more diagrams, an easier solution to indicate the information is to label the data points in the Black space diagram, although the addition of an extra axis is also possible to make the space three-dimensional.

The temperature sweep results at 10 rad/s of binders were analysed in the Black space in Section 4.2.1 of this report. They are examples of how to employ the Black space diagram for linear viscoelastic evaluation of bitumen. Precise quantitative evaluations were done for the studied binders with iso-modulus parameters by interpolation (Equations 6 and 7). A calculation template may make the determination much easier in practice.

While these determined parameters can be adopted as the technical requirements for binders, the use of these parameters is not limited to the binder evaluation only. The correlation analysis presented in the previous chapter has suggested that these iso-modulus parameters have a very strong correlation with the asphalt mixture property. This makes it possible to predict the performance of the bitumen in asphalt pavements based on binder testing, which can be an advantage for the purpose of bitumen selection.

6.2. PEDRO model for performance prediction based on binder data

The regression analysis results presented in Figures 34 and 35 link the binder parameters ($T_{G^*=50\ kPa}$ and $T_{G^*=15\ kPa}$ after RTFOT) to the asphalt mixture viscosity η at the maximum phase angle at the chosen reference temperature of 10 °C. To use the PEDRO model, the material inputs a_1, a_2 and a_3 according to Equation 5 need to be estimated without testing the asphalt mixture.

6.2.1. Estimation of PEDRO parameter values

Given a bituminous binder, it can be tested for the parameters $T_{G^*=50\ kPa}$ and/or $T_{G^*=15\ kPa}$ after RTFOT. The regression relationships in Figures 34 and 35, both based on the minimum allowable binder content, lead to the estimated viscosity η of the asphalt mixture at the maximum phase angle at the reference temperature of 10 °C. This viscosity can then be shifted to other reference temperatures by using the Arrhenius equation, as Equation 13.

$$\log(\eta_T) = \log\left(\eta_{T_{ref}}\right) + K_a\left(\frac{1}{T+273} - \frac{1}{T_{ref}+273}\right)$$

Equation 13. Shifting equation of the viscosity based on the Arrhenius equation.

In Equation 13, η_T is the asphalt mixture viscosity at the maximum phase angle at the target reference temperature of T (in °C), T_{ref} is the chosen reference temperature of 10 °C in this study. Without testing the asphalt mixture, the value of the constant K_a for determining the shift factor is unknown. However, the determined results in Table 3 suggest that it is fair to assume K_a to be 10000 K. With this, the asphalt mixture viscosity η can be estimated at different reference temperatures. And then, the PEDRO parameter values can be determined according to Equation 5 and used for performance prediction.

This estimation approach was demonstrated for the binders in asphalt mixtures with the minimum allowable binder content because the regression analysis considered that as the benchmark. The bitumen test results listed in Table 10 ($T_{G^*=50\ kPa}$ and $T_{G^*=15\ kPa}$) were used to estimate the asphalt mixture viscosity at the maximum phase angle at the reference temperature of 10 °C. The estimation results are listed in Table 21. It is noted that there are small differences between the values estimated with the two binder parameters. There are also certain differences between these estimated values and the determined values based on asphalt mixture testing (Table 4).

Table 21. Estimated asphalt mixture viscosity at the maximum phase angle, T_{ref}=10 °C (asphalt mixtures with the minimum allowable binder content).

Binder type in the asphalt mixture (binder content)	**Pen. 50/70 (6.2%)**	**Pen. 70/100 (6.0%)**	**Pen. 160/220 #2 (5.6%)**	**PMB 1 (6.0%)**	**PMB 2 (6.2%)**
Estimated log(η) with $T_{G^*=50\ kPa}$ after RTFOT	4.47	4.19	3.70	4.06	4.19
Estimated log(η) with $T_{G^*=15\ kPa}$ after RTFOT	4.38	4.14	3.71	4.11	4.28

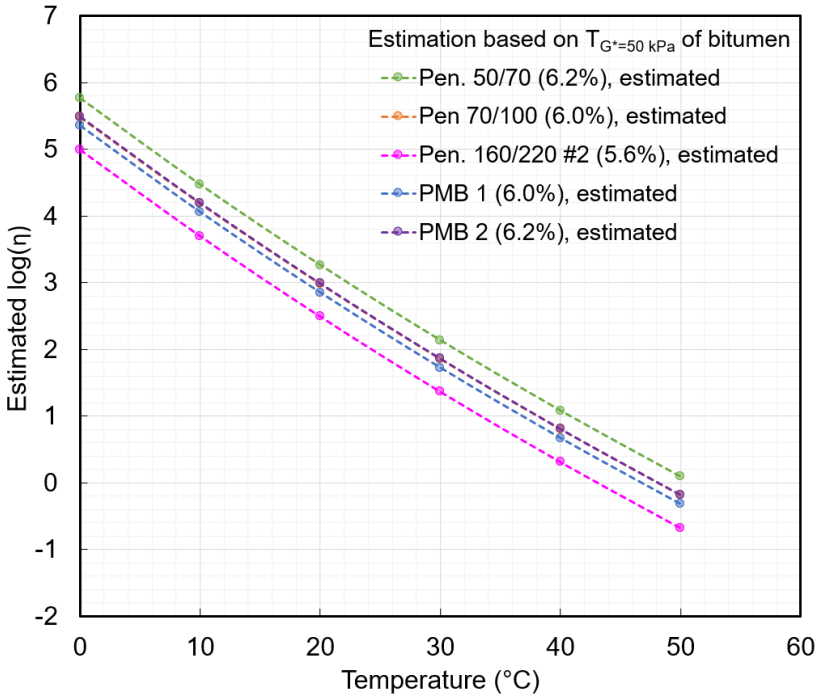

Figure 37. Estimated asphalt mixture viscosity at the maximum phase angle at different reference temperatures, with $T_{G^*=50\ kPa}$ after RTFOT.

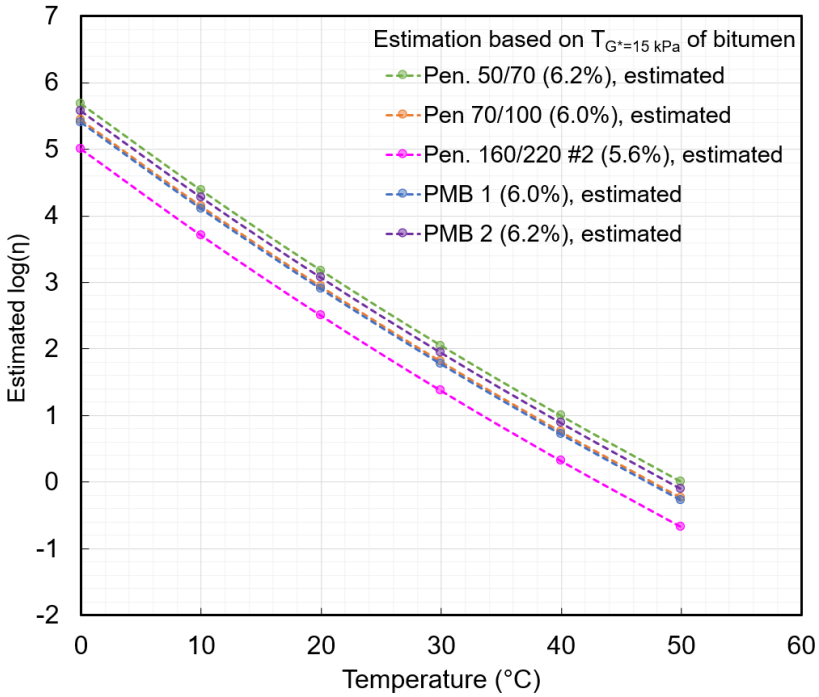

Figure 38. Estimated asphalt mixture viscosity at the maximum phase angle at different reference temperatures, with $T_{G^*=15\ kPa}$ after RTFOT.

After that, the estimated values at the reference temperature of 10 °C were shifted to other reference temperatures by using Equation 13. The shifted results are plotted in Figures 37 and 38 with the two binder parameters, respectively. It is noted that, with the constant K_a assumed the same for all, the lines in Figures 37 and 38 are all parallel. Based on these estimations, the values of the PEDRO material parameters were determined according to Equation 5 and are listed in Tables 22 and 23 with the two binder parameters, respectively.

Table 22. Estimated PEDRO material parameters with $T_{G^*=50\ kPa}$ after RTFOT.

Binder type in the asphalt mixture (binder content)	**Pen. 50/70 (6.2%)**	**Pen. 70/100 (6.0%)**	**Pen. 160/220 #2 (5.6%)**	**PMB 1 (6.0%)**	**PMB 2 (6.2%)**
Estimated a_1	3.81×10^{-4}	3.81×10^{-4}	3.81×10^{-4}	3.81×10^{-4}	3.81×10^{-4}
Estimated a_2	-0.132	-0.132	-0.132	-0.132	-0.132
Estimated a_3	5.759	5.479	4.991	5.349	5.485

Table 23. Estimated PEDRO material parameters with $T_{G^*=15\ kPa}$ after RTFOT.

Binder type in the asphalt mixture (binder content)	**Pen. 50/70 (6.2%)**	**Pen. 70/100 (6.0%)**	**Pen. 160/220 #2 (5.6%)**	**PMB 1 (6.0%)**	**PMB 2 (6.2%)**
Estimated a_1	3.81×10^{-4}	3.81×10^{-4}	3.81×10^{-4}	3.81×10^{-4}	3.81×10^{-4}
Estimated a_2	-0.132	-0.132	-0.132	-0.132	-0.132
Estimated a_3	5.672	5.434	4.996	5.398	5.569

In Tables 22 and 23, it is noted that all the a_1 and a_2 values estimated from the binder data were the same for all asphalt mixtures. This is due to the assumption of the fixed K_a value for all. From the previous experience of the authors on the PEDRO model, the a_1 and a_2 values of asphalt mixtures do not vary very much, while the a_3 value is more critical for the prediction results (Said *et al.*, 2020).

6.2.2. Evaluation of prediction results

To evaluate the accuracy of the approach described above, the estimated values listed in Tables 22 and 23 were put into the PEDRO model (web version at https://pedro.vti.se/) to predict the rutting development in the same structure of asphalt mixture under the same traffic and climate conditions as it was done in Section 3.4. The prediction results based on the binder parameters were compared with the ordinary prediction based on asphalt mixture testing, as shown in Figures 39-43.

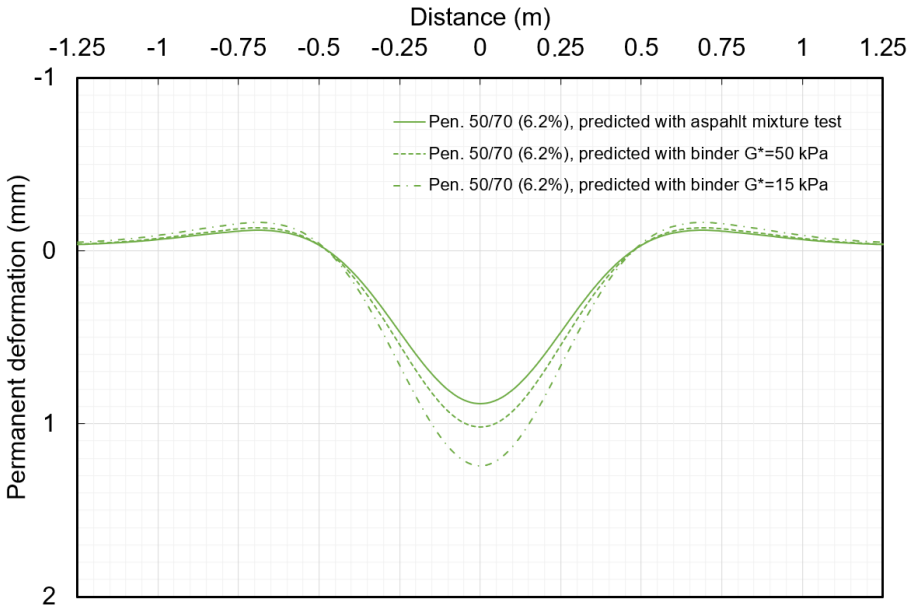

Figure 39. Comparison of predicted rut profiles in 20 years between different approaches by the PEDRO model, ABT16 asphalt mixture Pen. 50/70 (6.2%).

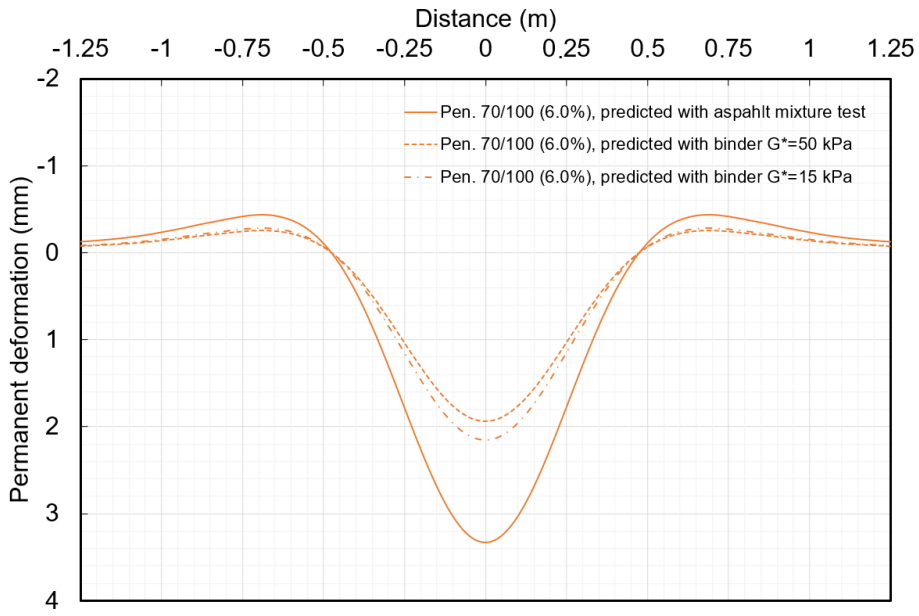

Figure 40. Comparison of predicted rut profiles in 20 years between different approaches by the PEDRO model, ABT16 asphalt mixture Pen. 70/100 (6.0%).

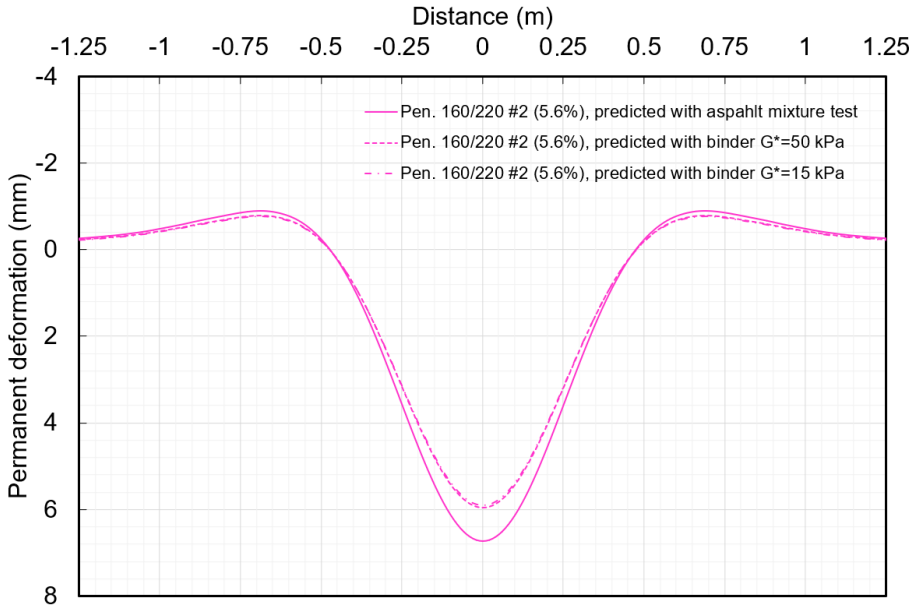

Figure 41. Comparison of predicted rut profiles in 20 years between different approaches by the PEDRO model, ABT16 asphalt mixture Pen. 160/220 #2 (5.6%).

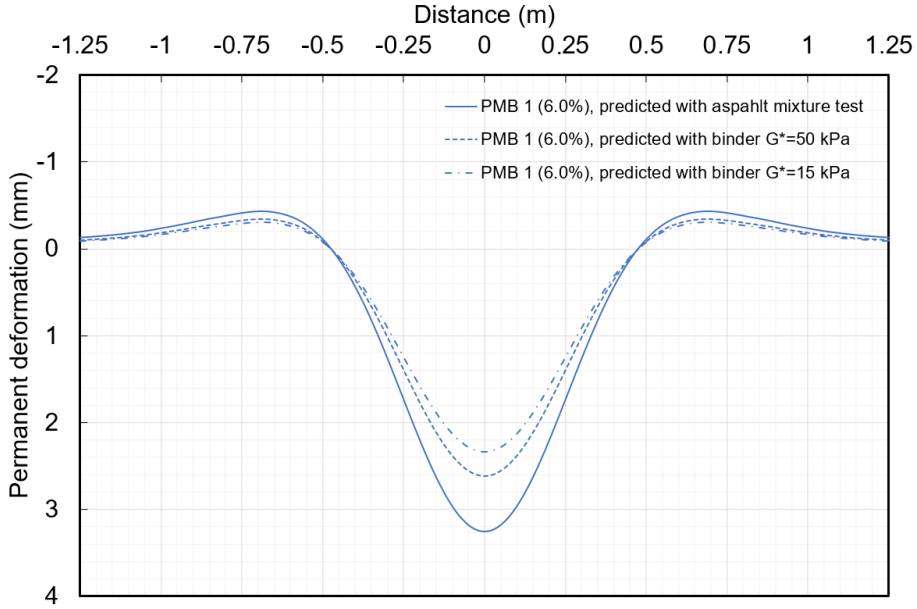

Figure 42. Comparison of predicted rut profiles in 20 years between different approaches by the PEDRO model, ABT16 asphalt mixture PMB 1 (6.0%).

The results indicate that the prediction based on binder testing is feasible. There is a difference between the prediction based on binder testing and the ordinary prediction based on asphalt mixture testing. This difference was up to about 1 mm (about 10%-40%) in 20 years for the studied cases in this report. In four of the five cases, the prediction based on binder testing underestimated the rut depth. In one case, it overestimated the rut depth. Considering that the prediction based on binder testing is conducted upon more unknown factors, such as the shift factor, this difference is assessed as small. Figure 44 presents the comparison of predicted rut depth development during the whole period of 20 years. Comparing the two binder parameters, the difference between their prediction results was not big. The prediction with $T_{G^*=50\ kPa}$ after RTFOT was closer to the ordinary prediction with asphalt mixture test in four of the five cases. In one case, the prediction with $T_{G^*=15\ kPa}$ after RTFOT was closer. In terms of ranking, both binder parameters ranked Pen. 50/70 (6.2%), Pen. 160/220 #2 (5.6%) and PMB 2 (6.2%) the same as the prediction with asphalt mixture test. Pen. 70/100 (6.0%) and PMB

1 (6.0%) show very similar rut depth development according to the prediction based on asphalt mixture test. The prediction with $T_{G^*=15\ kPa}$ after RTFOT ranked them closer to each other than that with $T_{G^*=50\ kPa}$. Due to the great popularity of $T_{G^*=15\ kPa}$, in addition, it can be more practical to use $T_{G^*=15\ kPa}$ after RTFOT for the prediction.

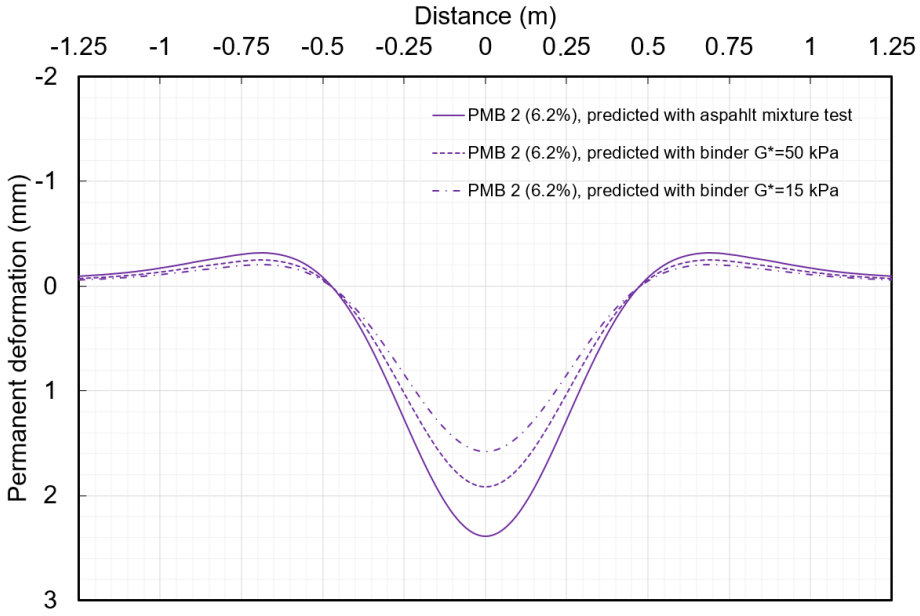

Figure 43. Comparison of predicted rut profiles in 20 years between different approaches by the PEDRO model, ABT16 asphalt mixture PMB 2 (6.2%).

6.3. Limitations

The Black space diagram is for the linear viscoelastic evaluation of bitumen. The PEDRO model uses linear viscoelastic properties of asphalt mixtures for the rutting performance prediction. Thus, the bitumen selection tool discussed in this chapter is based on the linear viscoelasticity of the materials. The non-linear behaviour is not covered.

The regression relationship between binder parameters and the asphalt mixture viscosity is crucial for the performance prediction based on binder testing in this chapter. By now, this relationship has been developed and investigated only for ABT16 asphalt mixtures with the minimum allowable binder content according to the Swedish Transport Administration specification (Trafikverket, 2020). However, it is possible to extend this relationship to other binder contents and mixture types in the future.

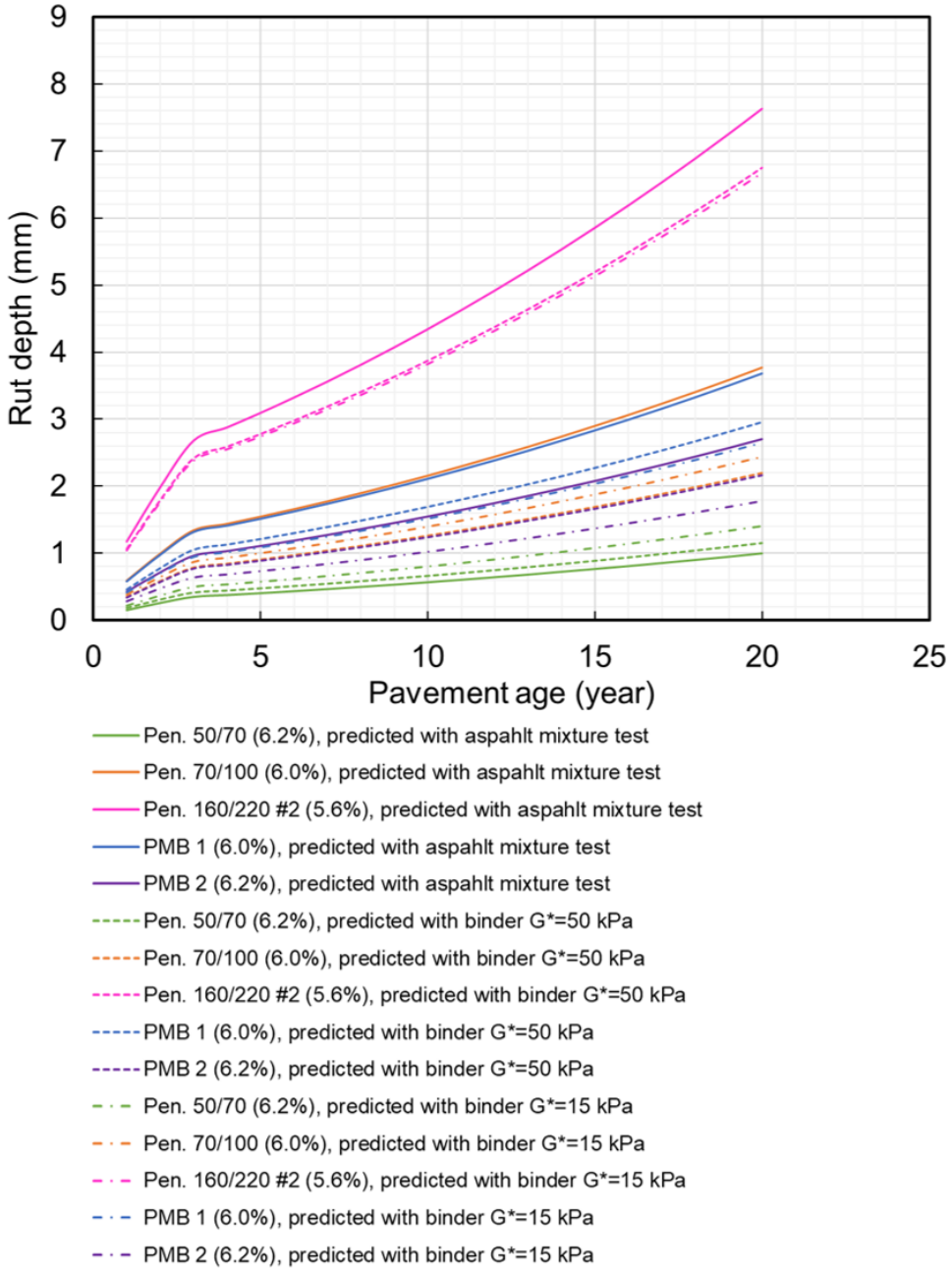

Figure 44. Comparison of predicted rut development (profile centre) during 20 years between different approaches by the PEDRO model.

7. Conclusions and recommendations

7.1. Conclusions

This report presents an experimental investigation on the shear resistance of asphalt mixtures and its relationship with the bitumen properties. The correlation between them is analysed using the experimental results. Based on the correlation analysis, a feasible approach is proposed from bitumen evaluation to the rutting performance prediction of asphalt pavements with the PEDRO model. Through such an approach, a bitumen selection tool is put forward, consisting of two linked parts respectively for bitumen evaluation and performance prediction. On the basis of the results and discussion described in previous chapters, the following conclusions can be drawn:

1. It is demonstrated that the Black space diagram is an efficient tool for the linear viscoelastic evaluation of bituminous binders. It combines the modulus and phase angle of bitumen in the same space and can thus integrate various linear viscoelastic parameters into one single diagram. This enables straightforward evaluations of bitumen, especially together with the common test method of temperature sweep by DSR at 10 rad/s. The adoption of the Black space diagram is not only compatible with the current technical specifications regarding high-temperature evaluation, but it also holds great potential to cover a wider service temperature range and even to include new linear parameters based on the up-to-date research.
2. By the correlation analysis between shear properties of asphalt mixtures and bitumen properties, it is confirmed that the shear modulus G of asphalt mixtures at the maximum phase angle is in a relatively narrow range and does not vary very much. The asphalt mixture viscosity η at the maximum phase angle is thus largely dependent on the frequency of the maximum phase angle.
3. The iso-modulus temperatures of RTFOT-aged bitumen by DSR testing at 10 rad/s have very strong correlations with the asphalt mixture viscosity η at the maximum phase angle. They can thus be used to estimate material parameters for the performance prediction by the PEDRO model. This is valid for both unmodified bitumen and PMBs.
4. For unmodified bitumen, the softening point of bitumen after RTFOT has a very strong correlation with the asphalt mixture viscosity η at the maximum phase angle. When both unmodified bitumen and PMBs are included in the analysis, however, the correlation is not strong anymore. In addition, the MSCR parameter with 3200 Pa stress does not show very strong correlation with the asphalt mixture viscosity η at the maximum phase angle. This might be because the investigated viscosity η is a linear viscoelastic property of asphalt mixture, but the MSCR parameter of binder (at 60 °C in this study) is not always within the linear viscoelastic region.
5. For both unmodified bitumen and PMBs, the LSV (0.001 Hz) at 10 °C after RTFOT has a very strong correlation with the asphalt mixture viscosity η at the maximum phase angle. In contrast, the correlation of the LSV at 60 °C after RTFOT is not as strong as at 10 °C. Despite the correlations, the large uncertainty associated with the determination of LSV from both the model fitting and the selection of target frequency can limit its practical use for bitumen evaluation and estimation of PEDRO material parameters.
6. By the regression analysis, the relationship between binder parameters and asphalt mixture viscosity η at the maximum phase angle is quantified at the minimum allowable binder content. This relationship links the binder parameters to the asphalt mixture property used by the PEDRO model, and thus makes an approach viable from bitumen evaluation to the rutting performance prediction.

7. Based on the above-mentioned aspects, a bitumen selection tool is foreseeable, consisting of two linked parts respectively for bitumen evaluation and rutting performance prediction. The Black space diagram allows efficient evaluations of bitumen with various parameters, while the PEDRO model can be employed for the rutting performance prediction with binder properties (mainly iso-modulus temperatures of RTFOT-aged binders) as the material inputs. Such a tool is expected to enable not only the control of bitumen parameters but also the evaluation of bitumen's long-term influence on pavement (rutting) performance with the binder testing results.

7.2. Recommendations

On the basis of this study, the following recommendations are given for the future implementation and further actions:

1. Some simple calculation templates can make it much easier in practice to use the Black space diagram, to determine iso-modulus parameters of bitumen, and to estimate PEDRO material parameters based on the binder testing. These templates are expected to provide various options, such as the calculation of different parameters and their use as alternatives for the estimation/prediction, to ease the possible implementation of the research results.
2. In this study, the regression relationship between binder parameters and the asphalt mixture viscosity was developed and investigated only for ABT16 asphalt mixtures with the minimum allowable binder content according to the Swedish Transport Administration specification (Trafikverket, 2020). Its validity for ABT asphalt mixtures of other nominal maximum aggregate sizes is probable but still needs to be analysed with more test data. Furthermore, it is recommended to extend this relationship to other binder contents and mixture types in the future. This will facilitate the implementation of a new prediction option based on binder testing in the PEDRO program.
3. This study was conducted along with the validation and calibration of the PEDRO model (version 1.10, January 2019). Any major revision/update of the model in the future may affect the validity and precision of the approach proposed in this study. It is thus recommended to review this approach when major updates are released in the future.

References

Alisov, A., Riccardi, C., Schrader, J., Cannone Falchetto, A., & Wistuba, M.P. (2020). A novel method to characterise asphalt binder at high temperature. Road Materials and Pavement Design, 21(1), 143-155.

Asgharzadeh, S.M., Tabatabaee, N., Naderi, K., & Partl, M. (2013). An empirical model for modified bituminous binder master curves. Materials and structures, 46(9), 1459-1471.

Asgharzadeh, S.M., Tabatabaee, N., Naderi, K., & Partl, M.N. (2015). Evaluation of rheological master curve models for bituminous binders. Materials and Structures, 48(1-2), 393-406.

Bari, J., & Witczak, M.W. (2006). Development of a new revised version of the Witczak E* predictive models for hot mix asphalt mixtures. Journal of the Association of Asphalt Paving Technologists, 75, 381-423.

Christensen, D.W., & Bonaquist, R. (2015). Improved Hirsch model for estimating the modulus of hot-mix asphalt. Road Materials and Pavement Design, 16(S2), 254-274.

Christensen, D.W., Pellinen, T., & Bonaquist, R.F. (2003). Hirsch model for estimating the modulus of asphalt concrete. Journal of the Association of Asphalt Paving Technologists, 72, 97-121.

De Visscher, J., & Vanelstraete, A. (2004). Practical test methods for measuring the zero shear viscosity of bituminous binders. Materials and Structures, 37(5), 360-364.

Glover, C.J., Davison, R.R., Domke, C.H., Ruan, Y., Juristyarini, P., Knorr, D.B., & Jung, S.H. (2005). Development of a New Method for Assessing Asphalt Binder Durability with Field Validation. Report No. FHWA/TX-05/1872-2. College Station, T.X.: Texas Transportation Institute.

Hagner, T., 2018. German Experiences with DSR Test Methods. Presentation on the DSR seminar in Stockholm, 8 October 2018.

Havriliak, S., & Negami, S. (1966). A complex plane analysis of α-dispersions in some polymer systems. Journal of Polymer Science Part C: Polymer Symposia, 14, 99-117.

Liu, H., Zeiada, W., Al-Khateeb, G.G., Shanableh, A., & Samarai, M. (2020). Use of the multiple stress creep recovery (MSCR) test to characterize the rutting potential of asphalt binders: A literature review. Construction and Building Materials, 121320.

Morea, F., Agnusdei, J.O., & Zerbino, R. (2010). Comparison of methods for measuring zero shear viscosity in asphalts. Materials and Structures, 43(4), 499-507.

Morea, F., Agnusdei, J.O., & Zerbino, R. (2011). The use of asphalt low shear viscosity to predict permanent deformation performance of asphalt concrete. Materials and Structures, 44(7), 1241-1248.

Olard, F., & Di Benedetto, H. (2003). General “2S2P1D” model and relation between the linear viscoelastic behaviours of bituminous binders and mixes. Road Materials and Pavement Design, 4(2), 185-224.

Oscarsson, E. (2011). Mechanistic-Empirical Modeling of Permanent Deformation in Asphalt Concrete Layers. Doctoral thesis. Lund University.

Pellinen, T.K., Witczak, M.W., & Bonaquist, R.F. (2004). Asphalt mix master curve construction using sigmoidal fitting function with non-linear least squares optimization. In 15th Engineering Mechanics Division Conference: Recent Advances in Materials Characterization and Modeling of Pavement Systems (pp. 83-101). Columbia University, N.Y.

Rowe, G.M. (2014). Interrelationships in rheology for asphalt binder specifications. In Proceedings of the Fifty-Ninth Annual Conference of the Canadian Technical Asphalt Association (pp. 457-483). Winnipeg, Manitoba.

Said, S., Ahmed, A., Jelagin, D., Lu, X., Gudmarsson, A., Nilsson, R., Oscarsson, E., & Jarlsson, H. (2020). Prediction of Rutting in Asphalt Concrete Pavements - The PEDRO Model. VTI Report No. 1016A. Linköping: VTI.

Said, S.F., Hakim, H., & Eriksson, O. (2013). Rheological characterization of asphalt concrete using a shear box. Journal of Testing and Evaluation, 41(4), 602-610.

Schrader, J., & Wistuba, M.P. (2019). On the use of a novel Binder-Fast-Characterization-Test. In RILEM 252-CMB-Symposium on Chemo-Mechanical Characterization of Bituminous Materials (pp. 123-128). Cham: Springer.

Siegle, D., 2015. Critical Values of the Pearson Product-Moment Correlation Coefficient. Retrieved from https://researchbasics.education.uconn.edu/r_critical_value_table/.

Soenen, H., 2018. Multiple Stress Creep Recovery Test. Presentation on the DSR seminar in Stockholm, 8 October 2018.

Sybilski, D. (1994). Relationship between absolute viscosity of polymer-modified bitumens and rutting resistance of pavement. Materials and Structures, 27(2), 110-120.

Sybilski, D. (1996). Zero-shear viscosity of bituminous binder and its relation to bituminous mixture's rutting resistance. Transportation Research Record, 1535(1), 15-21.

Sybilski, D. (1997). New simplified equation for the computation of absolute viscosity of polymer-bitumens. Materials and Structures, 30(3), 182-187.

Trafikverket (2020). KRAV - Bitumenbundna lager. TDOK 2013:0529, Version 4.0. Borlänge: Trafikverket. (In Swedish)

Zhang, H., Chen, Z., Xu, G., & Shi, C. (2018). Evaluation of aging behaviors of asphalt binders through different rheological indices. Fuel, 221, 78-88.

Zhu, J., Ghafoori, E., & Dinegdae, Y. (2020). Characterization of Asphalt Mixtures and Bitumen to Minimize Shear-Related Distresses in Asphalt Pavement: State of the Art. VTI Report No. 1056A. Linköping: VTI.

Zhu, J., Lu, X., Langfjell, M., & Gudmarsson, A. (2021). Quantitative relationship of fundamental rheological properties of bitumen with the empirical Ring and Ball softening point. Road Materials and Pavement Design, 22(S1), S345-S364.

Appendix 1 Comparison of different fitting models for asphalt mixture

Three master curve fitting models are compared in this appendix, including the Havriliak-Negami model (Havriliak and Negami, 1966), 2S2P1D model (Olard and Di Benedetto, 2003), and sigmoidal/compound unimodal-sigmoidal model (Pellinen *et al.*, 2004; Said *et al.*, 2013). The measurement data of asphalt mixture with PMB 1 (6.0%), as presented in Figure 5 of this report, were employed for the comparison. The fitting results are presented as follow.

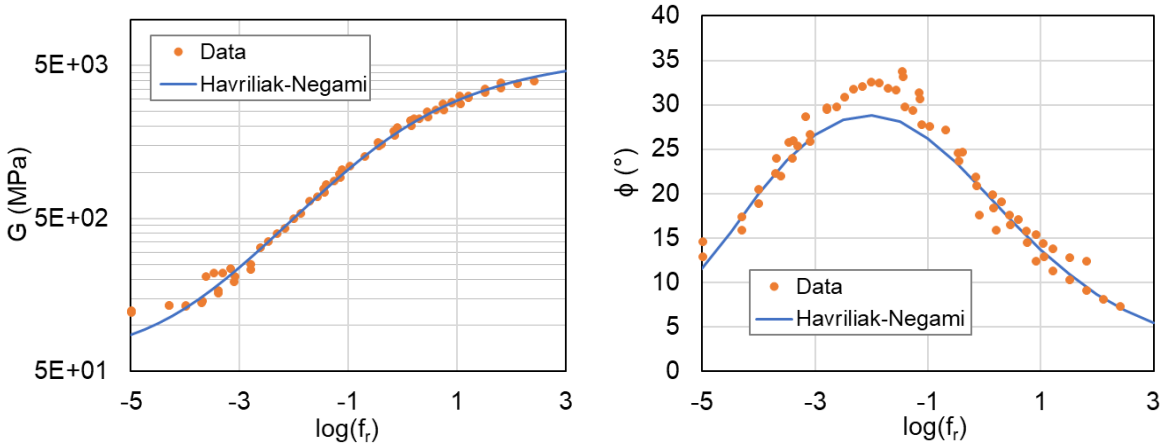

Figure A1. Master curve fitting with the Havriliak-Negami model, T_{ref}=10 °C.

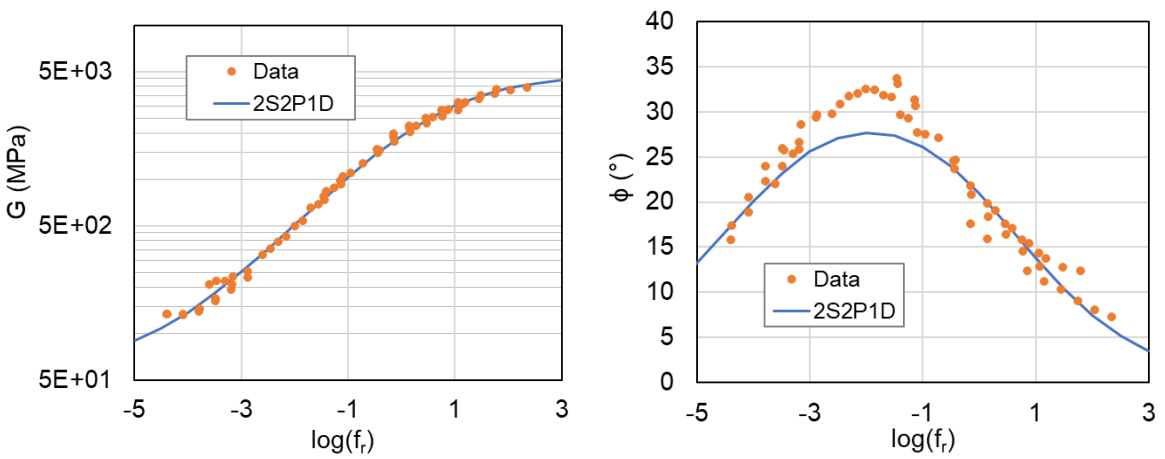

Figure A2. Master curve fitting with the 2S2P1D model, T_{ref}=10 °C.

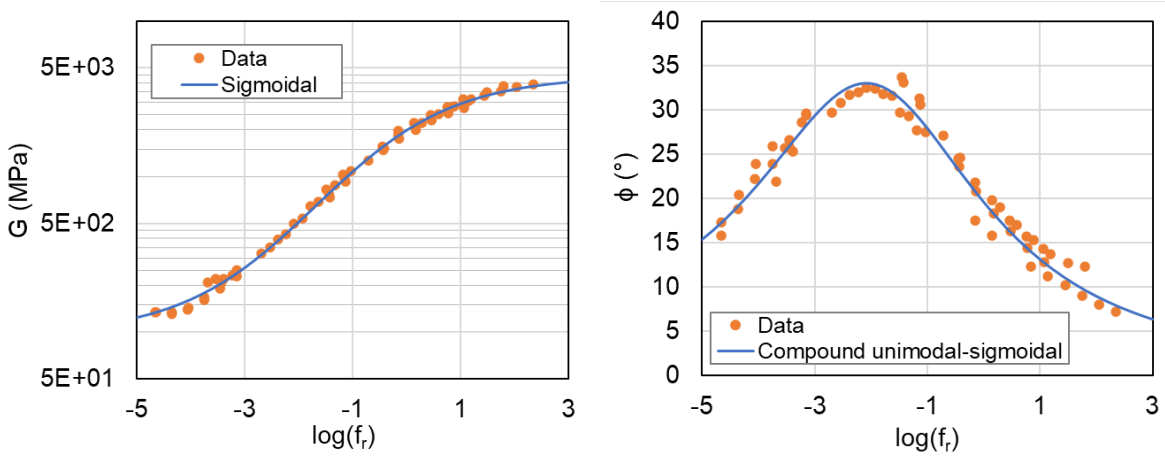

Figure A3. Master curve fitting with the sigmoidal/compound unimodal-sigmoidal model, T_{ref}=10 °C.

Appendix 2 Master curve fitting parameters of asphalt mixtures

The values of parameters for fitting master curves of asphalt mixtures are presented in this appendix. The detailed description can be found in Section 3.2 of this report.

Table A1. Master curve fitting parameters of asphalt mixture shear modulus G (MPa).

Binder type in the asphalt mixture (binder content)	**Pen. 50/70 (6.2%)**	**Pen. 70/100 (6.0%)**	**Pen. 160/220 #1 (6.0%)**	**Pen. 160/220 #2 (5.6%)**	**PMB 1 (6.0%)**	**PMB 2 (6.2%)**
v	76.7	80.1	89.5	98.7	102.8	92.3
α	5205	4879	4602	4157	4067	4087
β	-0.0798	0.2698	1.2533	0.2840	0.1511	0.2208
γ	0.9654	1.0492	1.2993	1.0340	1.0172	0.9464

Table A2. Master curve fitting parameters of asphalt mixture phase angle ϕ (°).

Binder type in the asphalt mixture (binder content)	**Pen. 50/70 (6.2%)**	**Pen. 70/100 (6.0%)**	**Pen. 160/220 #1 (6.0%)**	**Pen. 160/220 #2 (5.6%)**	**PMB 1 (6.0%)**	**PMB 2 (6.2%)**
a	-2.7793	-2.1469	-1.0520	-1.9353	-2.0425	-2.2717
b	2.2461	2.1020	1.9924	2.4118	2.5201	2.6388
c	34.244	36.606	40.739	32.769	31.951	30.495
d	3.0466	3.4082	2.6510	2.7530	2.2146	3.1548
g	1.5297	1.1128	2.1602	2.4073	1.2495	1.0609

Appendix 3 Master curve fitting parameters of bituminous binders

The values of parameters for fitting master curves of bituminous binders are presented in this appendix. The detailed description can be found in Section 4.2.2.1 of this report.

Table A3. Master curve fitting parameters of original binder G (Pa).*

Binder type	Pen. 50/70, original	Pen. 70/100, original	Pen. 160/220 #1, original	Pen. 160/220 #2, original	PMB 1, original	PMB 2, original
α	6.99×10^{7}	5.87×10^{7}	5.22×10^{7}	5.24×10^{7}	4.34×10^{7}	7.19×10^{7}
β	1.0301	1.7877	3.2501	6.3449	2.0116	2.6905
γ	1.9833	1.9994	2.0731	2.0652	1.9114	1.5566

Table A4. Master curve fitting parameters of RTFOT-aged binder G (Pa).*

Binder type	Pen. 50/70, after RTFOT	Pen. 70/100, after RTFOT	Pen. 160/220 #1, after RTFOT	Pen. 160/220 #2, after RTFOT	PMB 1, after RTFOT	PMB 2, after RTFOT
α	4.78×10^{7}	4.92×10^{7}	4.76×10^{7}	4.02×10^{7}	4.97×10^{7}	5.90×10^{7}
β	0.2380	1.0300	2.5585	5.8272	3.5959	2.2166
γ	1.9090	1.9101	1.9868	1.9880	1.7969	1.5550

Table A5. Master curve fitting parameters of original binder phase angle (°).

Binder type	Pen. 50/70, original	Pen. 70/100, original	Pen. 160/220 #1, original	Pen. 160/220 #2, original	PMB 1, original	PMB 2, original
a	0.3968	1.0208	1.9424	1.2465	-	-
g	1.8126	1.8492	1.7772	1.5107	-	-
δ_P	-	-	-	-	71.3	65.0
f_P	-	-	-	-	5.04×10^{-3}	3.00×10^{-3}
S_R	-	-	-	-	0.0396	0.0380
δ_L	-	-	-	-	16.8	-3.0
S_L	-	-	-	-	0.3662	5,0000

Table A6. Master curve fitting parameters of RTFOT-aged binder phase angle (°).

Binder type	Pen. 50/70, after RTFOT	Pen. 70/100, after RTFOT	Pen. 160/220 #1, after RTFOT	Pen. 160/220 #2, after RTFOT	PMB 1, after RTFOT	PMB 2, after RTFOT
a	-0.0747	0.5552	1.5476	0.7638	-	-
g	2.0290	2.1506	2.0441	1.7737	-	-
δ_P	-	-	-	-	69.2	63.5
f_P	-	-	-	-	8.09×10^{-4}	1.00×10^{-3}
S_R	-	-	-	-	0.0302	0,0320
δ_L	-	-	-	-	15.7	-3.0
S_L	-	-	-	-	0.4703	5.0000

ABOUT VTI

The Swedish National Road and Transport Research Institute (VTI), is an independent and internationally prominent research institute in the transport sector. Our principal task is to conduct research and development related to infrastructure, traffic and transport. We are dedicated to the continuous development of knowledge pertaining to the transport sector, and in this way contribute actively to the attainment of the goals of Swedish transport policy.

Our operations cover all modes of transport, and the subjects of pavement technology, infrastructure maintenance, vehicle technology, traffic safety, traffic analysis, users of the transport system, the environment, the planning and decision making processes, transport economics and transport systems. Knowledge that the institute develops provides a basis for decisions made by stakeholders in the transport sector. In many cases our findings lead to direct applications in both national and international transport policies.

VTI conducts commissioned research in an interdisciplinary organisation. Employees also conduct investigations, provide counseling and perform various services in measurement and testing. The institute has a wide range of advanced research equipment and world-class driving simulators. There are also laboratories for road material testing and crash safety testing.

In Sweden VTI cooperates with universities engaged in related research and education. We also participate continuously in international research projects, networks and alliances.

The Institute is an assignment-based authority under the Ministry of Infrastructure. The Institute holds the quality management systems certificate ISO 9001 and the environmental management systems certificate ISO 14001. Certain test methods used in our labs for crash safety testing and road materials testing are also certified by Swedac.

vti

Swedish National Road and Transport Research Institute • www.vti.se • vti@vti.se • +46 (0)13–20 40 00